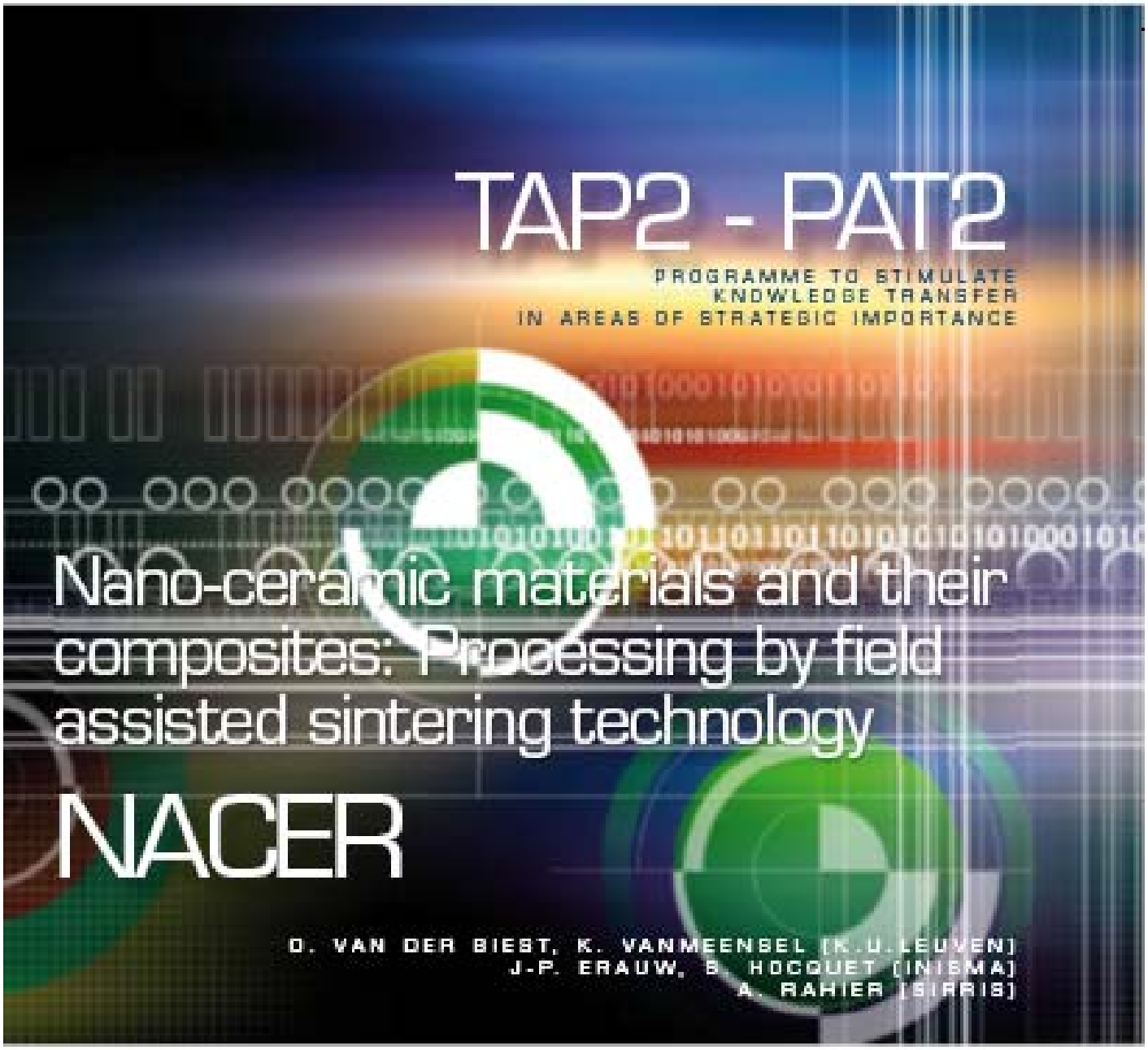
TAP2 - PAT2
PROGRAMME TO STIMULATE
KNOWLEDGE TRANSFER
IN AREAS OF STRATEGIC IMPORTANCE
Nano-ceramic materials and their composites: Processing by field assisted sintering technology
NACER
O. VAN DER BIEST, K. VANMEENSEL [K.U.LEUVEN]
J-P. ERAUW, B. HOCQUET [INISMA]
A. RAHIER [SIRRIS]
STANDARDISATION
TELECOMMUNICATIONS
SPACE SECTOR
CLEAN TECHNOLOGIES
NEW MATERIALS
.be

PROGRAMME TO STIMULATE KNOWLEDGE TRANSFER IN AREAS OF STRATEGIC IMPORTANCE

TAP2

FINAL REPORT

NANO-CERAMIC MATERIALS AND THEIR COMPOSITES: PROCESSING BY FIELD ASSISTED SINTERING TECHNOLOGY

NACER

P2/00/07

Promoters

Omer Van der Biest

Katholieke Universiteit Leuven, Department of Metallurgy and Materials Engineering

Kasteelpark Arenberg 44, B-3001 Leuven

Francis Cambier

INISMa – INstitut Interuniversitaire des Silicates, sols et Matériaux

Avenue Gouverneur Cornez 4, B-7000 Mons

André Rahier

Sirris-Wallonie, Centre de recherche des Industries de Fabrication Métallique

Rue du Bois St Jean 12, B-4102 Seraing

Authors

O. Van der Biest, K. Vanmeensel (K.U.Leuven)

J-P. Erauw, S. Hocquet (INISMa)

A. Rahier (Sirris)

KATHOLIEKE UNIVERSITEIT LEUVEN

sirris driving industry by technology

bcrc inisma

D/2010/1191/17
Published in 2010 by the Belgian Science Policy
Avenue Louise 231
Louizalaan 231
B-1050 Brussels
Belgium
Tel: +32 (0)2 238 34 11 – Fax: +32 (0)2 230 59 12
http://www.belspo.be

Contact person: *Anna Calderone*
Secretariat: +32 (0)2 238 34 80

O. Van der Biest, K. Vanmeensel, J-P. Erauw, S. Hocquet, A. Rahier, ***Nano-ceramic materials and their composites: Processing by field assisted sintering technology (NACER)***, Final Report, Belgian Science Policy (Programme to stimulate knowledge transfer in areas of strategic importance – TAP2), Brussels, 2010, 105 p.

TABLE OF CONTENTS

SUMMARY

A. Context

The discovery of new materials may enable entirely new technologies. The discovery of superconductors is one example but in recent years materials and in particular ceramics, with entirely new combinations of properties have been developed. The use of very fine nanosized or nanostructured powders is one of the key aspects of these developments. Hence materials development in general and nanotechnology can be considered as strategic areas which may have vast repercussions in development of new technologies in many sectors.

B. Objectives

The scientific goal of the NACER project is to build on the experience and knowledge in the partnership to obtain the most advanced nanostructured ceramics and ceramic composites in close collaboration with interested Belgian industry.

The fabrication process for nanostructured ceramics starts with the synthesis of powders with particles in the range 10 to 100 nm. The objective of Sirris was to synthesize and characterize carbide and nitride nanopowders using a RF high power plasma system as well as laboratory equipment, and to supply these powders to the partners for further testing. In the course of the project Sirris observed that maintaining the reproducibility of the powder characteristics while preserving the perspective of scaling the production up to an industrial scale was a challenge. For this reason, and in agreement with the partners, Sirris focused exclusively on the synthesis of SiC, with a strong accent on the end-product quality.

To prepare nanostructured objects from nanopowders, the powders need to be formed into the desired shape using colloidal techniques based on suspensions. These lead to more homogeneous microstructures and also they will make for safer handling of the nanopowders. After shaping one needs to eliminate the pores between particles by heating to high temperatures in a process which is generically called sintering. A major challenge is to retain the nanostructure by minimising other high temperature processes competing with sintering such as grain growth, which tend to destroy the nanostructure. Field assisted sintering technology (FAST) also known as spark plasma sintering (SPS) or pulsed electric current sintering (PECS) is one of only a few techniques which have the potential to meet this challenge. The

main and specific objective of the project was to broaden the scientific and practical knowledge regarding the field assisted sintering technology for the make-up of new promising ceramics and composites. The further processing of the nanopowders, either obtained from Sirris or from other sources was carried out in collaboration by INISMa in Mons and at K.U.Leuven, Department of Metallurgy and Materials Engineering, where the FAST equipment is located.

C. Conclusions

Sirris succeeded in mastering the process variables in such a way that the end product characteristics (specific area, mean particle diameter, granulometry distribution, specific gravity, XRD signatures, and overall stoichiometry) are reproducible. 23 batches of SiC nanopowder were produced for a total of 1400 g of SiC nanopowder. Part of this material was made available to the partners, even beyond the end date of the project.

INISMa has focused on an understanding of the densification mechanisms of an ultrafine commercial alumina powder, which served as a model for an electrically insulating powder. It was made clear that as the density of the alumina increases the grains also grow significantly in this single phase material. Particular attention has been paid to **the modelling of the thermal conductivity as function of porosity and grain size of the aluminas.** From an extensive literature study, the Effective Medium Percolation Theory (EMPT) model appeared to be most appropriate. In order to match data on porous and very fine grained aluminas it is necessary to take into account the thermal resistivity of the grain boundaries.

The **thermal properties of ZrO_2-TiN ceramic composites** were investigated and modelled. Among the analytical models the Maxwell model appears to approximate the experimental data more closely. A numerical object oriented finite element technique (OOF) was also used. In this approach actual pictures of the microstructure are the starting point. The OOF approach leads to a realistic estimate of the thermal conductivity values compared to experimentally determined values. There is also a good correspondence with the analytically calculated values using the Maxwell model. Apparently in this system the thermal resistivity of the internal interfaces can be neglected.

Al_2O_3–WC composite powders with up to 80 vol% WC could be fully densified by means of FAST. The higher the WC content, the higher the sintering temperature needed to achieve fully dense composites. The dispersion of 20–60 vol% WC

particles significantly suppressed Al_2O_3 grain growth, resulting in ultrafine grained composites with high stiffness. The electrical conductivity of these composites is high enough for the materials to be suitable for electrical discharging machining (EDM).

For **electrically conductive ZrO_2-$TiC_{0.5}N_{0.5}$ (60/40) composites** a number of process variables were investigated. With respect to the stabilisers the highest toughness was obtained for 1Y2Nd-ZrO_2 matrices which were tougher compared to 3Y-ZrO_2 matrices with values up to 9 MPa.$m^{1/2}$ reached. Generally, the mechanical properties of the processed composite materials decreased with decreasing TiCN particle size. This was attributed to a partial dissolution of TiCN in Y-ZrO_2 which increases as the contact area between the two phases increases. Further proof for this hypothesis is being sought. In contrast for **ZrO_2-WC (60/40) (vol%) composites** we observed improved mechanical properties compared to ZrO_2-TiCN (60/40) composite materials, due to the absence of any chemical interaction between the Y-ZrO_2 matrix and the secondary WC phase.

Fully dense, binderless WC ceramics can be obtained by FAST whereby the grain size of the initial starting powder (150 nm) was maintained in the fully densified material. **This is an example of a material that could only be made by FAST and where indeed the promise of the technique has been fully realised.** This material exhibits exceptional mechanical properties such as a Vickers hardness of 28 GPa and a 3-point bending strength of nearly 1 GPa.

Also **WC-Co materials with a dispersion of diamond particles** were investigated and promising results obtained.

In another **case study on TiO_x / TiO_2 materials**, the main conclusions are that it was possible to retain the crystallographic structure of the TiO_x phase after densification with FAST. In contrast this was not possible for the TiO_2 phase with anatase structure which had transformed to the rutile structure after densification.

In the FAST technology **the electrical and thermal properties of the die assembly** play a crucial role in the temperature distribution that can be achieved. The **mechanical properties of the die material also determine the pressures that can be applied** to assist the densification. Hence research on the development of a die set-up which allows the application of higher pressures than the currently used graphite dies was successfully concluded.

Another limitation of the FAST technology is that at present only rather simple shapes such as discs can be obtained. In order to make **more complicated shapes**

possible the deformation behaviour of fully dense material was investigated in the FAST equipment. **Super plastic deformation rates** could be achieved which opens prospects of more complex shaping by the technique. In order to understand this deformation behaviour one needs an accurate thermal-electrical modelling of the experiments.

D. Contribution of the project in a context of scientific support to transfer of knowledge and innovation

The work plan included case studies driven by the industrial members of the Follow-up committee. Four case studies have been worked on which have given the industrial members the opportunity to evaluate the FAST technology on nanopowders for their interests.

The novel approach based on chemical engineering tools and reasoning as used by Sirris to tune the process variables of the synthesis of consistent nanopowders is being further exploited to provide specific powders to several industrial partners. Sirris is also ready to transfer the necessary knowledge to partners who would be interested in scaling the synthesis up to an industrial scale.

The research partners also participated in a number of events on a national and international level on the subject of nanotechnology and ceramics. They gave some introductory and overview papers on the subject of the project.

The three partners are active in regional and European projects on nanomaterials and nanocomposites.

E. Keywords

Ceramics, composites, nanomaterials, RF plasma, nanopowder, sintering, FAST, SPS, PECS, silicon carbide, alumina, zirconia, tungsten carbide, titanium nitride, titanium oxide.

SAMENVATTING

A. Context

De ontdekking van nieuwe materialen kan aanleiding geven tot de ontwikkeling van totaal nieuwe technologieën. De ontdekking van de supergeleiders is daar een voorbeeld van maar meer recent werden er in het bijzonder keramische materialen ontwikkeld met een totaal nieuwe combinatie van eigenschappen. Het gebruik van zeer fijne poeders met nano afmetingen of met nanostructuur is een van de sleutel aspecten van deze ontwikkeling. Het is dus duidelijk dat materiaal ontwikkeling in het algemeen en ook de nanotechnologie als strategische gebieden moeten worden beschouwd die zeer brede naklank kunnen vinden in de ontwikkeling van nieuwe technologieën in vele sectoren.

B. Doelstellingen

Het wetenschappelijk doel van het NACER project is, om bouwend op de kennis en ervaring van de partners, de meest geavanceerde keramieken en keramische composieten met nanostructuur te produceren in samenwerking met de Belgische industrie.

Het fabricage proces voor nanogestructureerde keramische materialen begint met de synthese van de poeders samengesteld uit deeltjes in het bereik 10 tot 100 nm. De doelstelling van Sirris was de synthese en de karakterisering van nanopoeders (carbide en nitride) door gebruik van een hoog vermogen RF plasma toorts evenals geschikte laboratorium uitrustingen, vervolgens de poeders te leveren aan de verschillende partners voor verder onderzoek. In de loop van het project werd er vastgesteld dat de productie op industriële schaal van reproduceerbare nanopoeders was een uitdaging. Daarom boog Sirris zich uitsluitend op de synthese van SiC in overleg met de partners, met een sterk accent op de kwaliteit van het eindproduct.

Om van deze nanopoeders voorwerpen met macroscopische afmetingen te maken, zal aan deze poeders vorm worden gegeven via colloïdale vormgevingstechnieken op basis van suspensies. Deze leiden tot een meer homogene microstructuur en zijn ook veiliger bij het manipuleren van poeders met nano-afmetingen. Vervolgens dient men de poriën tussen de deeltjes te elimineren door op te warmen tot hoge temperatuur in een proces dat sinteren wordt genoemd. Een grote uitdaging bij dit proces is het behoud van de nanostructuur in het materiaal. Immers bij hoge temperatuur zijn er naast de transportprocessen die tot verwijdering van de poriën

leiden ook andere zoals korrelgroei die leiden tot een vergroving van de microstructuur. Sinteren in de aanwezigheid van een elektrisch veld (field assisted sintering technology, FAST, of spark plasma sintering, SPS, of pulsed electric current sintering, PECS) is een van de weinige technieken die het potentieel heeft om deze uitdaging aan te kunnen. De voornaamste en specifieke doelstelling van het project was om de wetenschappelijke en praktische kennis van het “field assisted sintering" proces te verbreden voor de bereiding van nieuwe veel belovende keramieken en composieten. Het verder verwerken van de poeders bekomen van Sirris of afkomstig van andere bronnen werd in samenwerking uitgevoerd door INISMa en de K.U.Leuven, Departement Metaalkunde en Toegepaste Materiaalkunde waar ook de FAST apparatuur zich bevindt.

C. Besluiten

Sirris slaagde erin de variabelen van het procedé aan te passen zodanig dat de eigenschappen van het eindproduct (specifiek oppervlak, gemiddelde diameter en distributie van diameters van de deeltjes, dichtheid, XRD spectra en algemene stoechiometrie) werden reproduceerbaar. 23 batches van SiC nanopoeder werden geproduceerd met een totale inventaris van 1400 g. Een gedeelte van dit materiaal is ter beschikking van de partners, zelfs na de einddatum van het project.

INISMa heeft gefocusseerd op het begrijpen van de verdichtingmechanismen van een ultrafijn commercieel aluminiumoxide poeder, dat als model dient voor een elektrisch isolerend poeder. Het werd duidelijk dat naarmate de dichtheid van het aluminiumoxide verhoogde de korrelgrootte ook significant toenam in die monofazig materiaal. Er werd ook bijzondere aandacht besteed aan **het modelleren van de thermische geleidbaarheid als functie van de porositeit en de korrelgrootte van het aluminiumoxide**. Uit een uitgebreide literatuur studie bleek dat EMPT theorie (Effective Medium Percolation Theory) het meest geschikt was. Om een goede overeenstemming te bekomen voor de poreuze en zeer fijnkorrelige aluminiumoxides is het nodig om ook de thermische weerstand van de korrelgrenzen in rekening te brengen.

De **thermische eigenschappen van ZrO_2-TiN keramische composieten** werden onderzocht en gemodelleerd. Het analytische Maxwell model benaderde het best the experimentele gegevens. Een numerieke methode OOF (Object Oriented Finite element technique), die vertrekt van een microscopisch beeld van de microstructuur werd ook gebruikt. De OOF benadering leidde tot een realistische schatting van de thermische geleidbaarheid. Er is ook een goede overeenstemming met het Maxwell

model. Blijkbaar kan in dit systeem de thermische weerstand van de grensvlakken tussen de fazen verwaarloosd worden.

Al_2O_3–WC composiet poeders met tot 80 vol% WC kunnen volledig verdicht worden met FAST. Hoe hoger het WC gehalte des te hogere de temperatuur die nodig is om volledig dichte materialen te bekomen. Een dispersie van 20 tot 60 vol% WC onderdrukt de korrelgroei in het aluminiumoxide op een significante manier waardoor ultra fijnkorrelige composieten met hoge stijfheid worden bekomen. De elektrische geleidbaarheid van deze composieten is hoog genoeg om ze met vonkerosie verder te bewerken.

Een aantal variabelen in het bereiden van **ZrO_2-$TiC_{0.5}N_{0.5}$ (60/40) composieten** werden onderzocht. Voor wat betreft de additieven die de werd De hoogste taaiheid werd bekomen wanneer een mengsel van additieven werd gebruikt die de tetragonale structuur van zirkoonoxide stabiliseren. Een 1Y2Nd-ZrO_2 matrix vertoonde een hogere taaiheid (tot 9 $MPa.m^{1/2}$) dan de standaard 3Y-ZrO_2 matrix. In het algemeen waren de mechanische eigenschappen van de composieten minder gunstig naarmate de deeltjes grootte van de secondaire TiCN faze kleiner werd. Dit wordt toegeschreven aan het gedeeltelijk in oplossing gaan van de TiCN in Y-ZrO_2, een verschijnsel dat toeneemt naarmate het contactoppervlak tussen beide fazen toeneemt. Er wordt nog verder gezocht naar een bevestiging van deze hypothese. In contrast hiermee werden voor **ZrO_2-WC (60/40) (vol%) composieten** wel een verbetering gevonden wanneer de secondaire faze zeer fijn verdeeld is in de matrix. In dit geval is er geen interactie tussen de Y-ZrO_2 matrix en de secundaire WC faze.

Volledig dichte WC keramieken zonder binder faze konden worden bekomen met FAST. In deze keramieken kon de originele deeltjesgrootte van het start poeder (150 nm) worden bewaard in het volledig verdichte materiaal. **Dit is een voorbeeld van een materiaal dat alleen met FAST kon worden aangemaakt waar inderdaad de belofte van de techniek werd waar gemaakt.** Dit materiaal vertoont uitzonderlijke mechanische eigenschappen zoals een Vickers hardheid van 28 GPa en een 3-punt buigsterkte van bijna 1 GPa.

Ook **WC-Co materialen met een dispersie van diamant deeltjes** warden onderzocht en veelbelovende resultaten werden geboekt.

In een **case studie op TiO_x / TiO_2 materialen** waren de voornaamste conclusies dat het mogelijke was om de kristallografische structuur van de TiO_x faze te bewaren na verdichten met FAST. Daarentegen voor de TiO_2 faze was dit niet mogelijk en werd de anatase structuur omgezet in de rutiel structuur na het verdichten.

In de FAST technologie spelen de elektrische en de thermische eigenschappen van de matrijs materialen een cruciale rol in de temperatuur distributie die kan worden gerealiseerd. De mechanische eigenschappen van het matrijsmateriaal bepalen ook de druk die kan worden aangelegd om het verdichten te bevorderen. Onderzoek op de ontwikkeling van een matrijs waar hogere drukken kunnen worden toegepast werd succesvol afgerond.

Een andere beperking van de FAST technologie is dat op dit moment alleen eenvoudige vormen zoals schijven kunnen worden bekomen. Om **meer complexe vormen** te kunnen aanmaken hebben we onderzocht hoe het materiaal zich gedraagt bij vervorming nadat het is verdicht. **Superplastische vervormingsnelheden** kunnen worden bereikt waardoor meer complexe vormen mogelijk worden. Om dit vervormingsgedrag te begrijpen was een accurate thermische elektrische modellering noodzakelijk.

D. Bijdrage van het project in een context van wetenschappelijke ondersteuning aan transfer van kennis en innovatie

Het werkplan omvat ook een actie rond case studies die werden aangebracht door de industriële leden van het Opvolgingscomité. Vier case studies werden uitgewerkt. Deze hebben de industriële partners de kans gegeven om de FAST technologie voor nanopoeders te evalueren voor hun interessegebieden

De op de chemische ingenieurstechniek gebaseerde nieuwe aanpak en redeneringen die door Sirris gebruikt werden om reproduceerbare eigenschappen van het eindproduct te verkrijgen door procesvariabelen te verfijnen worden thans verder gebruikt in het kader van de levering van andere poeders aan industriële partners. Sirris is ook klaar om de nodige kennis over te dragen naar partners die eventueel interesse aantonen in de synthese van nanopoeders op industriële schaal.

De onderzoekspartners hebben ook deel genomen aan manifestaties op nationaal en international niveau op gebied van nanotechnologie en keramische materialen. Ze hebben er inleidende voordrachten en overzichten gegeven over het onderwerp van het project.

De drie partners zijn actief in regionale en Europese projecten over nanomaterialen en nanocomposieten.

E. Trefwoorden

Keramische materialen, composieten, nanomaterialen, RF plasma, nanopoeder, sinteren, SPS, FAST, PECS, silicium carbide, aluminiumoxide, zirkoonoxide, wolfraamcarbide, titaannitride, titaanoxide.

RESUME

A. Contexte

Les matériaux céramiques nanostructurés promettent des combinaisons peu communes de propriétés. En ce qui concerne leurs propriétés mécaniques, on recherche en particulier un meilleur compromis entre dureté et ténacité. Ceci combiné à une excellente résistance chimique, rendra possible de nouvelles applications pour lesquelles cette combinaison particulière de propriétés s'avère déterminante dans le choix du matériau.

B. Objectifs

Le but scientifique du projet NACER est de développer, en s'appuyant sur l'expertise et le know-how des trois partenaires, des céramiques nanostructurées les plus avancées, tant monolithiques que composites, en collaboration étroite avec l'industrie belge intéressée.

Le procédé de fabrication commence par la synthèse de poudres présentant des tailles de grains dans la gamme des 10 à 100 nm. L'objectif poursuivi par Sirris consistait à synthétiser et caractériser des nanopoudres de carbures et de nitrures en utilisant un procédé à plasma de haute puissance ainsi que des équipements de laboratoire adéquats, et de livrer ensuite les poudres synthétisées aux différents partenaires en vue de réaliser les tests requis. Au cours du projet, nous avons constaté que maintenir une qualité constante du produit en sortie tout en préservant la perspective de produire à une échelle industrielle constitue un réel défi. Pour cette raison, en accord avec les partenaires, Sirris a concentré ses efforts sur la synthèse de SiC nanométrique avec un fort accent placé sur la qualité du produit final.

Partant de ces nanopoudres, la mise en forme d'objets macroscopiques s'effectue par le biais de techniques colloïdales au départ de suspensions. Ces techniques conduisent à des microstructures plus homogènes mais garantissent également une manipulation plus sûre des nanopoudres. Après le façonnage, la porosité intergranulaire est éliminée par un traitement thermique à température élevée connu de manière générique comme le frittage. Le maintien de la structure nanométrique en cours de frittage constitue ici le défi principal. En effet, à ces températures élevées de traitement, en plus des phénomènes de transport conduisant à la densification du compact, d'autres mécanismes prennent place tels que par exemple la croissance des grains tendant à détruire la structure nanométrique de départ. La

technique de frittage sous champ électrique (FAST – Field Assisted Sintering Technology), également connue sous les vocables SPS (Spark Plasma Sintering) ou PECS (Pulsed Electric Current Sintering – frittage sous courant électrique pulsé), est l'une des quelques techniques qui potentiellement permet de relever ce défi.

L'objectif spécifique principal de ce projet était d'élargir les connaissances scientifiques et l'expertise pratique quant à l'utilisation du frittage sous champ électrique pour l'élaboration de matériaux céramiques et de composites innovants. Le traitement de nanopoudres, tant celles synthétisées par Sirris, que celles provenant d'autres sources a été effectué, en collaboration avec l'INISMa de Mons, au département de métallurgie et d'ingénierie des matériaux (département MTM) de la K.U.Leuven, où l'équipement FAST utilisé est localisé.

C. Conclusions

Sirris a pu maîtriser les variables du procédé de synthèse de telle sorte que les caractéristiques du produit final (surface spécifique, diamètre moyen des particules, répartition granulométrique, densité, signatures DRX et stœchiométries globales) soient reproductibles. Vingt-trois lots ont été produits qui totalisent 1400 g de SiC nanométrique. Une fraction de ce matériau est mise à disposition des partenaires, même après l'échéance du projet.

L'INISMa pour sa part a mis l'accent sur la compréhension des mécanismes de densification d'une poudre commerciale d'alumine ultrafine, qui a servi de modèle pour le comportement de poudres électriquement isolantes. Il a été démontré que dans ce matériau monophasé, l'augmentation de la densité va de pair avec une croissance marquée des grains d'alumine. Une attention particulière a été accordée à **la modélisation de la conductivité thermique du matériau en fonction de la porosité et la taille moyenne des grains** après densification. Sur base d'une étude fouillée de la littérature, la théorie EMPT (Effective Medium Percolation Theory) apparaît la plus appropriée pour l'interprétation des résultats. Pour obtenir une corrélation entre les données expérimentales obtenues sur ces alumines poreuses et à grains très fins et le modèle, la prise en compte de la résistance thermique des joints de grains se révèle nécessaire.

Les **propriétés thermiques de composites céramiques ZrO2-TiN** ont été étudiées et modélisées. Parmi les modèles analytiques disponibles, le modèle de Maxwell semble le mieux approcher les données expérimentales. Une méthode de simulation numérique par éléments finis orientée objets (OOF) a également été utilisée. Dans cette approche, des micrographies des structures réelles sont prises comme point de

départ de la modélisation. L'approche OOF conduit à une estimation réaliste des valeurs de conductivité thermique par rapport aux valeurs déterminées expérimentalement. Une bonne corrélation avec les valeurs calculées analytiquement en utilisant le modèle de Maxwell est également relevée. Apparemment, dans ce système, la résistivité thermique des interfaces entre phases constitutives peut être négligée.

Des **poudres composites Al_2O_3-WC** avec des teneurs volumiques en WC jusqu'à 80% ont pu être complètement densifiées par la technique FAST. L'obtention de la densité totale de ces composites nécessite une température de frittage d'autant plus élevée que la teneur en WC augmente. L'incorporation de 20-60 vol% de particules de WC, réduit de manière significative la croissance des grains de la matrice Al_2O_3, résultant en l'obtention de composites présentant une microstructure ultrafine ainsi qu'une rigidité élevée. Par ailleurs, la conductivité électrique de ces composites est assez élevée pour permettre l'usinage de ces matériaux par électroérosion (EDM).

Dans le cas des **composites ZrO2-$TiC_{0.5}N_{0.5}$ (60/40) électriquement conducteurs**, un certain nombre de variables opératoires ont été étudiées. En termes de stabilisateurs de la zircone, les valeurs les plus élevées de ténacité ont été obtenues pour les matrices 1Y2Nd-ZrO2, qui se sont révélées plus tenaces que les matrices 3Y-ZrO_2, avec des valeurs allant jusqu'à 9 MPa.$m^{1/2}$. En général, les propriétés mécaniques des composites mis en œuvre diminuent pour une taille de particules de TiCN décroissante. Ceci a été attribué à une dissolution partielle du TiCN dans la matrice Y-ZrO_2, dissolution d'autant plus marquée que la zone de contact entre les deux phases augmente. Une recherche d'éléments complémentaires pour appuyer cette hypothèse est en cours. En revanche pour les **composites ZrO_2-WC (60/40) (vol%)**, une amélioration des propriétés mécaniques est observée par rapport aux composites ZrO_2-TiCN (60/40), en raison de l'absence de toute interaction chimique entre la matrice Y-ZrO_2 matrice et la phase secondaire WC.

Une **densification complète de céramiques WC exemptes de liant** a pu être obtenue par frittage FAST. De plus, par ce biais, la taille initiale des grains de la poudre de départ (150 nm) a été conservée dans le matériau densifié. **Ceci est un exemple d'un matériau qui ne peut être élaboré que par FAST et où les promesses de cette technique ont pu être pleinement concrétisées.** Ce matériau présente des propriétés mécaniques exceptionnelles telles qu'une dureté Vickers de 28 GPa et une résistance à la flexion 3-points de près de 1 GPa.

Des composites **WC-Co avec une dispersion de particules de diamant** ont été étudiées et des résultats prometteurs obtenus.

Dans une autre **étude de cas portant sur des matériaux TiO_x / TiO_2**, les principales conclusions sont qu'il est possible de conserver la structure cristallographique de la phase TiO_x après densification par la technologie FAST. En revanche ce maintien n'a pas été possible pour le TiO_2 dont la structure anatase d'origine est transformée en rutile après densification.

Dans la technologie FAST, les propriétés électriques et thermiques de l'outillage (assemblage matrice-poinçons) jouent un rôle crucial dans la répartition de température qui peut être atteinte. Les propriétés mécaniques du matériau d'outillage déterminent pour leur part, les pressions qui peuvent être appliquées pour faciliter la densification. C'est pourquoi le développement d'un outillage permettant l'application de pressions plus élevées que celles permises par le graphite actuellement utilisés a été entrepris. Ce développement s'est conclu avec succès.

Une autre limitation de la technologie FAST est qu'à l'heure actuelle, seules des géométries relativement simples telles que des disques peuvent être obtenues. Afin de rendre la **réalisation de formes plus complexes** possible, le comportement en déformation de matériaux complètement denses a été investigué dans l'équipement de FAST. Des **taux de déformation superplastique** ont pu être atteints ce qui ouvre des perspectives de mise en forme de formes plus complexes par cette technique. Afin de comprendre parfaitement ce comportement en déformation, une modélisation thermo-électrique précise est nécessaire.

D. Apport du projet dans un contexte d'appui scientifique au transfert des connaissances et à l'innovation

Le plan de travail comprenait également des études de cas proposées par les membres industriels du Comité de suivi.

Quatre études de cas ont été menées qui ont donné à ces membres industriels l'occasion d'évaluer la plus-value de la technologie FAST appliquée aux nanopoudres dans leurs domaines respectifs d'activité.

La nouvelle approche, basée sur des outils d'ingénierie chimique et qu'utilise Sirris pour ajuster les paramètres opératoires du processus de synthèse de nanopoudres et obtenir des produits de caractéristiques consistantes, se poursuit aux fins d'approvisionner plusieurs industriels en poudres spécifiques. Sirris est également prêt à transférer le know-how nécessaires à des partenaires qui seraient intéressés dans l'extension de la synthèse à l'échelle industrielle.

Les partenaires de recherche ont également participé à un certain nombre d'événements tant au niveau national qu'international sur le thème de la nanotechnologie et des matériaux céramiques. Ils ont à chaque fois donné des aperçus sur le contenu et les avancées du projet.

Les trois partenaires sont actifs dans des projets régionaux et européens dédiés aux nanomatériaux et nanocomposites.

E. Mots-clés

Matériaux céramiques, nanomatériaux, frittage, SPS, FAST, PECS, RF plasma, nanopoudre, carbure de silicium, alumine, zircone, carbure de tungstène, nitrure de titane, oxyde de titane.

1. Introduction

1.1. Subject and objectives

The main objective of the project is to unite the expertise of three Belgian research centres which have developed major complementary expertise in research on bulk inorganic materials with a nanostructure.

The three research centres have complementary strong points in this field. Sirris is building up a facility for the production of nanopowders with capacity sufficient to produce powders in kilogram quantities. K.U.Leuven, Department of Metallurgy and Materials Engineering (MTM) has been a pioneer in Europe in the development of equipment for field assisted sintering technology (FAST, also called SPS and PECS). Advanced prototype European equipment has been installed in its laboratory. INISMa has been studying nanoceramics and composites using more conventional technology. It has a very broad range of equipment to measure the properties of materials and in particular ceramics.

The broad **scientific goal of the NACER project** is to build on the experience and knowledge in the partnership to obtain advanced nanostructured ceramics and ceramic composites in close collaboration with interested Belgian industry.

Processing materials via powders has the potential to control the microstructure of materials on a nanoscale. This should start already with the synthesis of the powders. These can have themselves a size in the nanorange (10 to 100 nm) as is now possible for a number of ceramic compounds. Other powders are rather “nanostructured” than “nanosized” e.g. powders of metallic alloys with a nanodistribution of phases within each particle can for instance be obtained by rapid quenching of particles from the liquid.

Over the last few years, **several new technologies have been developed for the production of submicron, ultrafine or nanopowders with a narrow size distribution**. Nanopowders are generally produced by condensation of precursors (atoms, molecules or clusters) in a supersaturated gas environment. Such precursors are generated by various processes, such as laser evaporation of solid targets or plasma or laser-induced decomposition of gas mixtures. Other methods are related to ball milling (or mechanical alloying), self-propagating high temperature synthesis,

sol-gel, spray-drying of solutions, aerosol pyrolysis or chemical vapour condensation at low pressure.

Many technical and business issues however remain to be resolved before nanosized powders can be used in commercial applications. These issues involve:

- The lack of technology in handling and processing nanopowders, so that the fabricated materials show a very fine microstructure. Many nanopowders have been produced so far, but there is no competitive technology of their consolidation able to preserve small grain size yet keeping a high properties level.
- Nanopowders have proved to be difficult to densify using conventional processing routes and densification methods.
- The cost of fabricating bulk nanoscale materials is still very high (commercially available powders cost 50 - 500 $/kg), thus the components and devices of them are uneconomic for industrial use. It follows that R&D on nanostructured materials is highly risky for new business. Nanomaterials processing technology should be rather inexpensive to overbid high raw materials costs.
- In spite the fact that EU, USA and Japan are currently studying nanocomposites as a promising class of materials, there is a little understanding of behaviour of these materials during processing and assembling into final components.

To prepare objects in macro size from powders with nanosize or nanostructure, one needs to shape the powder first into the desired shape and subsequently heat it in order to form strong bonds between the particles and to make the pores between particles disappear. For this process of consolidation which one usually calls sintering, temperatures need to be high enough so that diffusion of atoms or ions becomes possible. This also entails that diffusion processes, which lead to coarsening, also have a chance. For example, small grains can shrink while larger grow at their expense (grain growth), or small crystals dissolve in favour of the growth of large ones (Ostwald ripening). The challenge in the processing of nanostructured materials from powders is to minimise the occurrence of these coarsening processes. Field assisted sintering technology (FAST) is one of a few techniques which have the potential to realise this.

FAST is also known under a number of other acronyms which emphasise true or assumed facets of the technique: SPS (spark plasma sintering), PECS (pulsed electric current sintering) and others. The principle is that the (nano)powder is inserted into a die and a high temperature is generated through a pulsed electric

current through the die and possibly, depending on the electrical properties of the powder compact, also through the powder. A high mechanical pressure is also applied to accelerate densification. The FAST process is in any case quicker than the classic heating and cooling in a furnace or in a hot press since the mass which is heated is reduced to the strictest minimum. The electrical voltage is relatively low (maximum 10 Volt) but the pulsed currents are high (of the order of thousands of Ampere). In addition to the speed of the process, literature mentions that also other effects may play a role to favour densification processes with respect to coarsening processes[1]. One supposes that sparks occur between particles and a plasma may be generated in the reduced pressure where the process is usually conducted. These are supposed to evaporate the contamination layer which often covers the surface of a powder and which may act as a barrier to densification. Proofs for these effects are as best incomplete since these processes occur in a closed die and measurement of the temperature of the densifying powder is difficult. The properties of the powder to be densified also should play an important role in these effects.

Innovative aspects of this project with respect to the state-of-the-art include:

- The **development of a facility for nanopowders with kgs/day production capacity.**
- Although the viability of FAST has been proven initially in Japan, it has been mainly applied to (insulating) oxide based materials. In this project, **FAST will be applied to conductive materials**. The study of the interaction of these conductive green compacts with the pulsed current and its relation with plasma generation shows a new application of this technique.
- **Colloidal processing** will be used to **enhance safe handling of nanopowders**, meanwhile ensuring optimised powder compaction for the sintering of nanosized powders.
- The FAST work will be supported and guided by **advanced modelling of the process**.
- **Modelling of the thermal properties of nanograined ceramics**.
- The field assisted sintering technology could have a high impact on the hard materials industry as it considerably reduces processing times and could lead to materials with higher hardness than those produced by conventional routes. Of particular interest are the **ceramic composite systems that have proven to be impossible to sinter conventionally without excessive grain growth**.
- **Production of homogeneous nanograined high hardness materials** for wear applications such as glass and metal forming tools, **hard and tough conductive composites which can be intricately shaped by electro**

discharge machining, nanograined conductive oxides, nanostructured SiC parts for space applications.

Economic, environmental and social aspects:

Improved safety and reliability, sustainable materials production and transformation technologies together with promotion of their efficient use, and improved quality of life constitute the broader objectives of the research work.

Within this project, the **understanding and application of structural nanocrystalline ceramics and cermets** (ceramic-metal composites) **will be improved** by establishing an efficient way to handle nanosized powders in order to obtain agglomeration-free green powder compacts, which facilitates easier sintering at lower temperatures than conventional ceramic powders.

A **range of applications are being targeted**: wear resistant nanostructured materials for tools of various kinds, in particular cutting tools, tools for metal, rock and glass processing; clinical biomaterials subject to wear, the development of multiscale porous materials, materials for space mirrors based on silicon carbide, etc.

The **industrial members of the Follow-up committee** have been chosen because of their interest in nanomaterials and their applications.

Taking as an example the development of cutting tools technology, it can be observed that it continuously develops to match changing requirements of the relevant market. To ensure higher machining productivity, tool manufacturers are promoting hard tool materials suitable for substantial productivity improvements in some metal cutting and rock drilling application. However, for a broadened range of machining utilisation, oxide based and silicon nitride based ceramic tooling still need further improvements in terms of flexural strength, toughness and hardness at high temperatures. One potential route to improved tool materials is the development of nano-grained ceramics and cermets, a key element of this proposal. **Advanced access to improved hard tool materials would place Belgian industry in a strong competitive position in terms of both machine tool design/development and efficient metalworking operations in key industries** such as automotive and aerospace.

A successful outcome of this project **will substantially stimulate employment and technical advances in powder manufacture (e.g. through a spin-off) as well as parts manufacture** thereby **further increasing the potential Belgian employment**.

Nanotechnology is viewed as a key strategic technology in the development of a sustainable society. For example, the **development of nanostructured ultralight materials** will result in energy, fuel and materials savings.

Using powder technology to process components, one utilises 95 % of raw materials. This is extremely more favourable from the point of view of natural resources, when compared to other processing routes.

FAST processing of nanostructured materials is therefore intrinsically much more energy efficient than conventional processes such as pressureless sintering, hot pressing and hot isostatic pressing.

This **project will have a positive impact on health and safety of the industrial workers involved in the manufacturing chain**. PM is already a relatively “clean” technology and the project aims to further improve this by colloidal processing to avoid dusting during powder handling.

The envisaged hard materials will increase workers safety by reducing the use of oil-based cutting fluids in metal working and machining operations. Indirectly, the project will contribute to enhancing the quality of life of all Belgian citizens by supplying wear parts for use in the next generation of automobiles, electric motors, household equipment, etc.

By the introduction of field assisted sintering in the production of wear resistant materials and the manufacturing of nanostructured lightweight materials, the project is focused on the establishment of a new processing technique enabling Belgian industry to be more competitive in world markets. This will actually lead to a significant increase in employment in the sector. By achieving major savings in raw materials and energy and reducing pollution, growth will be sustainable economically and environmentally.

1.2. Methodology, organisation and working method

Field Assisted Sintering Technology (FAST) is a new powder technology technique especially suited for nanosized powders or nanostructured particles because the time at high temperature, required to reach full density, is considerably reduced compared with conventional sintering processes. A number of difficult-to-process materials have been obtained with extremely fine microstructures at temperatures 200ºC lower than those required for conventional hot pressing.

Amongst the features of the FAST technique proven by our experience and/or reported in literature are:

- High heating rates are possibly accompanied by additional densification mechanisms.
- Lower temperatures of densification (typically 150 - 200ºC lower than hot pressing).
- Final products with full density and fine (nano)grain size.
- Short processing times : The short firing cycle offers many possibilities to produce novel ceramic materials with superior properties.
- Extremely promising for composite applications.
- Clean grain boundaries.
- Possibility for making it an automated continuous process.

Unresolved issues are the role of plasma mechanisms in ceramic samples with high loading of conductive second phases and the limitations in sample size. The latter is especially important for industrial applications. The process modelling method can give some clear guidelines on the upscaling of the process.

The main and specific objective of the project is to broaden the scientific and practical knowledge regarding the field assisted sintering technology (FAST) for the make-up of new promising ceramics and composites.

The major competencies of the three partners form a logical materials processing chain. This facilitates the integration of their efforts within the project : powders produced by Sirris will be forwarded to K.U.Leuven for shaping and FAST densification. INISMa will characterise the powders and materials produced and will also measure the essential data to control the FAST process (thermal and electrical properties). The management structure of the project is designed to streamline and facilitate these interactions between the partners.

The work has been organized in work packages which follow the sequence of steps when one is processing materials from powders. It begins with the synthesis of nanosized or nanostructured powders. In the present project the synthesis of nanosized ceramic powders was pursued in WP 1. After synthesis these powders need characterization with respect to morphology, particle size distribution, chemical and structural purity. Also powders from other sources were characterized. Next these powders need to be shaped in a body with a suitable shape. A suitable way to green shape nanosized powders is crucial in order to obtain high quality densified nanostructured composites. This was the concern in workpackage 2. The colloidal method is also a very safe way to handle and process nanopowders and was

investigated in NACER. Initially it was proposed to study hygiene and security Issues as part of WP 1 (Task 1.3) but no manpower was available for this. Of course the best and safest practices were used in the synthesis and subsequent processing of the powders by all the partners. The main factors that affect the sinterability of shaped advanced ceramics include agglomerates and inclusions. Due to their very small size nanosized powders are very susceptible to agglomeration simply due to Van der Waals attraction forces. The colloidal method is also an effective processing method in which the detrimental inhomogeneities can be removed by dispersing the powder in a liquid medium in a suspension. This was investigated in WP2. After shaping one obtains a so-called green part (this means not-sintered) product that needs further densification to a usable ceramic product.

As was explained in 1.1 the Field assisted sintering technique (FAST) carries a lot of promise to preserve the nanostructure from the green compact to the final ceramic material. This technique was investigated for a range of materials in WP3. Since the FAST process is intrinsically quick, it is important to know the temperature distribution within the densifying powder as well as its evolution in time. Hence it is important to be able to predict this temperature distribution as a function of time by computer simulation so that the temperature history at each location within the material is known. One of the attractions of the FAST technique is the versatility in terms of powders which can be used, the die materials, the construction and geometry of the die as well as the die and cycle parameters i.e. power/temperature and pressure as a function of time. This creates a wide range of processing parameters. To quickly identify an optimum combination of these, the central idea is to use the simulations as a guide in the FAST experimentation. It is believed that it is only through the development of accurate models that the full potential of the FAST technique will be realised not only on a laboratory scale but also later in industry. Hence in WP3 two tasks can be identified. On the one hand the experimental work with the FAST machine (Task 3.1.), on the other hand the computer simulations (Task 3.2.) which included among others also the modelling of two critical properties of the densifying compacts, namely their thermal and electrical transport properties.

After densification the resulting materials were characterised with respect to microstructure and with respect to properties in WP 4. Some of the materials investigated were model materials or were recommended by members of the Follow-up committee. Some resulted in actual case studies in collaboration with individual members of the committee. The state-of-the art in the field in terms of literature and technology development was also followed up. The bar chart below shows the Workpackages and tasks in the project with the expected timing at the start. This timing was by and large adhered to.

WORKPACKAGE BARCHART																
Workpackage descriptions	Partner's ManMonths			Duration												
				1st year				2nd year				3rd year				
	KUL	CRIF	INISMa													
WP1: Nanopowder production and characterisation																
Task 1.1: Synthesis of nanopowders							M1									
Task 1.2: Characterisation of nanopowders																
Task 1.3: Study of hygiene and security problems																
WP2: Shaping of nanopowders using suspensions																
Task 2.: Shaping of nanopowder suspensions							M2									
WP3: Field assisted sintering technology studies																
Task 3.1: Densification of nanopowders through FAST									M3							
Task 3.2: Modelling of the FAST process									M4							
WP4: Properties and performance of materials and composites processed																
Task 4.1: Characterisation of basic properties of densified products									M5							
Task 4.2: Measurement of functional properties																
WP5: Exploration of and preparation for applicationsDatabase development																
Task 5.1: Case studies																
Task 5.2: Technology watch and market study																
WP6: Project management																

1.3. Materials investigated

In order to ensure the long term viability and the extrapolation of the projects' results on the industrial scene, Sirris has put a strong accent on the reproducibility of the nanopowders' properties. Due to the inherent complexity of the plasma synthesis and in order to be able to provide powders of acceptable quality, Sirris agreed with the project partners to focus exclusively on the synthesis of SiC. Sirris provided also the other partners with nanopowders obtained from other sources.

Other materials which were investigated are:

- Aluminium oxide (alumina): in research on advanced ceramics alumina is often taken as a reference material because it is available with relatively high purity in a wide range of particle sizes and shapes. There is also a lot of knowledge on the properties of alumina hence in research it has often served as a "model" material. However it has found also technical applications in a number of niche markets;
- Al_2O_3-WC composites;
- Zirconia and zirconia based composites;
- TiO_2, TiO_x, materials;
- WC and WC-Co based materials.

1.4. Structure of the report

Rather than reviewing the progress that has been made in the different Workpackages during the course of the project, it appears more opportune to group the results according to the materials investigated and thus integrate the information that has been generated within the project for a particular type of material. Clearly within the scope of the project and with the means available not everything, from powder synthesis to properties characterisation, could be done for all materials. A separate section is also devoted to the modelling of a new die material. In the past and in most publications graphite dies are used for densification of ceramic materials. There is a need for designing dies with other materials with the aim to increase the mechanical loads on the powder during densification. In the course of the project the use of a molybdenum die was investigated.

At the end we will briefly review what has been done for the different case studies that have been carried out in close collaboration with members of the Follow-up committee. Finally we will review the main conclusions of the project.

2. Results for Silicon Carbide

2.1. Nanopowder production and characterisation

2.1.1. Synthesis of nanopowders

Sirris synthesizes nanopowders using a 60 kW inductively coupled plasma torch running at 5 MHz. This process is suitable for the production of nanopowders at industrial scale. Contrary to the cases where a DC plasma torch is being used, the RF plasma system should allow minimizing the contamination of the end product by structural components (e.g. electrode material). The process can be described as follows (Figure 1):

1. The plasma torch is fed by three different gases (sheath gas, central gas and solid precursor carrier gas) containing essentially argon and hydrogen (or oxygen) and flowing down under the coil, which is powered by the RF generator;
2. The intense electromagnetic field tears the dielectric and causes a current to flow into the gas. A rapid heating results from the Joule effect, causing a fast increase of the temperature (up to 10000 K in the hottest zones);
3. A solid precursor is also fed into the plasma, where it vaporizes and partially dissociates quasi instantly;
4. The vapours progress down to the quench zone where a large flow of cooling gas is introduced into the circuit. This causes the nucleation of nano-particles without favouring their growth;
5. The flow is further cooled down and directed towards a battery of filters where the nano-particles are collected;
6. Filters are regularly unloaded by a blow-back procedure. The powders are further transferred to a secondary filter, which can be discharged into a glove box under inert atmosphere (Ar);
7. Finally, the powders recovered in the glove box are conditioned and transferred to the laboratory for characterization.

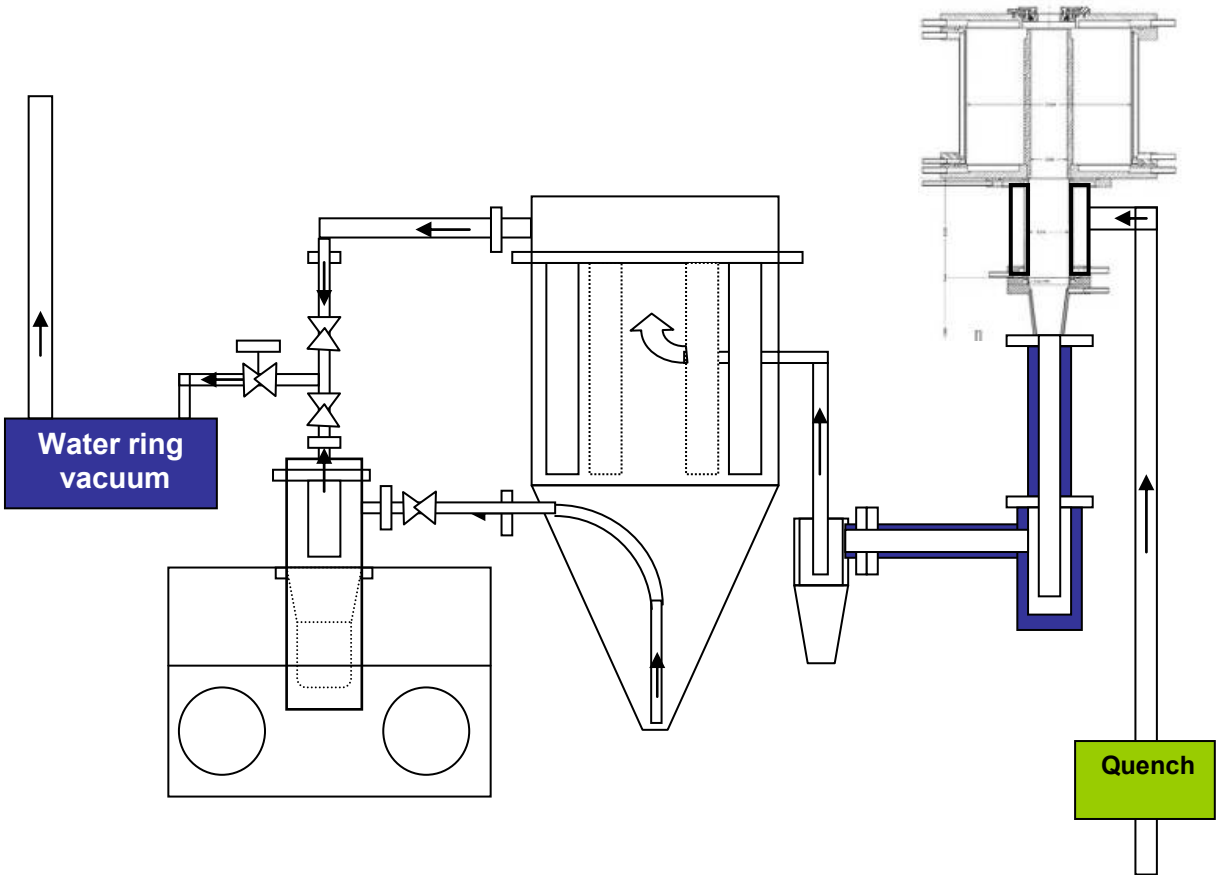

Figure 1: Schematic overview of the overall plasma torch process. Upper right part: plasma torch followed by quench section. Middle part: heat exchanger followed by filter battery. Left part: secondary filter and glove box.

Sirris exploits several instruments for the characterization of nanopowders. The available techniques are:

- An XRD instrument (PANalytical X'Pert PRO) for the identification and semi quantitative measurement of crystalline phases. This equipment allows also estimating the mass percentage of vitreous phases;
- A centrifugal disc model DC20000 from CPS (Florida, USA) for the determination of granulometry distributions;
- Two helium pycnometers (Pycnomatic, ThermoFinnigan) for the determination of specific gravities;
- Three BET instruments (Model Qsurf and Sorptomatic from Thermo Electron Corporation) for the determination of specific areas;
- A scanning electron microscope (JEOL JSM-6460LV);
- An Autolab PGSTAT302 potentiostat from Metrohm (Ecochemie, The Netherlands) for the determination of impurities as well as product stoichiometry;

- A CHN-O analyzer model Flash 2000 from Interscience.

Besides using existing procedures (for e.g. BET, pycnometry, granulometry distribution and XRD measurements), Sirris carries out also literature studies to find out adequate complementary techniques[2, 3] and develops also specific procedures based on past and new experience[4, 5]. More particularly, in the framework of the NACER project, we adapted an electrochemical technique[4] to the measurement of silicon in excess found in nanostructured SiC (i.e. the sum of free Si and SiO_2 in the product). The adapted technique relies on the chemical aggressiveness of singlet oxygen at moderately high pH to selectively dissolve silicon containing species. As explained in [4], the further sensitive determination of Si (LOD = 10 ng $Si.mL^{-1}$) is carried out by differential pulse anodic stripping voltammetry of the β-silico-dodecamolybdate in a tartrate medium buffered at pH 10. Raw data are treated using a home-made code developed under VBA for Excel®. We developed also another code to facilitate the transfer, the analysis and the interpretation of CPS data under Excel®. Further work is still going on regarding the determination of total Si, total C and free C in SiC.

During the first two years of the project, we attempted to synthesize different nanopowders (SiC, TiC, ZrO_2, …) using our RF plasma torch. In all cases, we observed that the quality of the nanopowders was very poor (Table 1).

The poor results observed by that time were due to the high level of complexity of the system. Table 2 depicts a non exhaustive list of process variables together with some comments on their effects.

Evidently, these process variables are highly correlated, thereby explaining why it is so difficult to keep the quality of the end product under control.

Powder properties	Observed results	Diagnostics and remarks
Specific gravity	Very often different from the theoretical value	Attributed to the presence of impurities (water from cooling circuits or corrosion products)
Specific area	Huge spreading ranging from 10 to 300 $m^2.g^{-1}$	Due to the uncontrolled presence of the solid precursor into the final product (confirmed by SEM measurements) or to unbalanced stoichiometry of the end product
Granulometry	Multi modal and non reproducible	No evident correlation was found with process input variables
XRD	Presence of a vitreous phase (> 30 wt. %); various impurities observed depending of the specific cases (iron oxide, boron nitride, silicon oxide, silicon, graphite, …)	Quantification by XRD is neither accurate nor precise enough. It addresses only the crystalline phases
SEM	Huge amounts of coarse precursor in the final product	The reaction zone (plasma) may be hydro-dynamically short-circuited
Chemical composition	Unbalanced in most cases	Requires introducing additional gaseous chemicals into the plasma
Colour	Variable; depends on the impurities	
Overall reproducibility	Very bad	

Table 1: Overview of the quality and characteristics of the produced nanopowder batches throughout the first two years of the project using RF plasma torch.

Variable number	Process variable	Nature of the variable	Comments
1	Sheath gas flow rate	Input	Governs a/o the stability of the plasma
2	Sheath gas composition	Input	Governs a/o the stability of the plasma
3	Central gas flow rate	Input	Governs a/o the stability of the plasma
4	Central gas composition	Input	Governs a/o the stability of the plasma
5	Carrier gas flow rate	Input	Influences the residence times
6	Carrier gas composition	Input	Influences the end product stoichiometry
7	Deposited power	Input	Governs the conversion
8	Quench gas flow rate	Input	Influences the final granulometry distribution
9	Quench gas composition	Input	Ideally Ar
10	Position of the quench	Input	Influences the final granulometry distribution
11	Flow rate of the precursor	Input	Governs the production rate
12	Injection rate of the precursor	Input	Influences the residence times
13	Mass conversion into nanometric product	Output	Depends on residence times
14	Micrometric powder into the end product	Output	Depends on flow and temperature patterns
15	Specific area of the end product	Output	Depends on quench conditions
16	Stoichiometry of the end product	Output	Depends on gas composition
17	Density of the end product	Output	Depends on gas composition
18	Production rate	Output	Depends on deposited power and gas flow rates

Table 2: Overview of process variables that influence the quality and characteristics of the RF plasma torch.

Based on previous results, on data collected in the literature as well as on standard chemical engineering approaches, we revised the set of process input variables and started-up an experimental program in order to derive at least rough estimations of the effects of these variables on the properties of the end product.

Experimental conditions	Stoichiometry of the end product
Without addition of methane	10 wt. % free Si in excess
With finely tuned flow rate of methane in the carrier gas	Both free C and free Si < 0.6 wt. %

Table 3: Effect of methane addition on the stoichiometry of the end product.

One essential objective was to tune the stoichiometry of the final product. Indeed, when injecting the solid precursor as only chemical species into the plasma, we observed the presence of free silicon into the nano-sized product (Table 3). This was attributed to the decarburization of the silicon carbide according to equation 1:

$$SiC + 2H_2 \leftrightarrow Si + CH_4 \qquad \text{(equation 1)}$$

Note that hydrogen is necessary to maintain the long term stability of the plasma at quasi atmospheric pressure. Therefore, we had to add methane to displace the equilibrium described by equation 1 to the left. However, adding too much methane causes the formation of free carbon, with a dramatic increase of the specific area. One of our tasks consisted in determining the correct methane to SiC ratio at the input to get a well balanced stoichiometry at the output.

In several cases, we observed also the presence of the micrometric precursor into the end product. This was attributed to several input variables among which:

- The mean diameter of the precursor;
- The physical characteristics of the plasma, which depend on the deposited power, but also on all gaseous flow rates and compositions;
- The physicochemical properties of SiC.

A thorough experimental campaign was carried out to optimize the related variables in such a way that:

- The mass conversion of the precursor into nano-sized SiC remained larger than at least 70 %;

- The collection units downward from the reaction zone could selectively isolate the nano-sized product from any non-reacted precursor.

These corrections allowed us to stabilize the specific area of the product. Numerous technical difficulties had also to be solved regarding the possible contamination of the product by oxygen containing species (e.g. air ingress or internal water leaks). Each time oxygen or water entered the system, we got unacceptable amounts of SiO_2 into the final product. The presence of such impurity causes an immediate decrease of the density and has also a bad effect on the specific area as well as on the colour of the product. To avoid such contamination, we carefully limited the deposited power as well as the input flow rate of all reactive species. As a consequence, the production rate is limited to about 150 to 200 $g.day^{-1}$. But another feature limits severely the production rate, namely the direct hydraulic connection existing between the battery of filters and the plasma reactor. This configuration obliges us to interrupt the injection of reactive species during unloading of the filters otherwise the quality of the product is not preserved. Additional efforts will be needed to modify the configuration in such a way that the filter blow back operations can be carried out off line, using e.g. two batteries of filters mounted in parallel.

Property	Average value	Radius of the 95 % confidence interval associated to the average value
Specific area ($m^2.g^{-1}$)	68	4
Density ($g.cm^{-3}$)	3.08	0.03
Mean particle diameter (nm; derived from CPS data)	60	3
Free crystalline Si (wt. %)	< 0.6	not evaluated
Free crystalline C (wt. %)	< 0.6	not evaluated

Table 4: Characteristics of optimized SiC powder batches.

All the corrective actions cited above allowed the production of nano-sized SiC of acceptable quality. The main added value results from the reproducibility of the products' properties as explained below.

By the end of November 2009, 23 batches of nanometric SiC were produced whose properties are listed in Table 4.

Figure 2 illustrates the granulometry distribution as measured by CPS on 11 different batches. All curves show a mono modal distribution with practically zero signatures

above 250 nm. The maxima of all curves are acceptably distributed around 60 nm. Figure 3 demonstrates that the specific area of the product is also reproducible. On this figure, we intentionally show some results obtained in extreme conditions: the low value observed for one production on May 7th is an example of material that still contains the precursor when the process variables are not correctly tuned. Two points (end of May and beginning of July) are shown to illustrate the effect of free carbon resulting from an unbalanced stoichiometry. Correctly tuning the process variables allows obtaining a reproducible specific area as illustrated e.g. by the last three points compared to other results on Figure 3. Figure 4 demonstrates that the density of the product is remarkably constant.

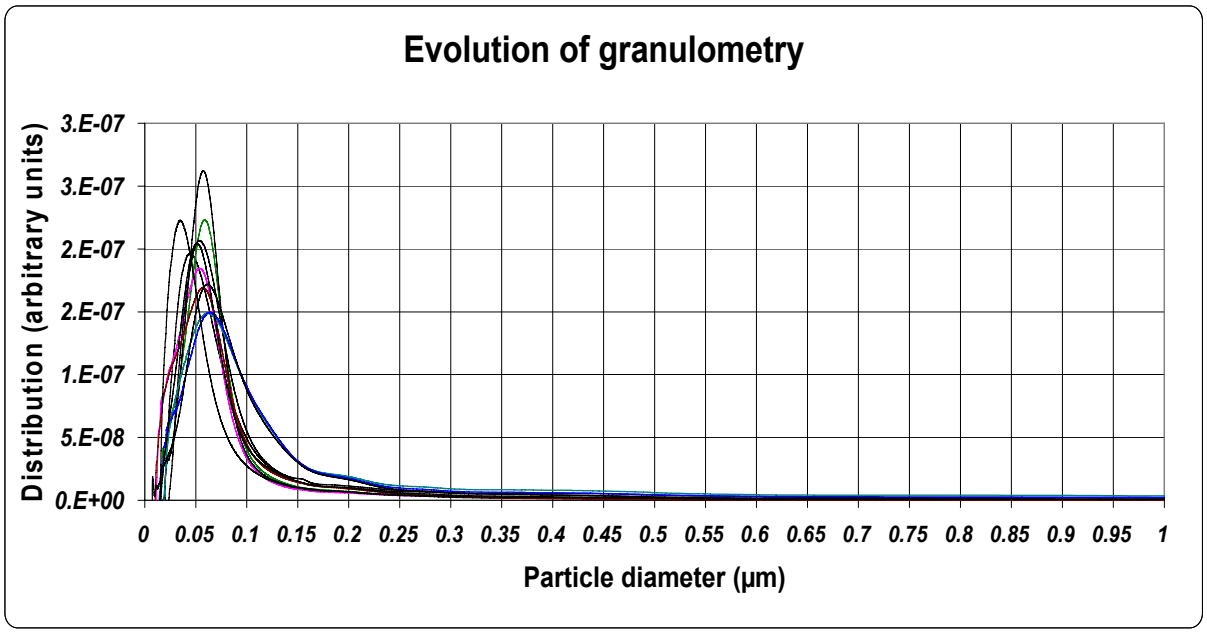

Figure 2: Illustration of the distribution of particle diameters for several successive batches.

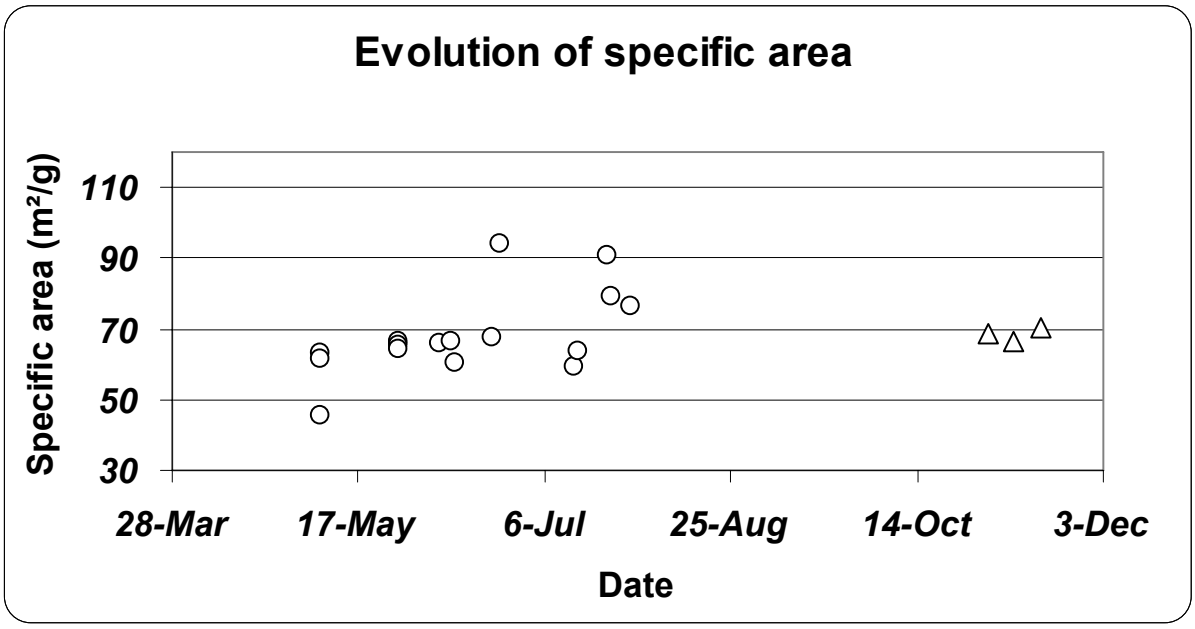

Figure 3: Specific area obtained since May 7th, 2009. The low response on the left corresponds to an experiment where the micrometric precursor could find a hydraulic path besides the plasma due to a badly tuned input process variable. The high responses correspond to experiments where the injection of the micrometric precursor was maintained during the regeneration of the filter unit. This caused the formation of free carbon.

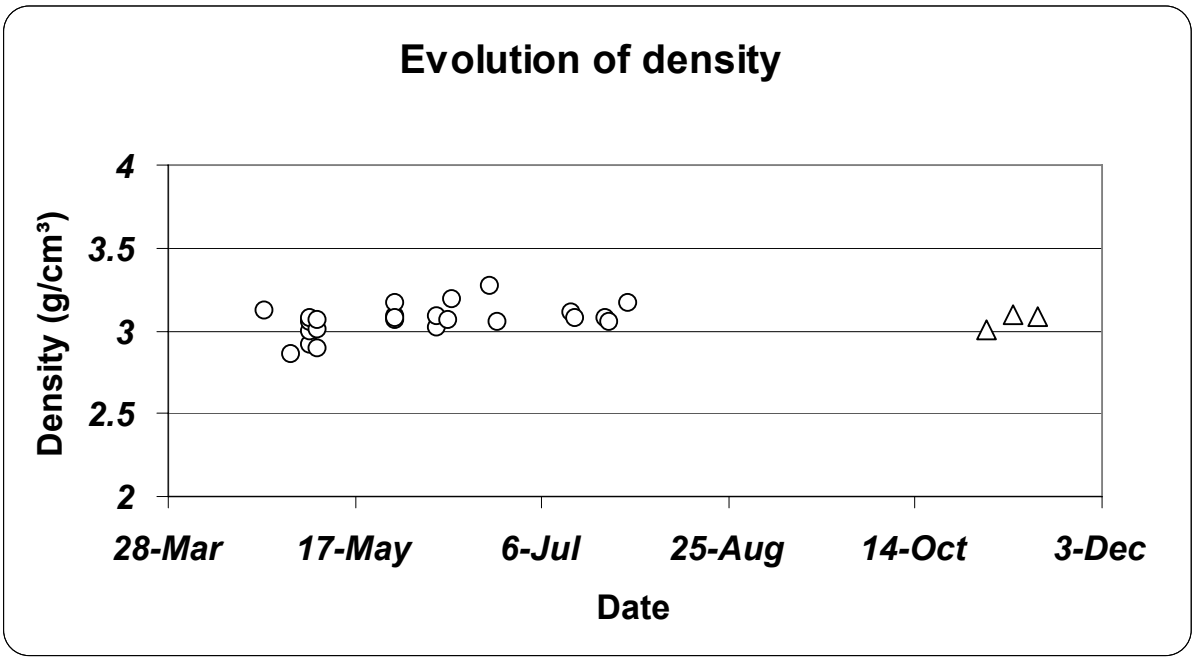

Figure 4: Evolution of the density of the product for several successive batches.

The characteristics of the product are further illustrated by Scanning Electron Microscopy (SEM) pictures.

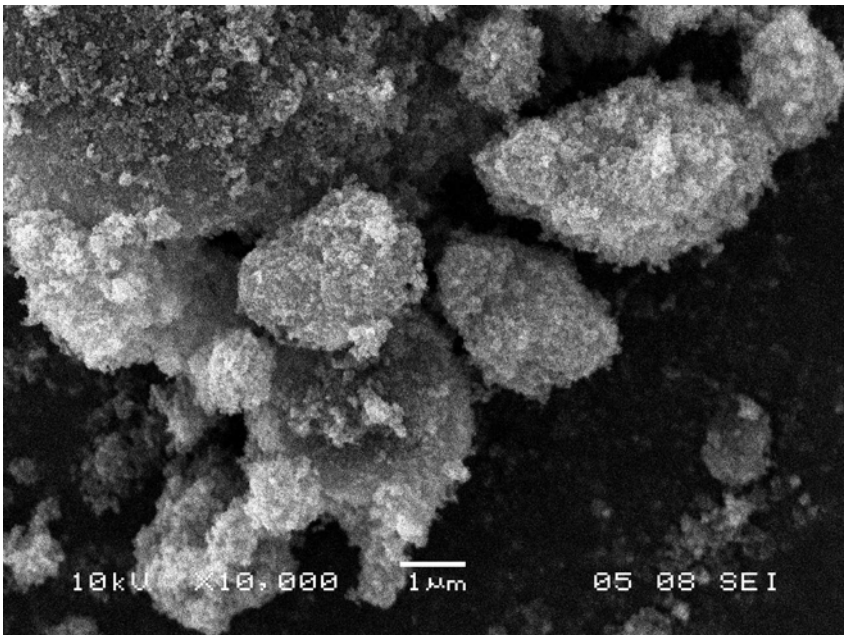

Figure 5: SEM picture of the end product showing agglomerated SiC nanoparticles.

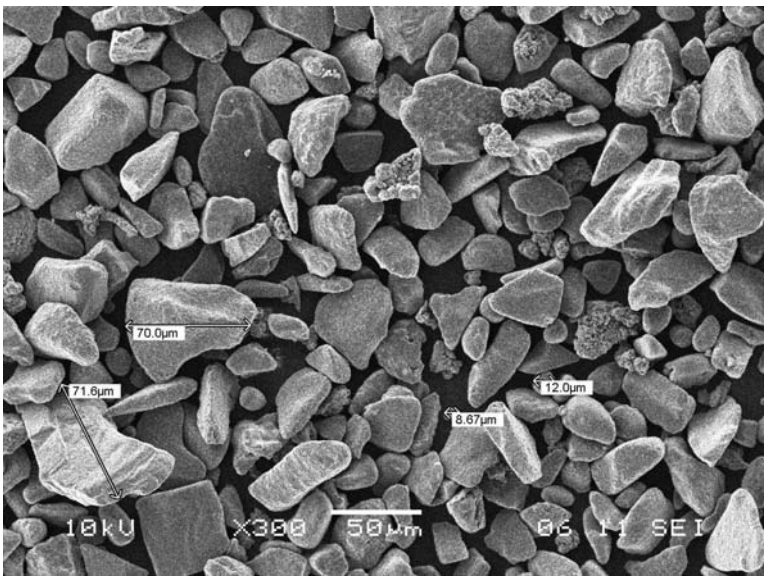

Figure 6: SEM picture of the precursor after separation from the nanopowder. Some agglomerated nano-sized particles can be identified.

Figure 5 illustrates the morphology of the end product. Nanoparticles are clearly agglomerated. Figure 6 depicts the precursor recovered after plasma treatment. The

mass fraction of un-reacted materials is less than 30 wt. % of the total mass injected during treatment.

2.1.2. Characterisation of SiC nanopowders from other sources

X-ray diffraction

The initial SiC batches, forwarded by Sirris were characterised by K.U.Leuven and INISMa using X-ray diffraction and compared with commercially available nanopowders, as shown in Figure 7. The plasma synthesised powder mainly consisted of beta silicon carbide and contained traces of free silicon.

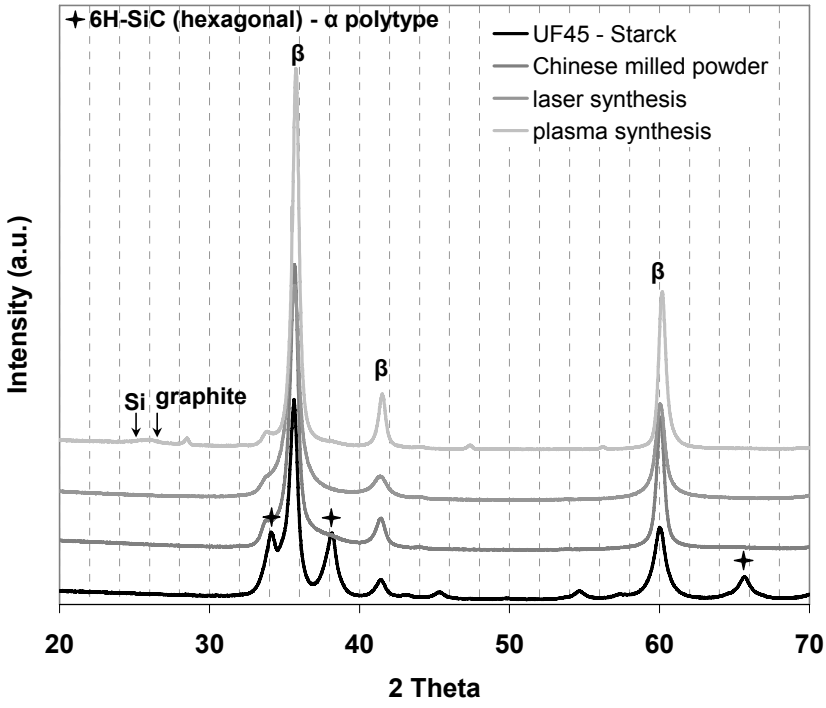

Figure 7: X-ray diffraction patterns of SiC nanopowders obtained from different sources.

Particle size distribution

In view of the oxygen contamination reported by SIRRIS, only the SiC batches obtained from external suppliers have been characterized by INISMa. The particle size distribution of these three nanometric SiC powders coming respectively from China (supposed to be produced by milling), from Latvia (plasma synthesized powder) and from France (CEA – laser synthesis) has been measured by means of the ESA or

attenuation technique, following a protocol established at the beginning of the project using ZnO commercial nanopowder.

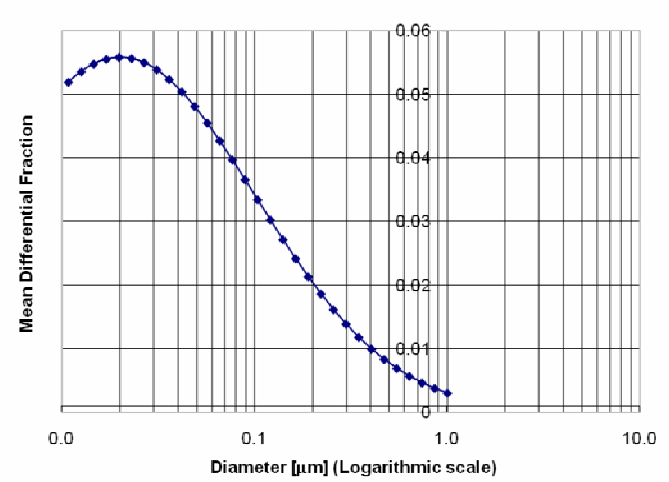

Figure 8: Particle size distribution obtained on the CEA laser synthesized SiC powder.

The powders have been measured as received and no attempt has been made to improve the dispersion behaviour thereof. The obtained average particle size values are respectively :

- Powder from China: d_{50} = 1.26 µm
- Powder from Latvia : d_{50} = 1.06 µm
- Powder from France : d_{50} = 40 nm (Figure 9)

As inferred from those experiments, the two first powders are fairly agglomerated and will need an extra conditioning step before their use. The CEA laser synthesized powder on the contrary shows, in the as received state a correct dispersion behaviour.

Attempt to produce a de-agglomerated suspension from the plasma synthesized powder from Latvia using the MiniCer® nanogrinder equipment available at the INISMa has been envisaged but the amount of powder received did unfortunately not allow to perform this test.

2.2. Densification of silicon carbides

A first batch of silicon carbide powders, SiC-nano 07-06-14/01, obtained from Sirris in 2007 was subjected to a FAST cycle (2100°C, 5 min, 60 MPa). Above 1700°C the material became soft and plastic, as indicated in the densification and degassing curve of this sintering experiment, shown in Figure 9 (a), so that it was extruded out of the

die. This is attributed to a large SiO_2 content in this powder. Remnant SiO_2 was found in the microstructure of the material even if it was densified at 2100°C, as shown in Figure 9 (b). In addition, due to the presence of a large amount of free carbon (C), the material could not be densified completely, as indicated in Figure 9 (b).

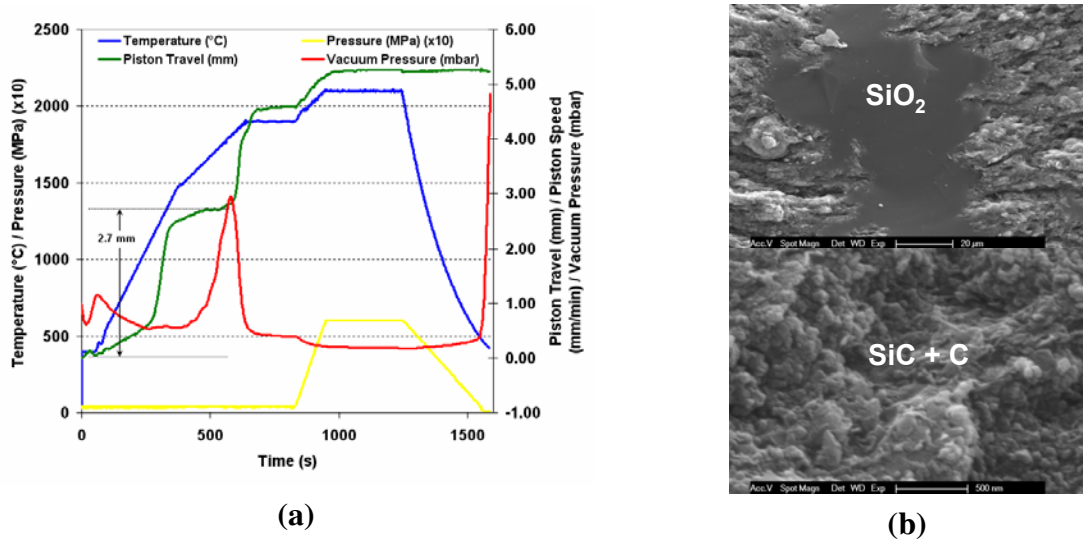

Figure 9: Densification behaviour (a) and secondary electron (SE) micrographs (b) of a Sirris nanopowder compact that was densified by FAST at 2100°C for 5 minutes applying 60 MPa pressure.

Comparative densification experiments were performed using commercial micrometre sized SiC powders, obtained from Superior Graphite. Two grades, undoped as well as B_4C doped batches, were densified using similar sintering conditions as shown in Figure 9 (a). The secondary electron micrographs of the densified materials are shown in Figures 10 (a-b), in case of the undoped and B_4C doped samples, respectively. The undoped sample contains visible porosity and had an overall relative density of 91.9%, while the doped sample was nearly fully dense, reaching a relative density of 98.9%. B_4C doping enhances the densification behaviour, but induces fast grain growth during the latter sintering stage at the same time. Therefore, similar densification experiments should be carried out using SiC nanopowder.

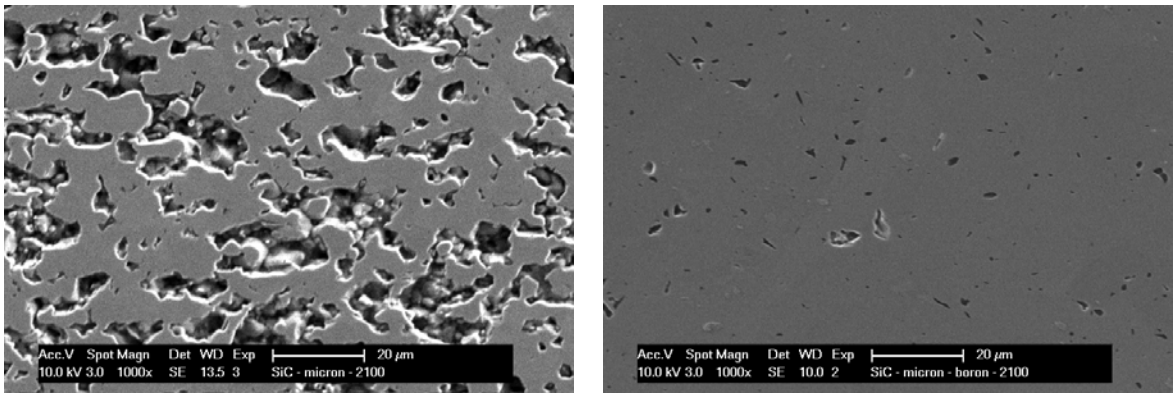

(a) **(b)**

Figure 10: Secondary electron micrographs of undoped (a) and B_4C doped (b) commercial micrometre sized SiC powder (Superior Graphite) that was FAST at 2100°C for 5 minutes applying 60 MPa.

2.3. Conclusions on SiC materials

The main lesson learnt from the R&D activities carried out on the synthesis of plasma powders is that the production of consistent nanopowders (i.e. having reproducible properties) is possible using a RF plasma torch capable of producing at least semi industrial amounts of end product within reasonable run durations. However, tuning the process variables for the sake of doing so requires a careful study of all process related aspects, ranging from the nature of the reactants to the post processing treatment operations, including the various difficult domains relevant to plasma chemistry. The main outcome of this research is the demonstration of the pertinence of chemical engineering tools and reasoning for overall process optimization purposes. Finally, we could also provide nanopowders to our partners, although quite late with respect to the schedule foreseen initially. Sirris believes that each specific nanopowder would require a study similar to the one reported here if they are ever to be produced at industrial scale while maintaining acceptable products' consistency. Further efforts will need to be devoted to the extension of characterization tools and methods as well as to dispersion and functionalisation of nanopowders.

For the densification of silicon carbide nanopowders with FAST an optimization of the additive levels is necessary. Whereas some free carbon is needed for the densification of silicon carbide[6], too much free carbon will prevent full densification.

One of the envisaged applications for SiC suggested by AMOS was lightweight and stiff mirror elements for use in space. This requires a smooth pore free silicon carbide. Pore free silicon carbide can not be obtained by standard hot pressing or pressureless sintering. By FAST experiments at 2100°C encouraging results were

obtained for a micrometre sized powder but some residual porosity remained. Further optimization of the FAST cycle and of the additives level with a nanosized powder could load to the desired result. This was not possible within the context of this project due to the difficulty of obtaining nanosized powders in sufficient quantity within the project duration.

3. Results on alumina

Alumina served as model for the behaviour of an electrically insulating powder in the FAST process. The commercially available ultrafine alumina powder (TM-DAR grade, mean particle size of 170 nm, Taimei Chemicals Co. Ltd, Nagano, Japan) was used throughout this study

3.1. Grinding and dispersion behaviour

Due to their very small size nanosized powders are very susceptible to agglomeration simply due to Van der Waals attraction forces as well as others that may be active between the particles. An effective way to remove this heterogeneity is the colloidal method, in which detrimental inhomogeneities can be removed by sedimentation. Also to obtain the most effective arrangement of particles in a green body, the achievement of complete dispersion of the particles in suspension is important. Hence for a given powder it is important to investigate what the degree of dispersion is that can be achieved. To this end the agglomerated particles need to be broken up into primary particles that were formed in the synthesis process. Once the powder is dispersed in the suspension renewed agglomeration needs to be prevented. This can be accomplished by assuring that the particles acquire an electrical charge so that they repel each other due to the electrostatic interaction. Repulsion can also be achieved by adsorbing on the particle surfaces long chained molecules (steric repulsion) which may also have an electric charge at their end (electro-steric repulsion).

To this end, the grinding and dispersion behaviour of the as-received TM-DAR powder was studied at INISMa using the MiniCer® nanogrinder (Netzsch) and the ACOUSTOSIZER II (Colloidal Dynamics) for determination of the particle size distribution.

Firstly, 10wt% of TM-DAR powder was mixed into distilled water. The zeta potential, pH and grain size distribution were measured directly (time = 0h), then after 1 and 2 hours (Figure 11). Surprisingly, the pH is acidic (around 4.5) and the zeta potential has a positive value. The d_{50} and d_{85} values are in a good agreement with the technical data for the powder. After two hours, the pH, zeta potential, d_{50} and d_{85} stabilized and a potentiometric titration was performed, by addition of KOH, in order to characterize the isoelectric point (IEP) of the powder. The IEP was found at a pH of 8.2 (Figure 11), just below the value currently observed for common alumina powder (~ 8.5).

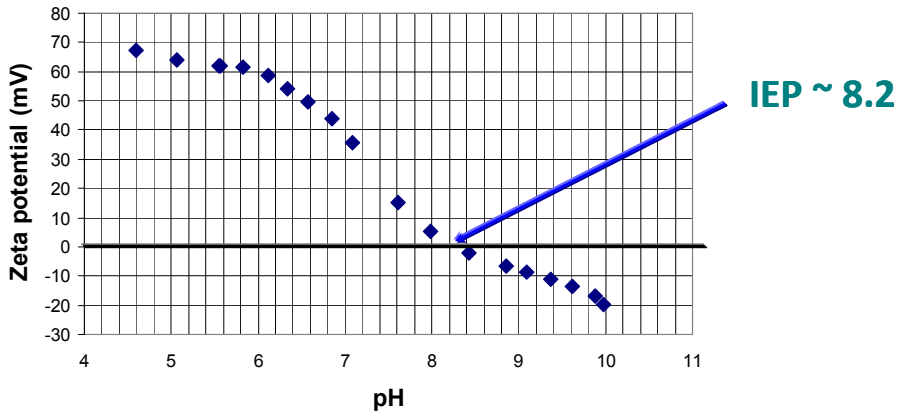

Figure 11: Potentiometric titration of 10wt% TM-DAR alumina powder in distilled water.

A foaming behaviour of a slurry with the same composition was observed after 15 min of slow stirring into the Minicer Grinder with ZrO_2 media (diameter 300 µm). Therefore, 1 µl of TEGO FOAMEX 8050 (antifoaming agent, styrene acrylic) was added to the next slurries in order to avoid bubble formation.

The grinding behaviour of a slurry composed of 10wt% of TM-DAR powder dispersed into distilled water with the addition of antifoaming agent, was studied by analysing the evolution of pH, zeta potential, d_{50} and d_{85}, after being ground at 4000 rpm during 90 minutes into the MiniCer® nanogrinder (in presence of ZrO_2 media).

- The pH reached a value around 8.8.
- The zeta potential decreased continuously till a negative value of -12 mV.
- The d_{50} and d_{85} remained constant (respectively 0.11 and 1 µm).

The slurry was stirred slowly over night and analysed in the next morning with the Acoustosizer system:

- The pH stayed at a constant value, around 8.7, a common value for alumina powder;
- The zeta potential decreased to -24 mV;
- The d_{50} was constant (0.10 µm).

But the d_{85} reached 3 µm, meaning that the slow stirring induced an agglomeration of the powder.

Then, the slurry was titrated by addition of volume of diluted dispersant (Dolapix CE 64), as shown in Figure 12.

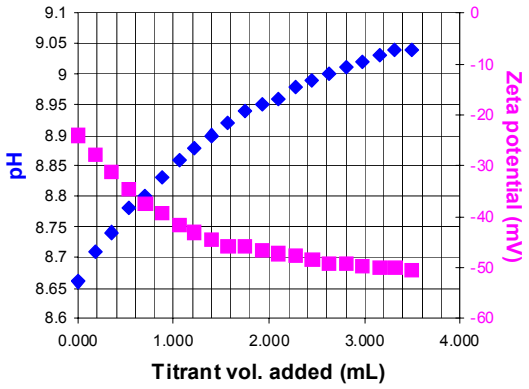

Figure 12: ***pH and zeta potential during titration of a slurry containing 10wt% TM-DAR, by addition of diluted Dolapix CE 64.***

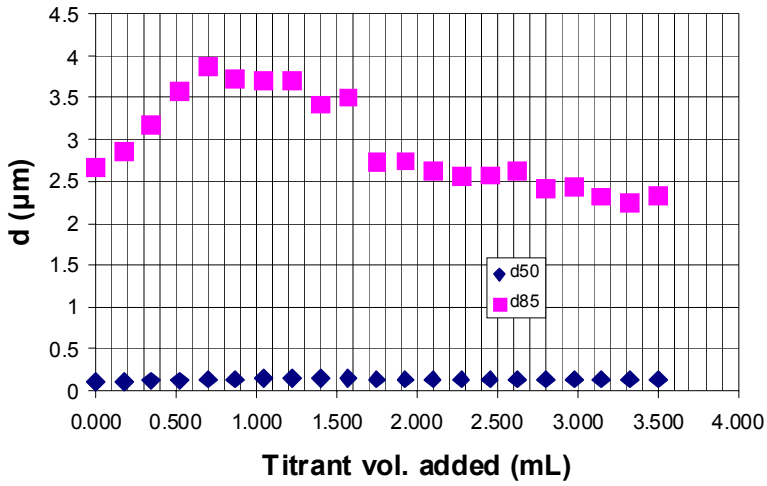

Figure 13: ***d_{50} and d_{85} during titration of a slurry containing 10wt% TM-DAR, by addition of diluted Dolapix CE 64.***

After addition of 2wt% of Dolapix, the pH increased from 8.65 to 9.05, as the zeta potential reached -50 mV, value currently observed when using this kind of dispersant.

The d_{50} parameter was not influenced by the dispersant. As far as the d_{85} was concerned, its value began to increase to a maximum of 4 µm, before a continuous decrease to around 2 µm (Figure 13).

After stirring overnight, the following parameters were measured in the next morning:

- Constant values of pH (~ 8.9), zeta potential (~ -50 mV) and d_{50} (~ 0.10 µm);
- The d_{85} decreased to ~ 0.80 µm.

In conclusion it can be stated that the first values of pH and zeta potential registered on the slurry composed with 10wt% of as-received TM-DAR alumina powder were found to

be different compared with currently observed values for common alumina powders. This might indicate that the powder contained organic surface groups. Furthermore, a foaming behaviour was observed after slow stirring into the MiniCer® nanogrinder.

After grinding at 4000 rpm in presence of zirconia media, the pH increased to recover a more “normal” value (between 8 and 9). Thanks to stirring, these unknown organics should be separated from the grain powder, leaving “new free surfaces” resulting in this increase of pH. After slow stirring over night, the d_{85} increased largely to more than 3 µm, due to an agglomeration of the powder. The addition of 2% of a dispersant (namely Dolapix CE 64) induced a defloculation of the powder thanks to a slow stirring over night.

3.2. Densification studies on Al_2O_3

The commercially available ultrafine TM-DAR alumina powder has been used to evaluate the densification kinetics under different conditions of pressures (8, 16 and 32 MPa), heating rates (50, 150 and 250°C), dwell temperatures (1200, 1250 and 1300°C) as well as dwell duration (between 0 and 6 minutes). The powder was pre-compacted in the graphite die (30 mm inner diameter) prior to heat treatment in order to limit grain rearrangement during the first part of the heating cycle. The load was applied from the start and kept constant throughout the thermal cycle.

The density, elastic modulus and thermal diffusivity of all samples was measured and compared with theoretical models, taking into account the grain size as well as the amount of porosity in the partially sintered samples. The main results are summarised hereafter.

3.2.1. Densification behaviour

The relative density values achieved are reported in Table 5 below, as a function of the sintering conditions.

As could be expected, the higher the temperature and/or the applied load, the higher the density. The effect of the heating rate if any is less clear; replication of some tests will be needed before clearly stating whether the observed differences are significant.

Using the recorded axial displacement of the plunger during the FAST runs, the continuous evolution of density with time has been calculated for the different conditions investigated. Figure 14 below shows representative evolution of density.

Analysis of the data has revealed that under some conditions, “large” temperature overshoots have taken place; resulting in fluctuating temperature profiles that can be observed on some densification curves during the dwell period. We have also observed that for the lowest applied load (8 MPa), all the specimens present a systematic radial shrinkage of a few percent. This precludes the use of the sole axial displacement of the plunger to derive the evolution of the density during the thermal cycle and additional assumptions need to be made. This being said, it is worth stressing that under the tested conditions in FAST the lower the heating rate, the higher the density achieved at the end of the heating ramp but that despite this non negligible difference in density, the compacts reach about the same densities at the end of the two minutes dwell.

Relative density (%)									
Temperature / Dwell	Applied Load (MPa)								
	8			16			32		
	Heating rates (K/min)								
	50	150	250	50	150	250	50	150	250
1200 °C 0 min	-	-	-	73	71	71	-	-	-
1200 °C 2 min	67	64	68	79	79	77	91	95°	90
1250 °C 0 min	-	-	-	94	85°	79	99	94	88
1250 °C 6 min	-	-	-	97	97	92	99	97	98
1300 °C 0 min	-	-	-	86	85	82	98	95	91
1300 °C 2 min	84	91	80	92	95	96	97	96	96

°average of two tests

Table 5: Relative density values of densified TM-DAR alumina.

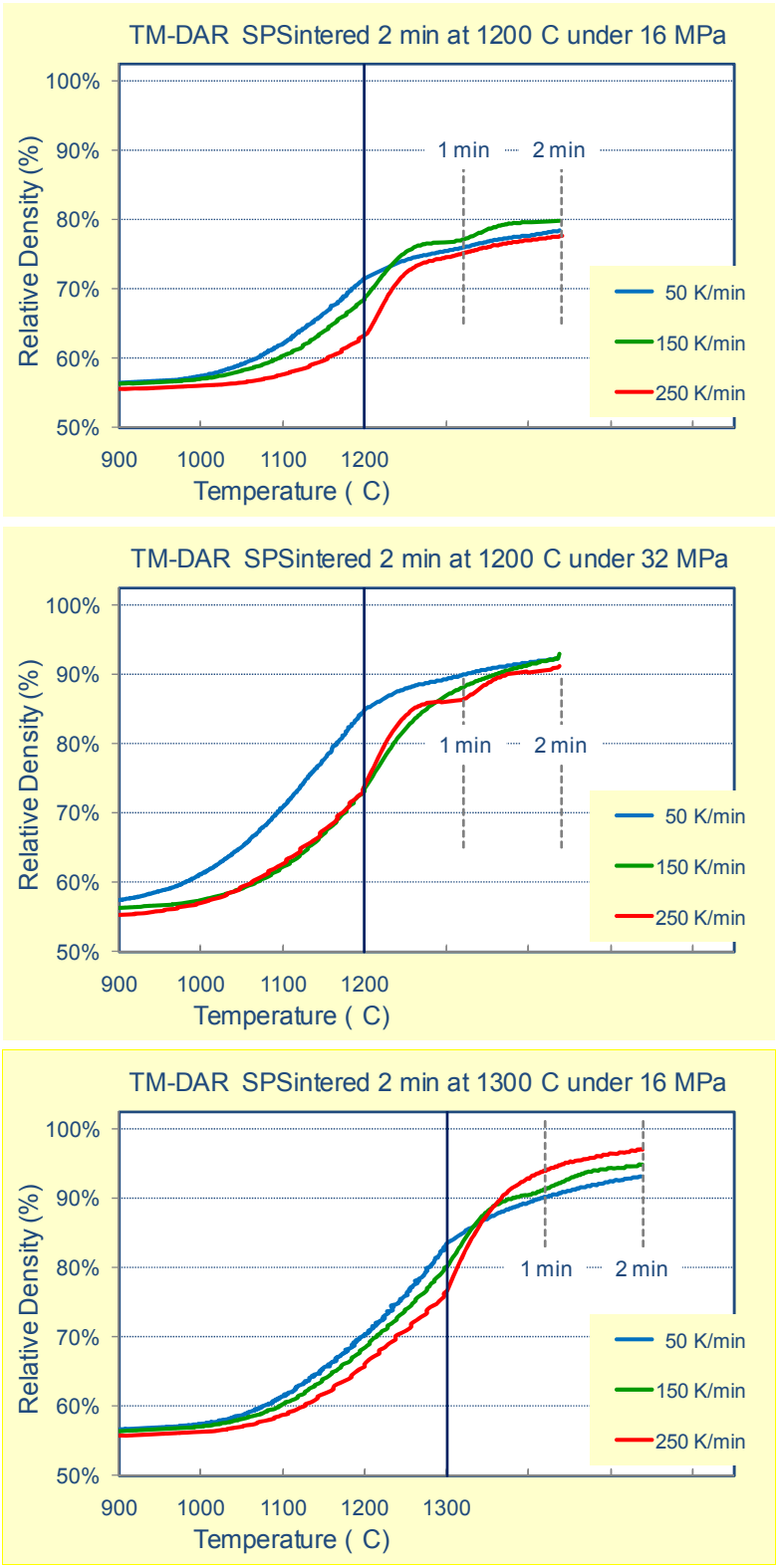

Figure 14: Evolution of relative density with time and temperature for FAST sintering runs a) 1200°C – 16 MPa, b) 1200°C – 32 MPa, c) 1300°C – 16 MPa.

3.2.2. Microstructural development

In parallel the detailed microstructural characterisation of the sintered specimens has been carried out. It is indeed of paramount importance in view of the objective of the project (development of nanoceramics) to assess the sintering trajectory (mean grain size vs. relative density) and its dependence on the operating conditions.

As will be obvious from what follows, the knowledge of the average grain size of the individual specimens is also needed to interpret and to model properly the thermal characteristics of dense and partially sintered nanomaterials. Figure 15 below shows the secondary electron micrograph of two Al_2O_3 TM-DAR samples sintered at 1200 and 1300°C applying a heating rate of 250°C/min and a pressure of 8 MPa.

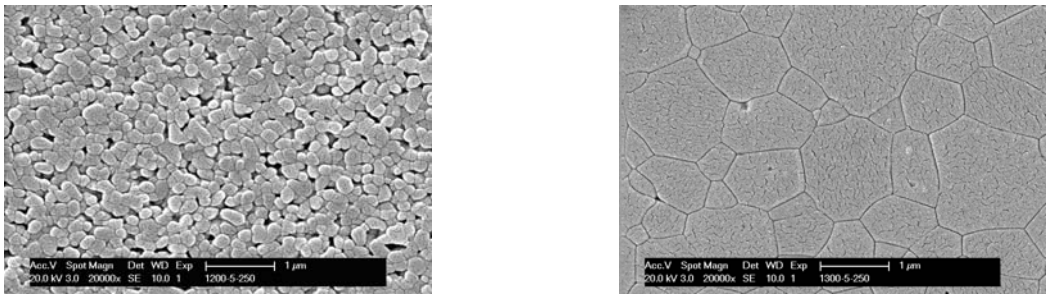

(a) **(b)**

Figure 15: Secondary electron micrograph of two Al_2O_3 TM-DAR samples sintered at (a) 1200 and (b) 1300°C applying a heating rate of 250°C/min and a pressure of 8 MPa.

3.2.3. Elastic properties

The FAST sintered TM-DAR alumina samples have, as mentioned before, been characterized in terms of elastic properties. This has been done using the impulse excitation technique on the disk shaped specimens. The obtained values are summarized as a function of sintering conditions in Table 6 below and represented as function of the porosity in Figure 16.

As could be anticipated, the elastic properties are primarily dictated by the density of the samples. Even if for similar density values, an effect of the sintering parameters (heating rate, applied load, ...) cannot be excluded, it is clear that it would be marginal. In the range investigated, the Young's modulus appears linearly dependent on the residual porosity in the sample, leading to a theoretical value of 402 GPa for fully dense alumina (Figure 16).

Elastic properties – E (GPa) / G (GPa) / Poisson's coefficient*									
Temperature / Dwell	Applied Load (MPa)								
	8			16			32		
	Heating rates (K/min)								
	50	150	250	50	150	250	50	150	250
1200 °C 0 min	-	-	-	-	131 86 0.21	130 54 0.21	-	-	-
1200 °C 2 min	99 42 0.17	98 41 0.20	112 47 0.21	200 82 0.22	209 86 0.21	170 70 0.20	-	351 141 0.24	-
1250 °C 0 min	-	-	-	351 142 0.24	251 102 0.23	196 80 0.22	391 157 0.25	342 138 0.24	303 123 0.23
1250 °C 6 min	-	-	-	387 155 0.25	371 149 0.24	324 131 0.24	394 158 0.25	377 152 0.24	384 154 0.24
1300 °C 0 min	-	-	-	260 106 0.23	250 102 0.23	223 91 0.23	394 158 0.25	339 136 0.24	305 123 0.24
1300 °C 2 min	252 103 0.22	313 127 0.23	202 83 0.21	355 143 0.24	353 143 0.24	385 155 0.25	-	377 152 0.24	378 153 0.24

* For each densification condition the first line gives the tensile E-modulus (GPa), the second line the shear modulus G (GPa) and the third line the Poisson ratio.

Table 6: Elastic properties of FAST densified TM-DAR alumina.

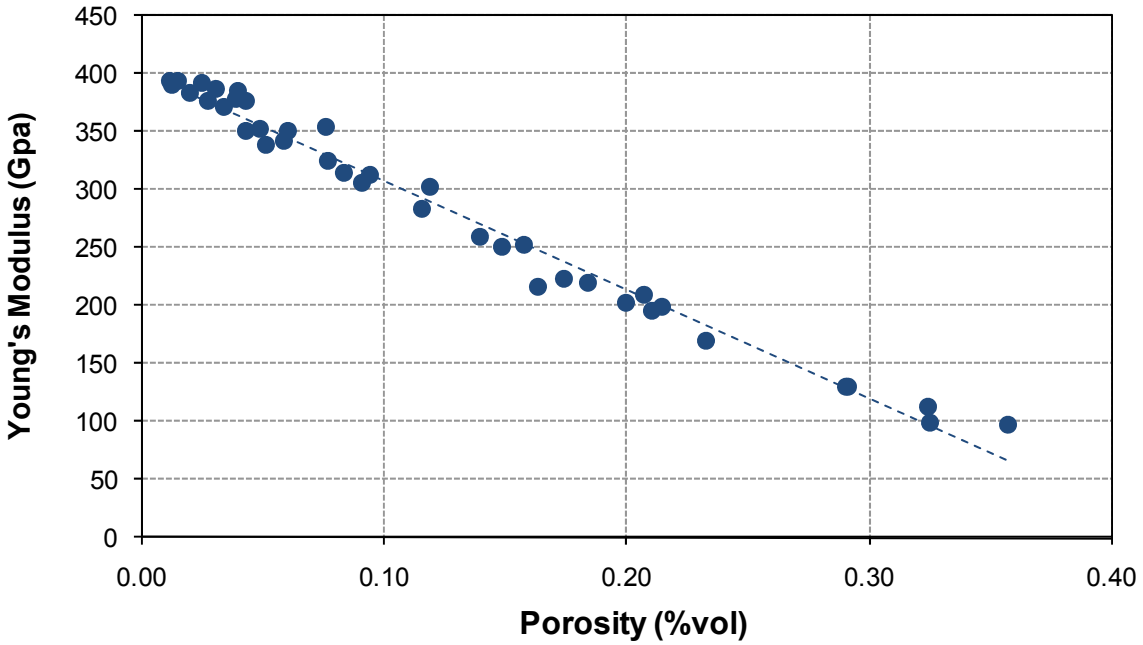

Figure 16: Young's modulus of partially sintered Al_2O_3 TM-DAR samples, densified by FAST, as function of their porosity content.

3.2.4. Thermal properties

The thermal conductivities of the (partially) densified Al_2O_3 TM-DAR samples, were evaluated by measurement of their thermal diffusivities using a Flashline 3000 system (Anter Corporation, Pittsburgh, PA) equipped with a HSXD (High Speed Xenon Discharge) pulse source to heat the bottom face of the disk-shaped samples.

The transient top-face temperature was monitored using a liquid-nitrogen-cooled InSb infrared detector. The 30 mm diameter samples were machined to 3 mm in thickness. In order to obtain reproducible values, a coating of Platinum and Graphite had to be applied on both faces of the specimens. The measurements were made under flowing Argon. Software incorporating the Clark and Taylor approximations was used to determine the thermal diffusivity of each sample. The diffusivity of most Al_2O_3 samples was evaluated in the 20°C - 500°C temperature range.

Representative thermal diffusivity data are presented in Figure 17 below.

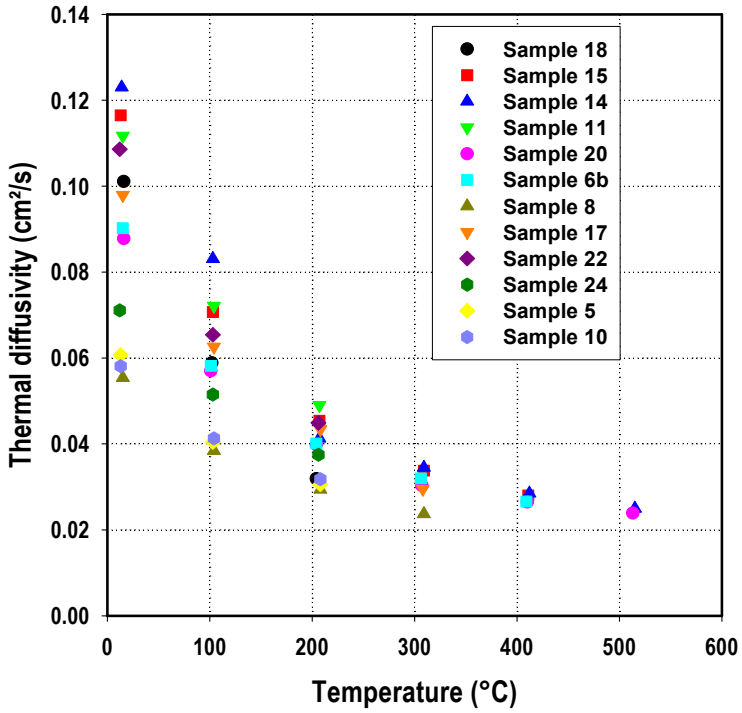

Figure 17: Evolution of thermal diffusivity with temperature of representative partially sintered Al_2O_3 TM-DAR samples, densified by FAST.

The specific heat of alumina at the corresponding temperatures has been theoretically calculated using the following equation:

$$C_p = a + b \cdot 10^{-3} \times T + c \cdot 10^{-6} \times T^2 + d \cdot 10^{5} \times T^{-2} \text{ en J/kg K} \qquad \text{(Equation 2)}$$

with a=756.0, b=992.6, c=-531.3 and d=-202.0

This equation has been obtained by least square fitting of a range of published data, as illustrated in Figure 18.

The thermal conductivity values for the TM-DAR alumina samples were then obtained by combining the measured diffusivity values, the calculated heat capacity values and their corresponding density values. The resulting evolution of the thermal conductivities with temperature is in fairly good agreement with the generally accepted dependence on T^{-1} (when T is expressed in Kelvin).

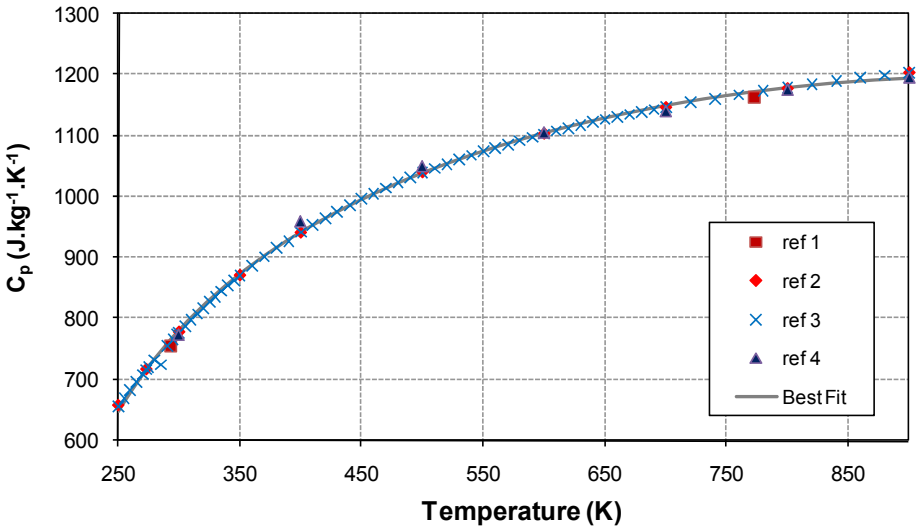

Figure 18: ***Literature based heat capacity data for alumina and best fit curve. For references see [7].***

In Figure 19 below, these thermal conductivity values are represented as a function of the porosity content of the samples and compared with theoretical values calculated according to the Effective Medium Percolation Theory (EMPT) model most commonly used for the prediction of the thermal properties of heterogeneous materials[8]. This model has been identified through a detailed bibliographical study carried out in the framework of this project.

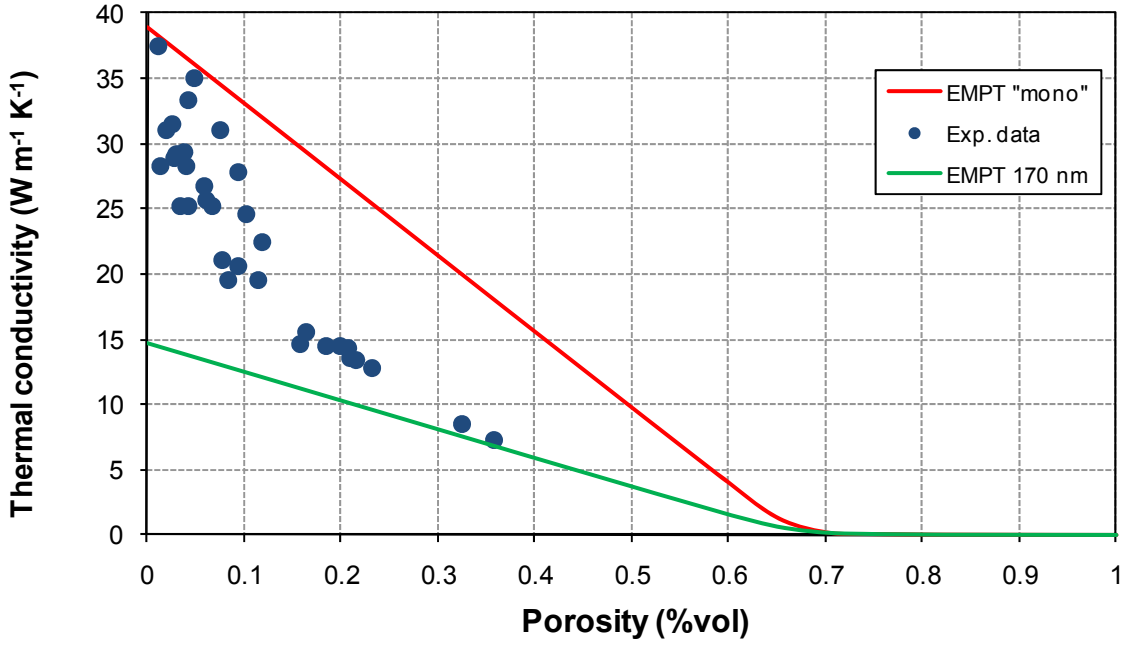

Figure 19: ***Experimentally determined thermal conductivity of FAST sintered TM-DAR alumina samples; the data are compared with the predictions from the Effective Medium Percolation Theory model using λ=14.8 and 39 W.m^{-1}.K^{-1} for alumina and λ =0.026 W.m^{-1}.K^{-1} for air.***

A significant discrepancy is observed between the theoretical predictions and the experimental data when using a thermal conductivity value of λ=39 $W.m^{-1}.K^{-1}$ corresponding to the generally admitted intrinsic thermal conductivity of dense alumina at room temperature. This discrepancy arises most probably from the fact that the contribution of the grain boundary thermal resistance is neglected whereas it has been shown that it significantly affects the overall thermal behaviour of the material when the average grain size is below typically a couple of micrometres. Assuming a grain boundary thermal resistance value of 10^{-8} $m^2.K.W^{-1}$ and taking as mean grain size the average grain size of the starting powder (170 nm), a thermal conductivity value of λ=14.8 $W.m^{-1}.K^{-1}$ is calculated for a corresponding fine-grained dense alumina. Using this last value as input in the EMPT model, the lower curve shown in Figure 19 is obtained, showing a better agreement with the lower density samples.

Accordingly, the observed behaviour of the FAST sintered TM-DAR specimens reflects the progressive coarsening of the structure as densification proceeds. Indeed, generally, densification and grain growth occur simultaneously, leading to a denser and coarser microstructure, respectively. Since both pores and grain boundaries act as barriers for phonon transport, the thermal conductivity increases with increasing density and grain size. The transition from open (relative density < 0.9) towards closed (relative density > 0.9) porosity is accompanied by a coarsening of the microstructure (Figure 15), resulting in fast increasing thermal conductivity values as observed here.

3.3. Conclusions Alumina

Well dispersed and a stable suspension could be obtained from the commercial TM-DAR powder by the use of the MiniCer® nanogrinder (Netzsch).

In order to gain insights into the operating densification mechanisms during the FAST process a series of experiments was carried out varying the pressures, heating rates, dwell temperatures as well as dwell duration. The data are still being analysed and in particular more detailed microstructural data are needed for the further elucidation. However it is clear that as the density of the alumina increases the grains also grow significantly. Further work is also in progress to compare density and microstructural evolution during FAST with the hot pressing technique.

The elastic properties of the aluminas depended primarily on the density of the samples. Other parameters do not have a discernible influence.

Particular attention has been paid to the modelling of the thermal conductivity as function of porosity and grains size. From an extensive literature study the Effective Medium Percolation Theory (EMPT) model appeared to be most appropriate. In order to match data on porous and very fine grained materials it is necessary to take into account the thermal resistivity of the grain boundaries.

4. Results on Al_2O_3-WC composites

At K.U.Leuven, Al_2O_3–WC composites were made from Al_2O_3 (TM-DAR, 0.2 μm, Taimei Chemicals Co. Ltd, Nagano, Japan) and WC (CRC-015, 0.15 μm, Wolfram Bergbau und Hütten GmbH, Austria) powders.

Different Al_2O_3-WC materials with varying WC content were processed by means of FAST. The WC content was varied between 0 and 80 vol% in order to be able to determine in which region percolation takes place. Representative microstructures of the different materials are shown in Figure 20. Materials with a WC content ≤ 40 vol% could be densified at 1450°C, while a temperature of 1650°C was needed for composites with larger WC content. In the absence of WC particles, Al_2O_3 grain growth occurs very fast, as confirmed by the microstructures of pure Al_2O_3 at 1250 and 1450°C. The presence of WC, however, inhibits the Al_2O_3 grain growth, hereby improving the mechanical properties of the composite materials as compared to monolithic Al_2O_3. The 3-point bending strength of the Al_2O_3-WC (60/40) material reached a value of 1187 +/- 117 MPa, as compared to 530 and 622 MPa, for the Al_2O_3 materials sintered at 1250 and 1450°C, respectively. The Vickers hardness and fracture toughness of the different materials is summarised in Figure 21 (a), while the electrical conductivity is logarithmically plotted in Figure 21 (b). Both the Vickers hardness and the fracture toughness increase with increasing WC content. Percolation takes place between 30 and 40 vol% of secondary phase particles.

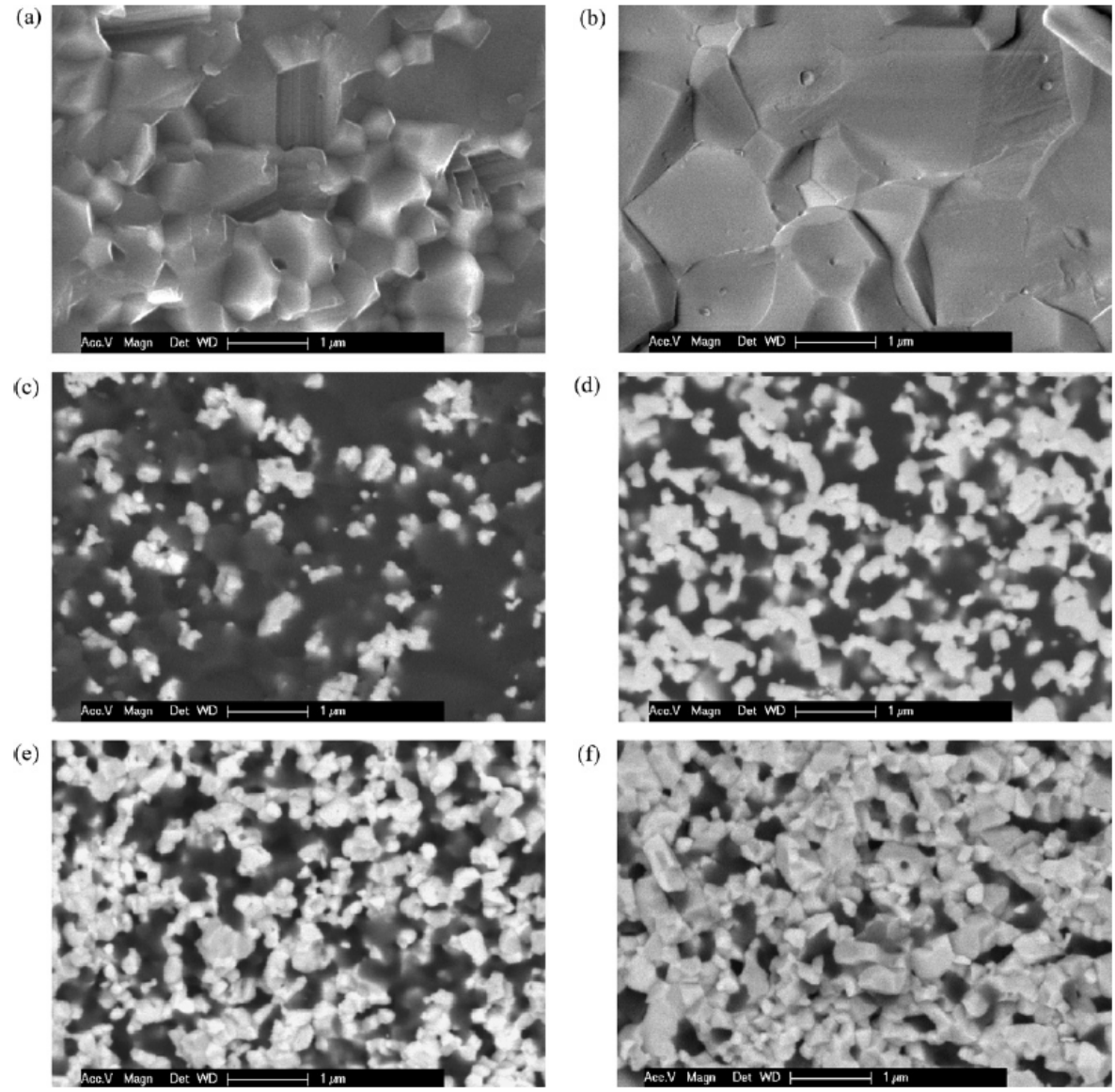

Figure 20: ***Representative back-scattered electron images of the different Al_2O_3-WC materials with different WC content: (a) 0 vol% - 1250°C, (b) 0 vol% - 1450°C, (c) 20 vol%, (d) 40 vol%, (e) 60 vol%, and (f) 80 vol%.***

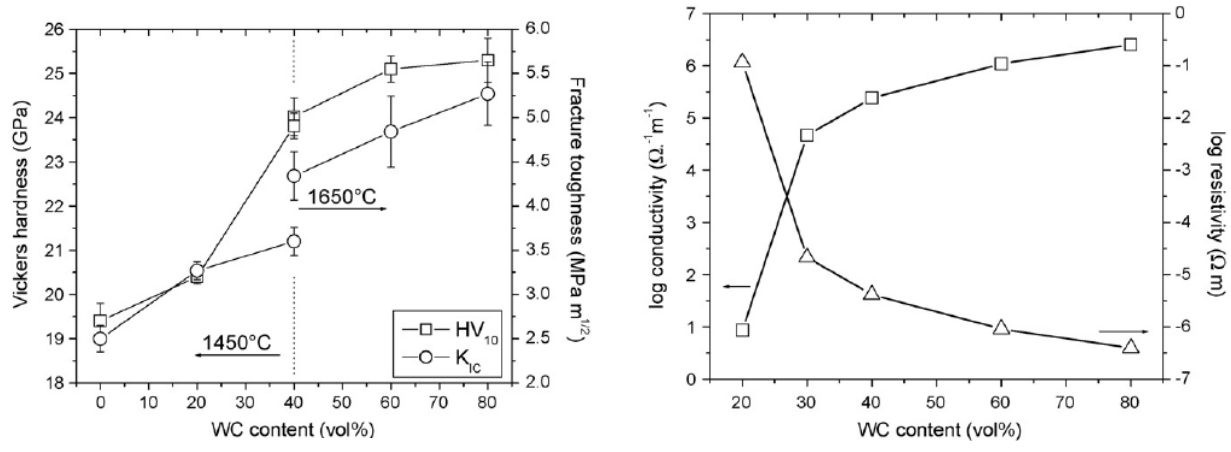

(a) **(b)**

Figure 21: ***Vickers hardness, fracture toughness (a) and electrical conductivity (b) of the different Al_2O_3-WC materials as function of their WC content.***

Conclusions Alumina-WC composites

Al_2O_3–WC composite powders with up to 80 vol% WC could be fully densified by means of pulsed electric current sintering within 4 min in the 1250–1750 °C range under a pressure of 60 MPa. The higher the WC content, the higher the sintering temperature needed to achieve fully dense composites.

The dispersion of 20–60 vol% WC grains significantly suppressed Al_2O_3 grain growth, resulting in ultrafine grained composites with high stiffness. The hardness of the Al_2O_3–WC composites linearly increased from 20.0 GPa for pure Al_2O_3 to 24.0 GPa for the 40 vol% and 25.1 GPa for the 60 vol% WC composites.

The FAST sintered Al_2O_3–WC composites with 40 or 60 vol% WC combine an excellent hardness of 24 GPa or higher with a quite acceptable fracture toughness of 4 $MPa.m^{1/2}$ or higher and a high flexural strength in the range 1000–1200 MPa. The electrical conductivity of these composites is high enough for the materials to be suitable for electrical discharging machining.

5. Results for zirconia based materials

5.1. Characterisation of zirconia powders

In the framework of a case study, unstabilised zirconia powder, was forwarded by Umicore to K.U.Leuven for characterisation. The powder was characterised using X-ray diffraction and compared with commercially available unstabilised as well as 3Y-stabilised zirconia nanopowders, as shown in Figure 22. Although no stabiliser was present in the Umicore powder, it mainly consisted of tetragonal zirconia grains, indicating that the average grain size was very small, so that the tetragonal phase became metastable even without the presence of stabilising cations such as Y^{3+} or Ce^{4+}.

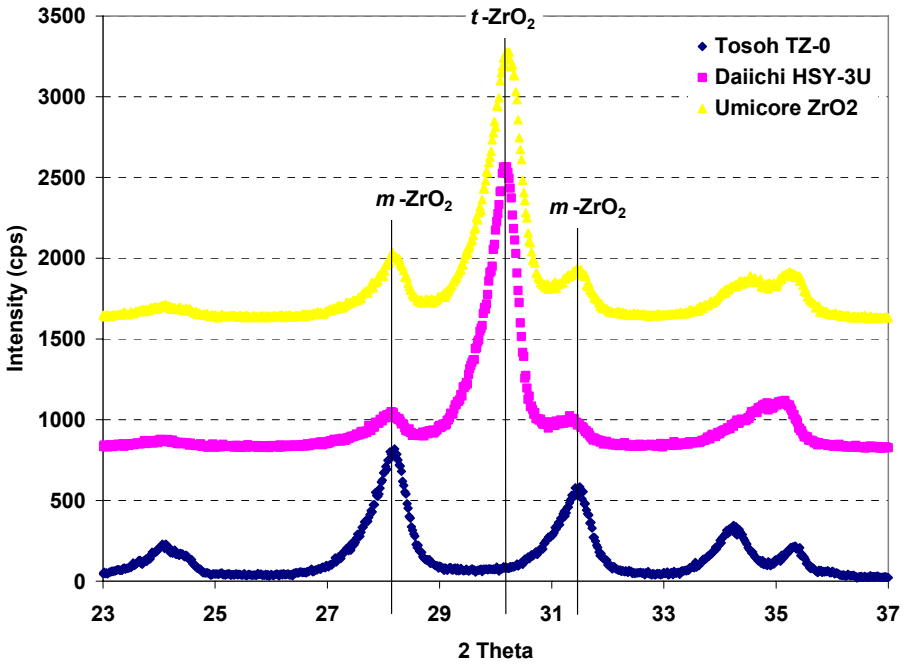

Figure 22: ***X-ray diffraction patterns of unstabilised ZrO_2 powder, supplied by Umicore, as well as commercial unstabilised (Tosoh TZ-0) and 3 mol% yttria stabilised (Daiichi HSY-3U) zirconia powders.***

As a prelude for the preparation of suspensions from a stabilised 3Y-ZrO_2 powder, its charging behaviour was characterised. The iso-electric point of this commercial powder and its zeta potential was measured in water using 0.1N HNO_3 and 0.1N KOH as titration agents, as shown in Figure 23.

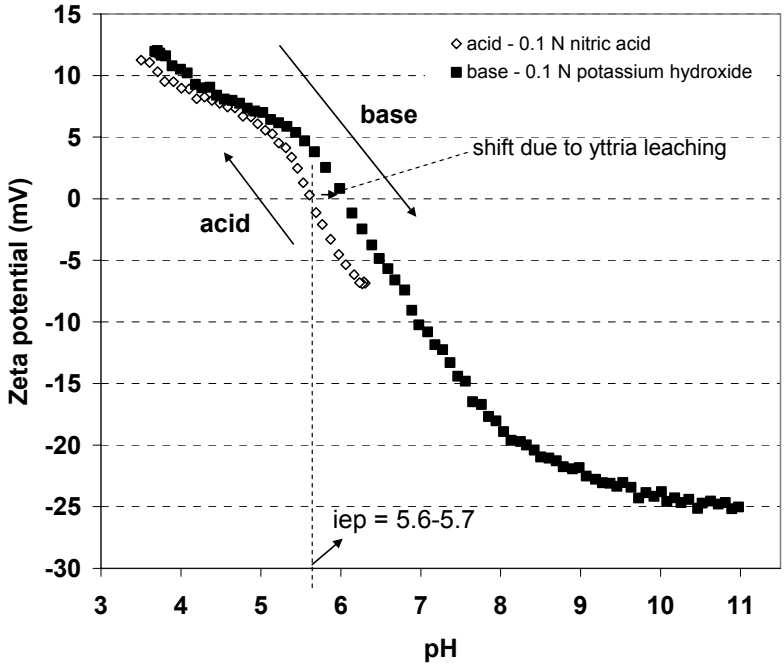

Figure 23: Zeta potential measurement and isoelectric point determination of commercially available 3Y-ZrO_2 nanopowder. A 20 wt% solids concentration was used. The titration was performed using 0.1N HNO_3 and KOH additives. KCl was used as background electrolyte.

5.2. Y-ZrO2 based ceramic composites

Y-ZrO_2 based ceramic composites containing either 30 vol% of an electrically insulating Al_2O_3 secondary phase or 40 vol% of an electrically conductive carbide (WC, TiC), nitride (TiN) or carbonitride ($TiC_{0.5}N_{0.5}$) phase were developed by means of FAST. Different stabilisers, stabiliser contents, ways of introducing the stabiliser and mixing techniques were applied, while the sintering temperature was varied. The most outstanding results are summarised below; first, the ZrO_2-Al_2O_3 (70/30) (vol%) are discussed followed by the ZrO_2-TiCN (60/40) (vol%) and ZrO_2-WC (60/40) (vol%) composite materials.

5.2.1. ZrO_2-Al_2O_3 (70/30) (vol%)

Throughout all experiments 2 mol% yttria stabiliser was used in the Y-ZrO_2 matrix, unless mentioned differently. The stabiliser was introduced either by a) mixing 3 mol% Y-TZP and unstabilised *m*-ZrO_2 powder or b) coating *m*-ZrO_2 powder with the appropriate amount of Y_2O_3 using a coating technique and a calcination step at 800°C. Figure 24 gives an overview of different ZrO_2-Al_2O_3 (70/30) (vol%) materials

that were densified at different temperatures, using different dwell times. Coated Umicore powder was used as the 2Y-ZrO_2 matrix powder.

The fracture toughness of the ZrO_2-Al_2O_3 composites was mainly dependent on a) the Y-ZrO_2 grain size, which was directly influenced by the temperature and the stabiliser content, b) the type and c) amount of stabiliser. Increasing temperatures and decreasing stabiliser contents (3→ 2.5 → 2Y) resulted in increased Y-ZrO_2 transformability. A fracture toughness value up to 6 MPa.$m^{1/2}$ were obtained.

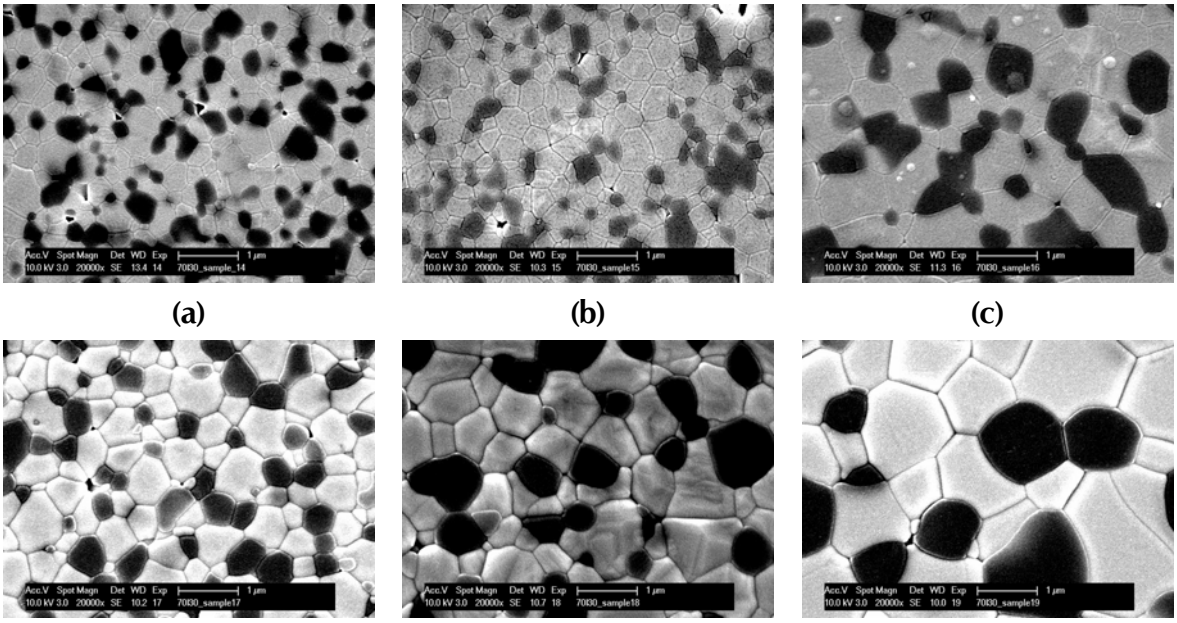

Figure 24: ***Secondary electron (SE) micrographs of ZrO_2-Al_2O_3 (70/30) (vol%) composites densified using FAST. The dwell time at 1450°C was varied between 2, 10 and 60 minutes (a-c), while the temperature was varied between 1550, 1600 and 1650°C (d-f), at 10' dwell time. The pressure was fixed at 60 MPa.***

5.2.2. ZrO_2-$TiC_{0.5}N_{0.5}$ (60/40) (vol%)

Different ZrO_2-$TiC_{0.5}N_{0.5}$ (60/40) composites prepared with different zirconia stabilisers, TiCN grain sizes, using different mixing/milling as well as densification (FAST vs HP) techniques, were prepared. Representative microstructures of FAST densified materials are shown in Figure 25 (a). Bead milling proved to be a suitable technique to a) homogeneously disperse nanometre sized TiCN particles in the Y-ZrO_2 matrix and b) break up micrometre sized TiCN particles into submicrometre sized particles.

With respect to zirconia stabilisers: 1Y2Nd-ZrO_2 matrices were tougher compared to 3Y-ZrO_2 matrices with toughness values up to 9 MPa.$m^{1/2}$.

Clear differences were observed when different starting powders as well as densification techniques were used. Generally, the mechanical properties of the processed composite materials decreased with decreasing TiCN grain size. A similar observation was done for the electrical conductivity. Neutron diffraction experiments revealed that the size of the Y-ZrO_2 unit cell was decreased more significantly when a) nanometre sized TiCN powder was used instead of micrometre sized TiCN powder and b) FAST was used instead of HP. This was attributed to a partial dissolution of TiCN in Y-ZrO_2, hereby inducing an inwards Ti^{4+} diffusion into the Y-ZrO_2 unit cell. The unit cell dimensions of the different materials are shown in Figure 25 (b).

5.2.3. Thermal properties of ZrO_2-TiN ceramic composites

Analytical models

Based on an exhaustive review of the literature, analytical models most currently used for the prediction of the properties of heterogeneous materials had been identified. Ab initio comparison of these was carried out for the compositions studied in this project, using thermal characteristics values reported in the literature for the pure components.

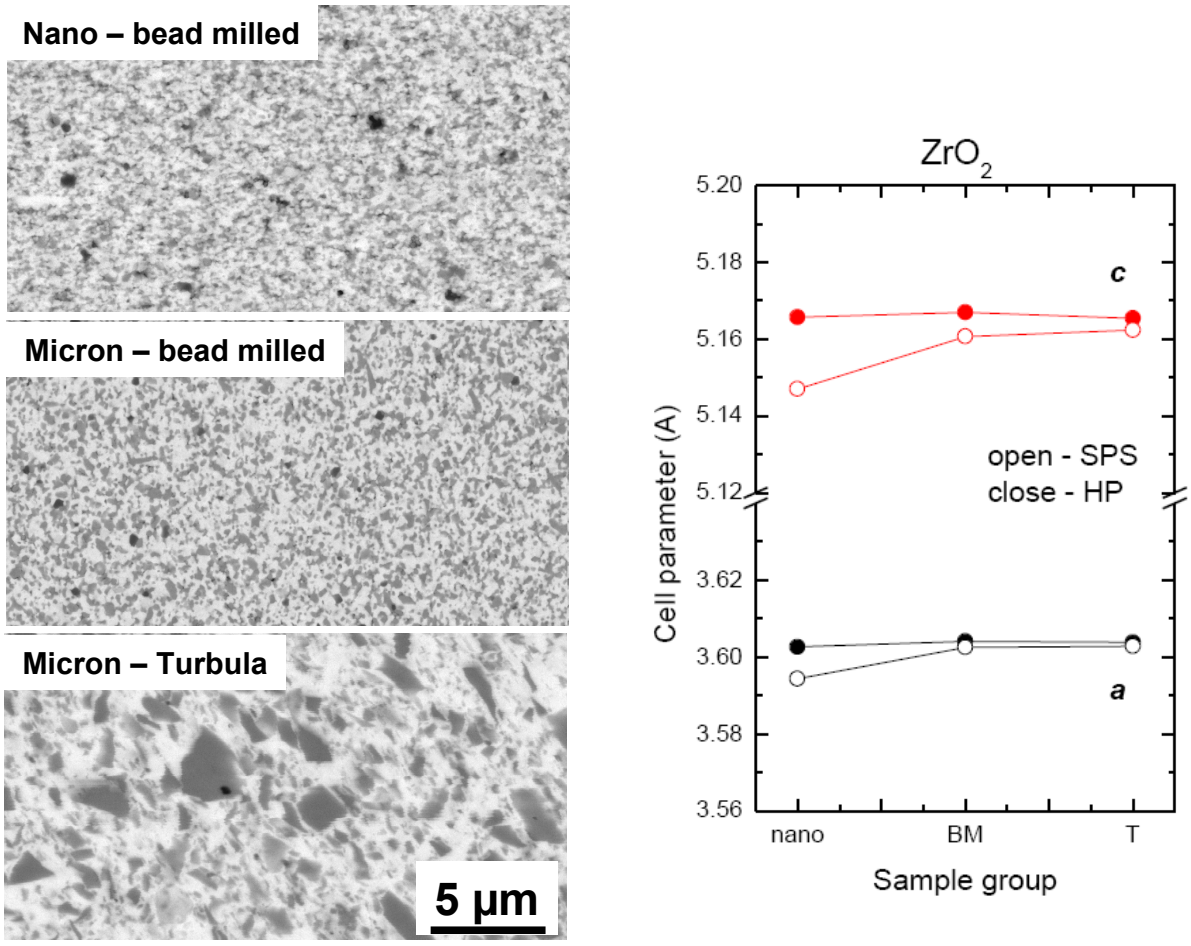

Figure 25: ***Representative microstructures of the different ZrO_2-TiCN (60/40) composites (a) and the unit cell dimensions of the concomitant Y-ZrO_2 matrix phase (b). Dark grey: TiCN.***

The validity of these models was further evaluated using the experimentally determined thermal properties of the pure components and comparing the predicted property of the composite(s) with that obtained experimentally (Figure 26).

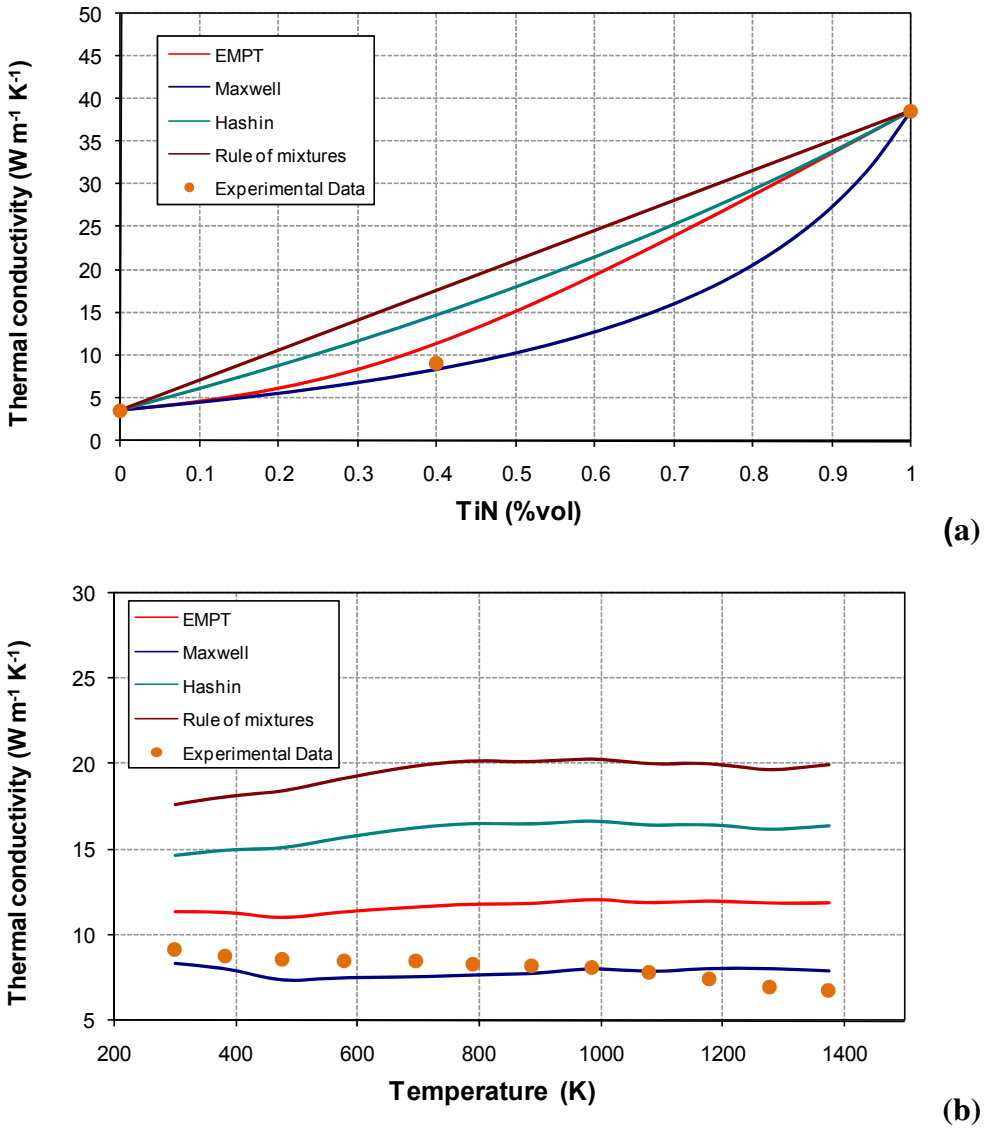

Figure 26: ***Example of the prediction of common analytical models for the thermal conductivity of a zirconia-titanium nitride composite; at respectively 273 K as function of composition (a) and for a 60/40 (vol%) composition as a function of temperature (b); the characteristics of the pure components are those determined experimentally.***

From the comparison it appears that the best agreement is obtained for these compositions with the Maxwell model. Thereupon, this agreement seems to be acceptable over a broad temperature range; at high temperature (typically above 900K), the experimental data slightly deviate from the trend provided by the analytical model.

A similar comparison can be done with thermal conductivity values obtained by numerical simulation using Object Oriented Finite element techniques, as shown in Figure 27.

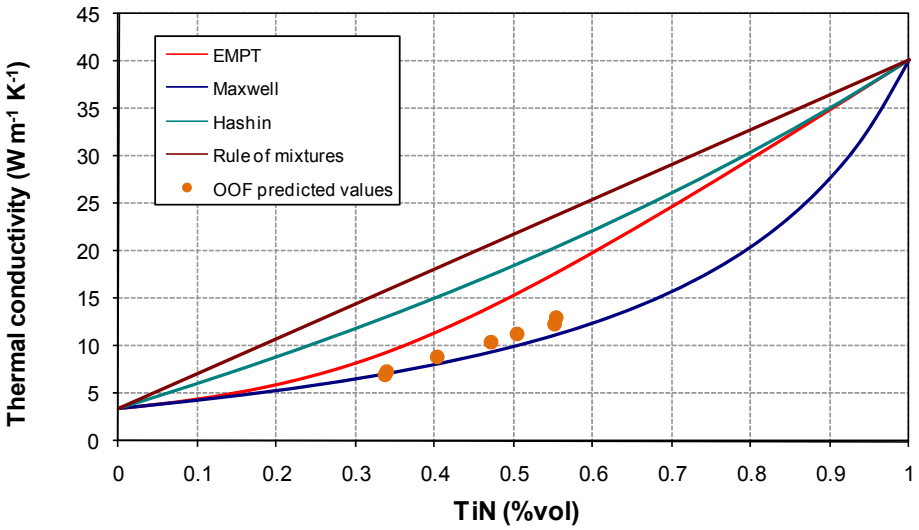

Figure 27: ***Comparison of predicted thermal conductivity values at 273 K for zirconia-titanium nitride composites; as function of composition, according to common analytical models and with predicted values resulting from OOF experiments.***

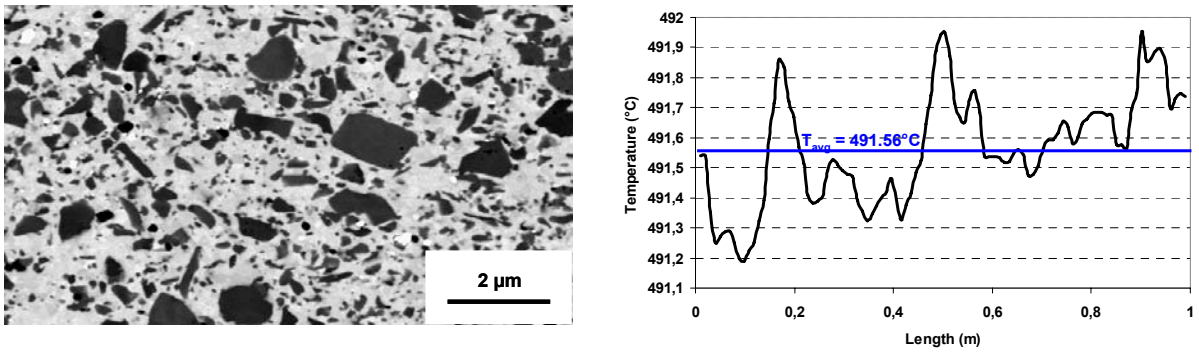

(a) **(b)**

Figure 28: ***BSE micrograph of a ZrO_2-TiN (60/40) (vol%) composite (a) and the calculation of the steady-state temperature profile on the top line of the microstructure after applying a constant bottom temperature of 500°C and a heat flux of 101.5 W/m² (b).***

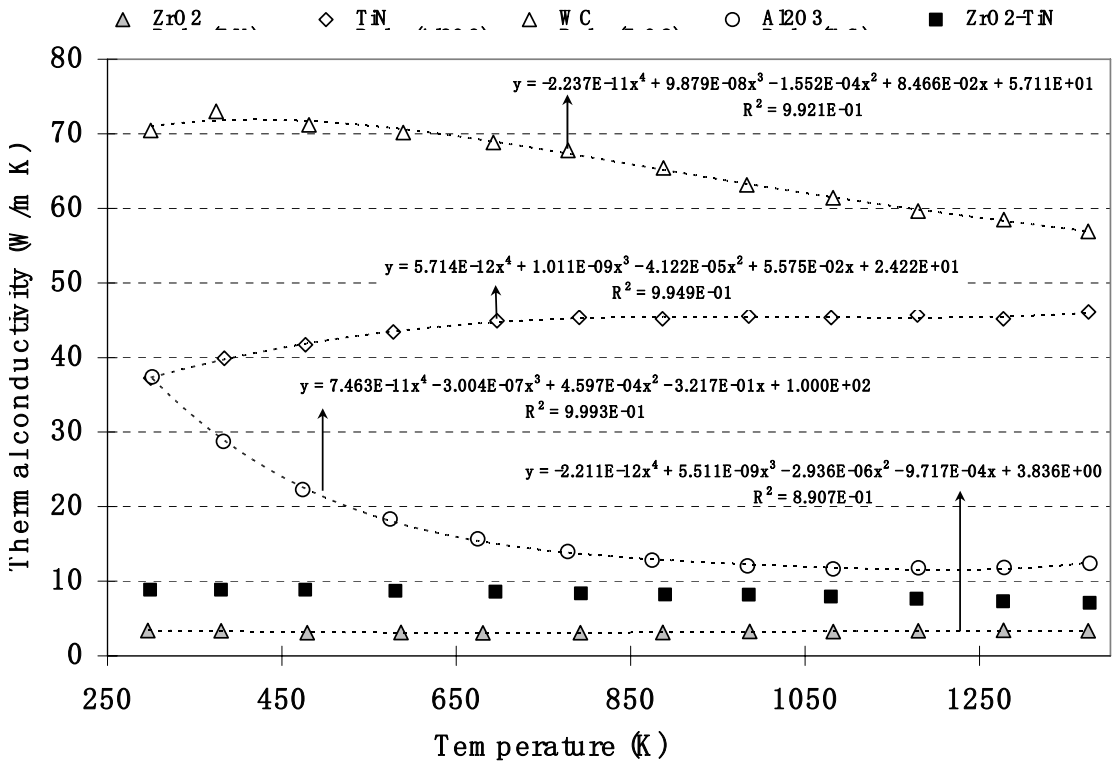

(a)

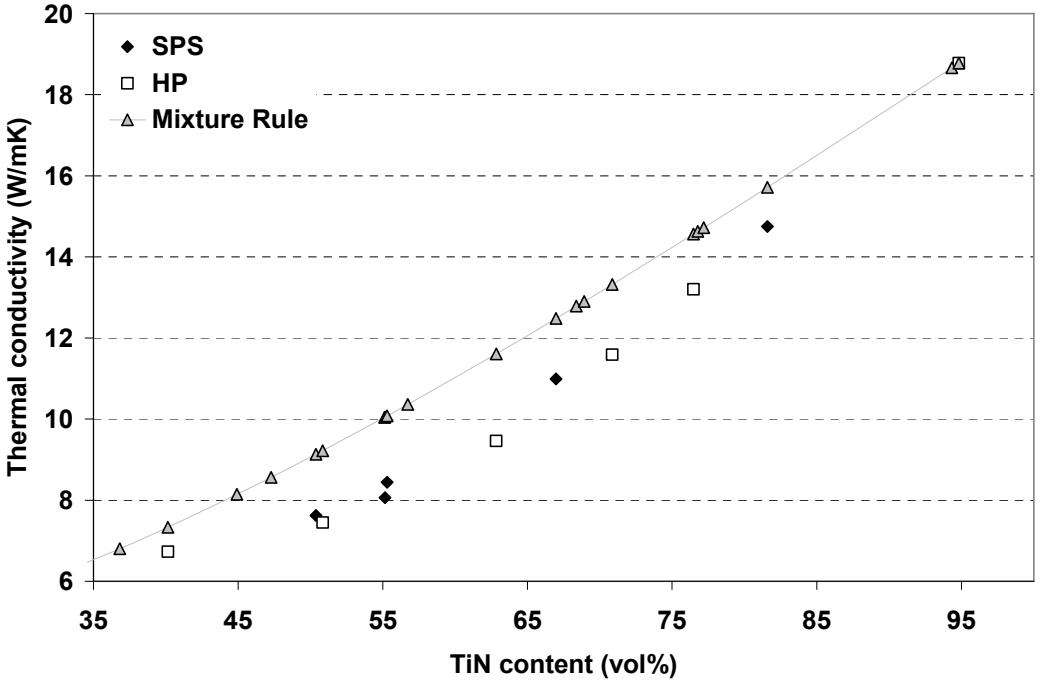

(b)

Figure 29: Experimentally measured (a) and OOF predicted (b) thermal conductivity values.

The thermal properties of a ZrO_2-TiN (60/40) composite material, of which the microstructure is shown in Figure 28 (a), were predicted using an object oriented finite element technique (OOF), shown in Figure 28 (b), using experimentally determined (at INISMa) thermal conductivity values of the constituting compounds, shown in Figure 29 (a). This method proves to be an excellent tool to qualitatively predict the thermal properties of composite materials based on 2D microstructures, as shown in Figure 29 (b). From Figure 28, it can be observed that, since the heat flux occurs in vertical direction, the vertical zones with an increased TiN content, exhibit a local higher heat flux, resulting in an increased temperature with respect to these zones with a lower TiN content.

The OOF approach, schematically shown in Figure 28, leads to a realistic estimation of the thermal conductivity values compared to experimentally determined values. Furthermore, this is confirmed by the comparison between the analytically calculated values using the Maxwell model and the OOF calculated values. The reason for this needs further investigation.

It has however to be pointed out that in both cases (analytical and numerical simulation), the potential effects of the interfaces (e.g. thermal resistance of the grain boundaries) on the overall apparent thermal behaviour of the material have been ignored.

5.2.4 ZrO_2-WC (60/40) (vol%)

ZrO_2-WC (60/40) (vol%) composites were processed using two different types of WC powder: nanometre sized powder and micrometre sized powder with average grain sizes of 200 nm and 1 µm, respectively. Three different composites, containing either pure nanometre or micrometre sized WC powders or a 50/50 (vol%) mix of both. Representative microstructures are shown in Figure 30, while Table 7 summarises the mechanical properties.

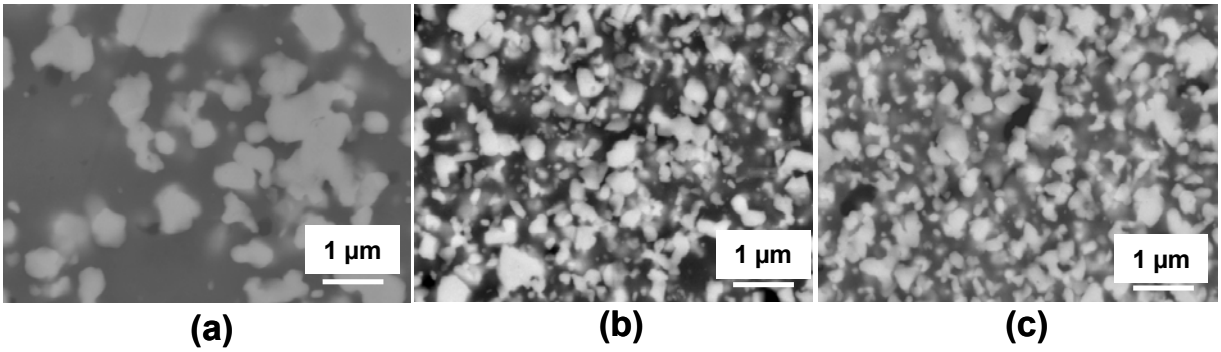

Figure 30: ***Representative BSE images of the different ZrO_2-WC (60/40) (vol%) materials with different WC grain sizes: (a) micrometre sized WC, (b) micrometre-nanometre sized WC (50/50) (vol%), (c) nanometre sized WC. Powder mixtures (b) and (c) were mixed using bead milling, while powder mixture (a) was mixed by Turbula. All materials were densified by means of FAST at 1550°C, applying a heating rate of 200°C/min and a pressure of 60 MPa. White: WC.***

WC source	Density (g/cm³)	E-modulus (GPa)	Vickers Hardness (kg/mm²)	Fracture toughness (MPa.m$^{1/2}$)
micro	9.58	345 ± 4	1624 ± 36	7.3 ± 0.4
nano/micro (50/50)	9.57	320 ± 4	1610 ± 30	6.1 ± 0.2
nano	9.69	334 ± 4	1660 ± 37	6.1 ± 0.3

Table 7: ***Summary of the mechanical properties of the different ZrO_2-WC (60/40) (vol%) materials using nanometre and micrometre sized WC particles.***

It can be observed that ZrO_2-WC (60/40) (vol%) composites exhibit improved mechanical properties compared to ZrO_2-TiCN (60/40) composite materials, due to the absence of any chemical interaction between the Y-ZrO_2 matrix and the secondary WC phase. The high temperature deformation behaviour of these composite materials will be discussed along with the finite element simulations of their deformation behaviour.

5.3. Conclusions zirconia based materials

As part of a case study together with Umicore an unstabilised nanosized zirconia powder was characterised. The large fraction of the tetragonal structure testifies to

the fine primary particle size for this powder. This powder among others was also used in the development of zirconia based composites.

The fracture toughness of the ZrO_2-Al_2O_3 composites was mainly dependent on a) the Y-ZrO_2 grain size, which was directly influenced by the temperature and the stabiliser content, b) the type and c) amount of stabiliser. Increasing temperatures and decreasing stabiliser contents (3→ 2.5 → 2Y) resulted in increased Y-ZrO_2 transformability and toughness values up to 6 MPa.$m^{1/2}$

For ZrO_2-$TiC_{0.5}N_{0.5}$ (60/40) composites a number of process variables was investigated. With respect to the stabilisers the highest toughness was obtained for 1Y2Nd-ZrO_2 matrices which were tougher compared to 3Y-ZrO_2 matrices with values up to 9 MPa.$m^{1/2}$reached. Generally, the mechanical properties of the processed composite materials decreased with decreasing TiCN grain size. This was attributed to a partial dissolution of TiCN in Y-ZrO_2 which increases as the contact area between the two phases increases. Further proof for this hypothesis is being sought. In contrast for ZrO_2-WC (60/40) (vol%) composites we observed improved mechanical properties compared to ZrO_2-TiCN (60/40) composite materials, due to the absence of any chemical interaction between the Y-ZrO_2 matrix and the secondary WC phase.

The thermal properties of ZrO_2-TiN ceramic composites were investigated and modelled. With respect to the analytical models the Maxwell model appears to approximate the experimental data more closely.

A numerical object oriented finite element technique (OOF) was also used. In this approach actual pictures of the microstructure are the starting point. The OOF approach, leads to a realistic estimation of the thermal conductivity values compared to experimentally determined values. There is also a good correspondence with the analytically calculated values using the Maxwell model. It is remarkable that for this system the potential effects of the interfaces (e.g. thermal resistance of the grain boundaries) on the overall apparent thermal behaviour of the material can be ignored.

6. Results on TiO_x / TiO_2 materials

These materials were investigated as part of a case study with Bekaert.

6.1. Densification behaviour

As-received (supplied by Bekaert), coarse TiO_x powders, were bead milled at 5000 rpm for 2, 4 and 6 hours using 2 mm diameter Y-TZP beads. Since no more significant reduction in grain size took place after 2h bead milling, all FAST experiments were performed using 2h bead milled TiO_x powder. A fully dense material with a density of 4.262 g/cm³ could be obtained after FAST at 1100°C. The crystallographic phase of the as-received powder could be maintained, both after bead milling and FAST densification.

The as-received TiO_2 nanopowder had the anatase crystal structure (JCPDF card 78-2486 - Anatase, tetragonal, ρ = 3.893 g/cm³). When the FAST densification temperature was lower than 900°C, the initial anatase phase was maintained. However, no fully dense specimens could be obtained at this temperature. When the temperature was increased, fully dense samples could be obtained, but the anatase phase transformed to rutile that was maintained during cooling.

6.2. Thermal properties

The (partially) sintered bead-milled TiO_x as well as the as-received nano TiO_2 materials, densified by FAST, were characterised in terms of thermal diffusivities. The tested samples and their corresponding densities are summarized in Table 8.

Sample Label	Processing Conditions	Density (g/cm³)
TiO_x-1000	Bead Mill (2h – 500rpm) FAST – 1000°C – 60 MPa	4.27
TiO_x-1100	Bead Mill (2h – 500rpm) FAST – 1100°C – 60 MPa	4.26
TiO_x-1200	Bead Mill (2h – 500rpm) FAST – 1200°C – 60 MPa	4.26
TiO_2-800	As received nanopowder FAST – 800°C – 60 MPa	2.73 (Anatase)
TiO_2-900	As received nanopowder FAST – 900°C – 60 MPa	3.55 (Rutile)
TiO_2-1000	As received nanopowder FAST – 1000°C – 60 MPa	4.16 (Rutile)

Table 8: Overview of the densities of different FAST sintered TiO_x / TiO_2 samples.

Thermal diffusivity values were only obtained on the densified TiO_2 nanopowder samples; a lack of reproducibility was systematically observed on the bead-milled TiO_x sintered samples. The evolution of the thermal diffusivity of the former is presented as a function of temperature in Figure 31. Despite the presence of one irregular data point, the general trends of increasing diffusivity with sample density and decreasing diffusivity with increasing test temperature were observed.

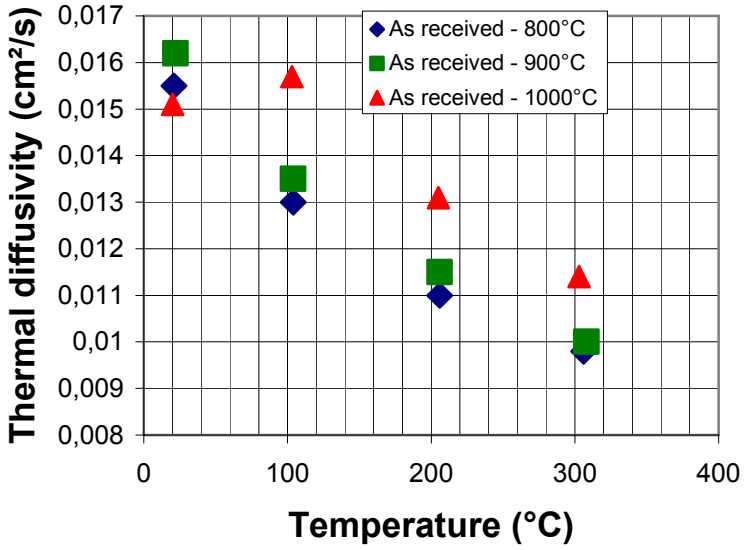

Figure 31: Evolution of thermal diffusivity of TiO_2 materials sintered by FAST.

6.3. Conclusions on TiO_x / TiO_2 materials

The main conclusions are that it was possible to retain the crystallographic structure of the TiO_x phase after densification with FAST. In contrast this was not possible for the TiO_2 phase with anatase structure which had transformed to the rutile structure after densification. For the latter the thermal diffusivity was measured and shown to decrease substantially from 25°C to 300°C.

7. WC-based and diamond dispersed WC-Co

7.1. Binderless WC

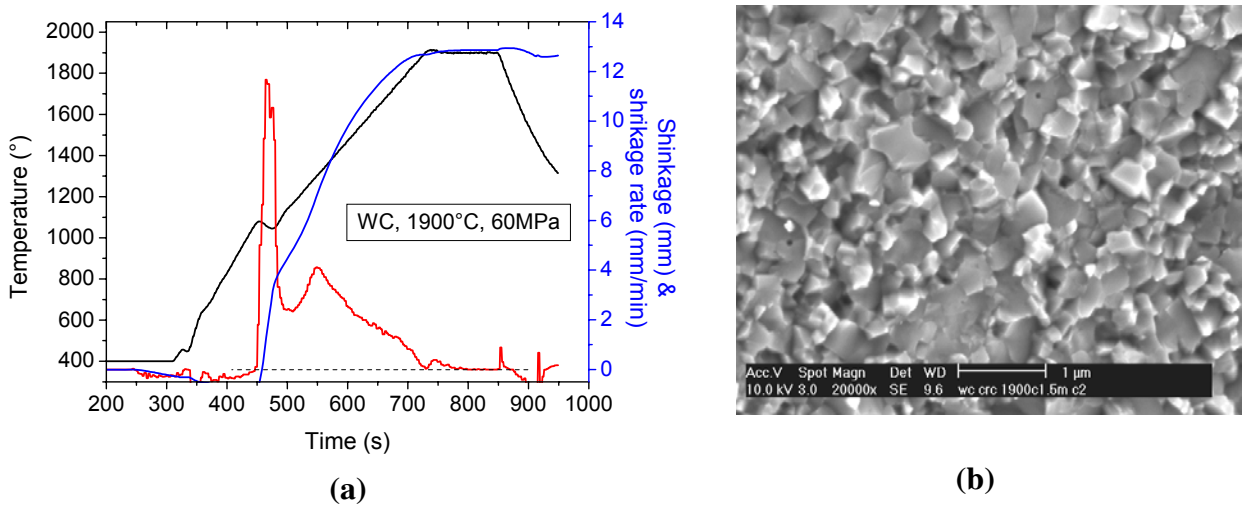

(a) **(b)**

Figure 32: Representative densification curve (a) and BSE micrograph of a fracture surface (b) of binderless WC densified by means of FAST at 1900°C for 1.5 min applying a pressure of 60 MPa.

Fully dense, binderless WC ceramics were processed by means of FAST at 1900°C, applying a pressure of 60 MPa. The densification curve is shown in Figure 32 (a). Submicrometre sized WC powder (CRC 015 grade, Wolfram-Bergbau, Austria) with an average grain size of 150 nm was used as starting powder. Figure 32 (b) indicates that the grain size of the initial starting powder was maintained in the fully densified material. Excellent mechanical properties such as a Vickers hardness of 28 GPa and a 3-point bending strength of nearly 1 GPa were obtained.

7.2. WC-Co materials

As part of a case study, a WC-Co powder, containing 6 wt% Co and two diamond dispersed WC-Co mixtures, containing either coarse or fine diamond particles were obtained from Diarotech, as summarised in Table 9.

All materials were densified successfully using FAST. In case of the WC-Co hardmetal, the sintering temperature was varied between 1050 and 1200°C, while the pressure was fixed at 60 MPa. Some eta phase was detected at the lower temperatures. At elevated temperatures, a bimodal WC grain size distribution

developed, as shown in the micrographs in Figure 33. In case of the diamond dispersed WC-Co materials, the pressure was increased to 100 MPa, while the sintering temperature was varied from 1100 to 1200°C. In all cases, a fully dense WC-Co matrix was obtained as well as a good integration between the diamond particles and the hardmetal matrix. With increasing sintering temperature, the amount of graphitisation on the outer surface of the diamond particles was enhanced, as indicated in Figure 34.

Label	Material	Theoretical Density (g/cm^3)	Size of diamond particles (µm)
Diarotech100622009_II	WC-6Co	14.99	-
Diarotech27082009_AI	WC-6Co + 46 vol% diamond	9.71	300-400 µm
Diarotech27082009_AII	WC-6Co + 30 vol% diamond	11.56	30-40 µm

Table 9: Overview of the different WC-6Co powder grades that were forwarded by Diarotech to KULeuven. Theoretical densities of 14.99 and 3.52 g/cm^3 were used for WC-6Co and diamond, respectively.

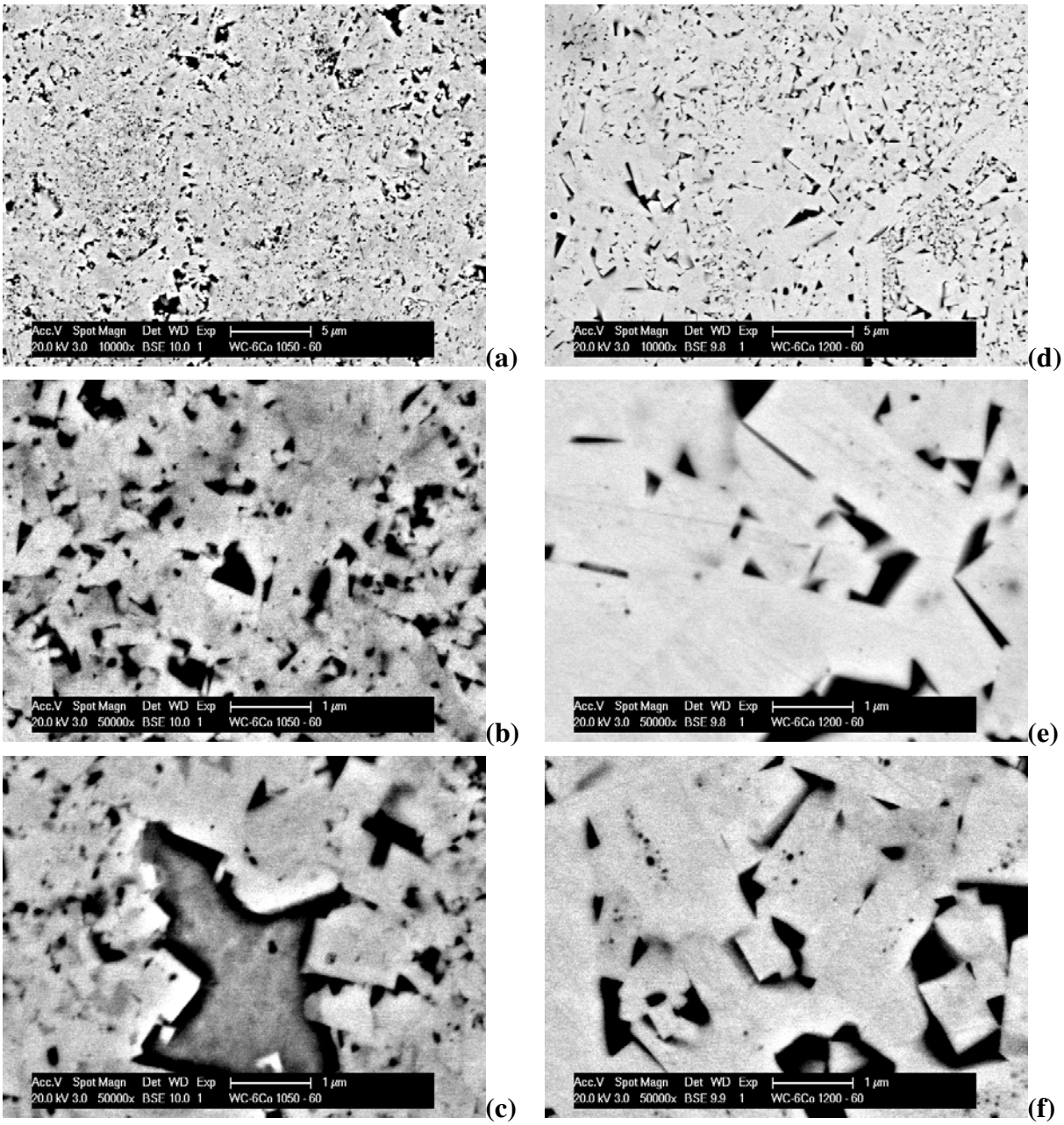

Figure 33: Representative Back Scattered Electron (BSE) images of the WC-6Co material densified by FAST at either 1050 (a-c) or 1200°C (d-f).

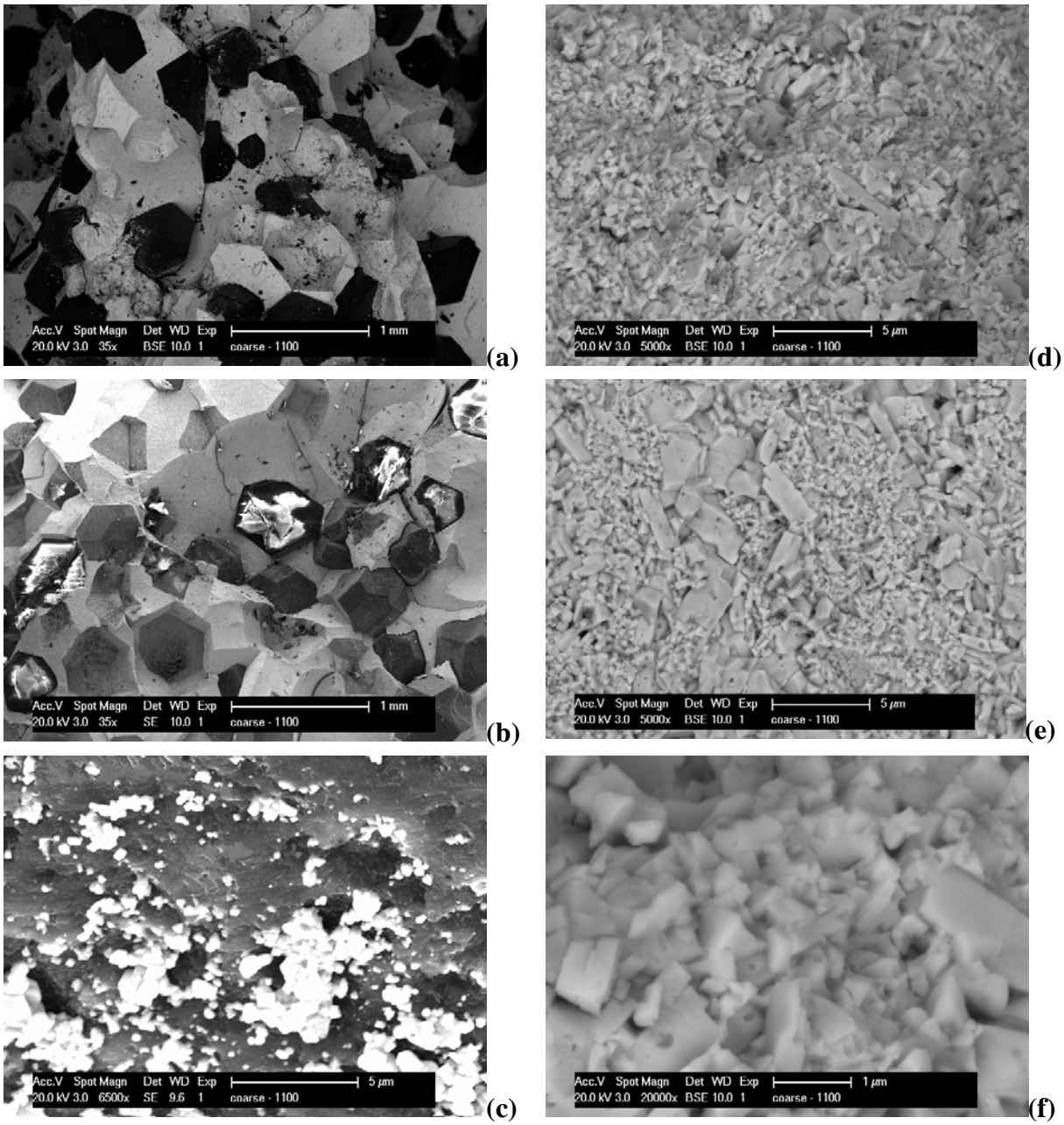

Figure 34: ***Representative Back Scattered Electron (BSE) (a; d-f) and Secondary Electron (SE) (b-c) images of the Al material containing 46 vol% of coarse (300-400 µm) diamond particles. The sample was densified using FAST at 1100°C applying a pressure of 100 MPa.***

7.3. Conclusions WC based materials

Fully dense, binderless WC ceramics can be obtained by FAST whereby the grain size of the initial starting powder (150 nm) was maintained in the fully densified material. This material exhibits exceptional mechanical properties such as a Vickers hardness of 28 GPa and a 3-point bending strength of nearly 1 GPa. The first experiments on a WC-Co material with diamond dispersions were promising.

8. Modelling FAST experiments with a molybdenum die

A previously developed thermal-electrical finite element model[9] was used and adjusted to simulate the temperature and current distributions inside a 30 mm diameter refractory metal (TZM: Ti, Zr dispersed Molybdenum) tool that allows FAST processing up to 1200°C applying pressures as high as 200 MPa. Different TZM dummy geometries, shown in Figure 35, were evaluated in order to determine the thermal and electrical contact resistances between the different parts of the TZM set-up. An overview of the experimentally measured Ohmic resistances of the different tools is shown in Figure 36, indicating that the presence of graphite papers between the punches and the conical protection plates significantly increases the overall tool resistance.

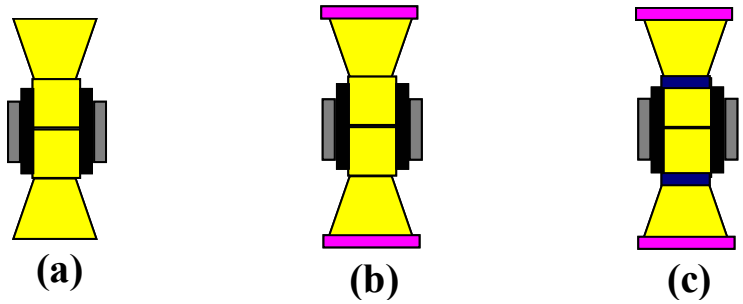

Figure 35: ***TZM dummy set-ups: TZM (a), TZM+steel plates (sp) (b) and TZM+steel plates (sp) + horizontal graphite papers (hp) (c).***

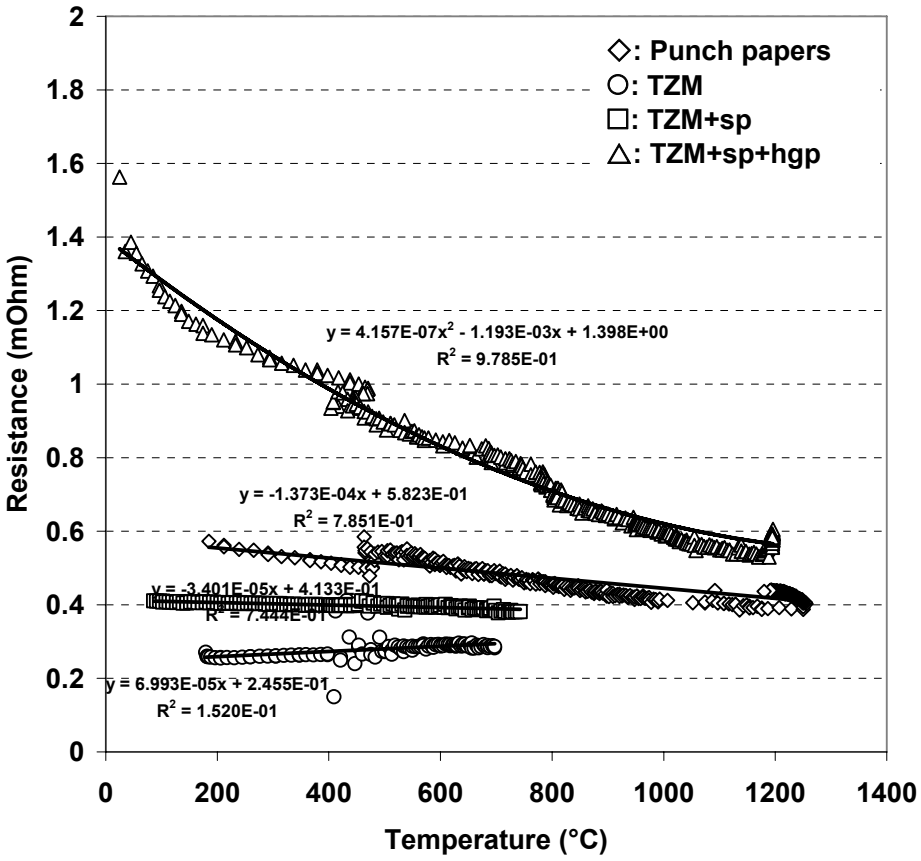

Figure 36: Experimentally measured Ohmic resistance curves of the different dummy set-ups used during the FE simulations. A constant pressure of 200 MPa was applied throughout all experiments.

Using an iterative approach, the experimentally measured Ohmic resistance values were inserted into the thermal-electrical finite element code as contact resistivities and optimised. The temperature distribution inside the different dummy set-ups at a fixed pyrometer temperature of 450°C, is shown in Figure 37. The overall resistance of the tool with only TZM parts is too low, so that overheating of the electrodes will occur. The simulation of the TZM + sp tool indicates that the steel plates are necessary to increase the overall tool resistance, in order to avoid overheating of the electrodes, while the graphite papers between the punches and protection plates are necessary to locate the heat generation in the centre of the tool. Therefore, the tool with steel plates and horizontal graphite papers was used throughout all high pressure FAST experiments

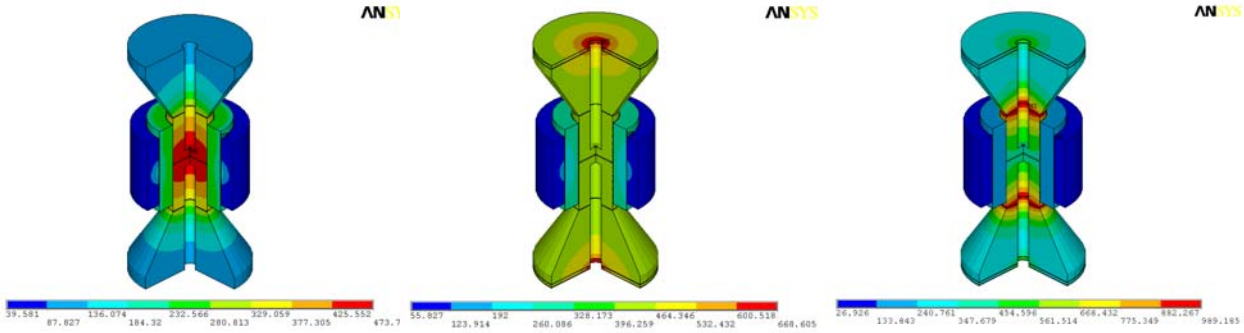

(a) (b) (c)

Figure 37: Simulated temperature distributions inside different TZM dummy set-ups, as calculated from the thermal-electrical finite element code. (a) TZM, (b) TZM + steel plates (sp) and (c) TZM + sp + horizontal graphite papers (hgp).

Conclusions

A TZM die assembly was successfully designed and experiments in this die set-up simulated. From these simulations emerged that the resistance in the set-up was too low and would have led to overheating of the electrodes. Incorporation of steel plates between the protection plates and the electrodes and horizontal graphite paper between the punches and the protection plates are necessary. The TZM die allows the use of significantly higher pressures than the traditional graphite dies although its maximum use temperature is limited to 1200°C.

9. Modelling material deformation during FAST experiments

A second set of macroscopic simulations coupled a thermal-electrical finite element model with a thermal-mechanical finite element model in order to predict the final shape of (super)plastically deformed ceramic cylinders under a constant load of 5 kN inside the FAST equipment. Two different materials were selected to be deformed at elevated temperatures ranging between 1250 and 1550°C: 3Y-ZrO_2 and 3Y-ZrO_2-$TiC_{0.5}N_{0.5}$ (60/40) (vol%), both hot pressed at 1450°C for 1 hour. The influence of the electrical current on the deformation behaviour was investigated by deforming the composite material as such or by positioning a SiC disc in between the cylindrical specimen and the graphite punches, as shown schematically in Figure 38 (a). Representative deformation curves of the two materials at 1450°C are shown in Figure 38 (b). A ZrO_2-WC (60/40) (vol%) composite was deformed at the same conditions as a reference experiment.

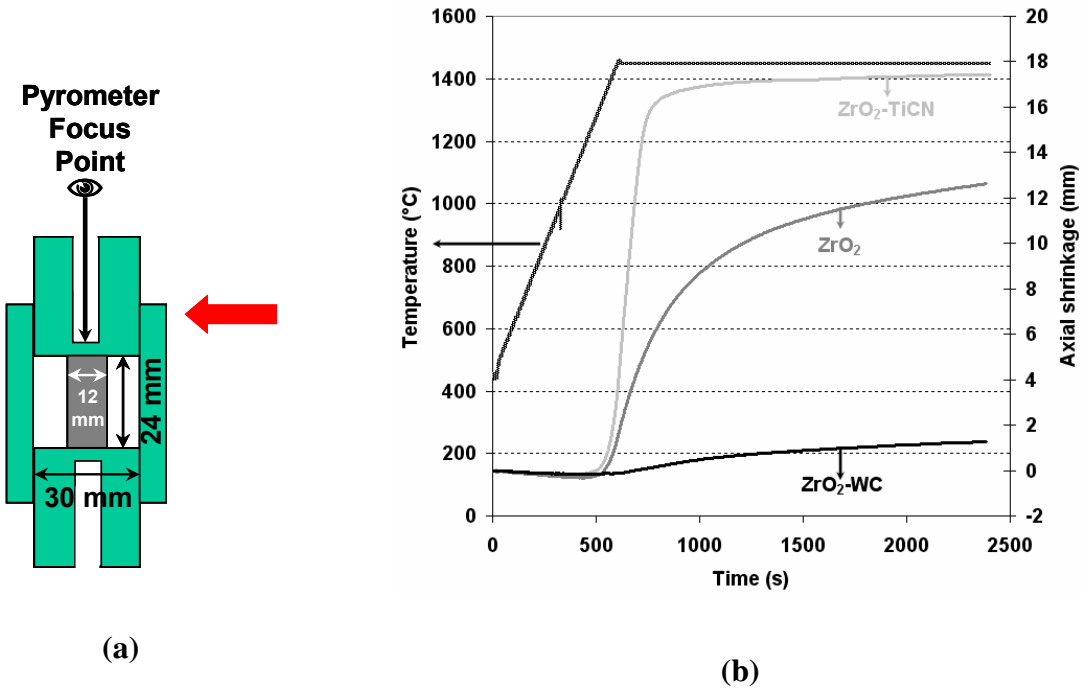

Figure 38: ***Experimental set-up (a) and constant load (5kN) deformation curves (b) of three ZrO_2 based materials at 1450°C – pyrometer temperature: ZrO_2-WC (60/40) (vol%) (black-reference), 3Y-ZrO_2 (dark grey) and ZrO_2-TiCN (60/40) (light grey).***

Although the deformation curves in Figure 38 indicate that ZrO_2-TiCN (60/40) deforms better than 3Y-ZrO_2, one must take into account the temperature gradient that is present inside the sample during densification. This gradient develops

because of the specific sample geometry but mainly because of the electrical properties of the deforming specimen. In case the material is electrically conductive, the sample centre is largely overheated as compared to the top of the sample, which has a temperature close to the temperature that is registered by the pyrometer, as shown in Figure 39.

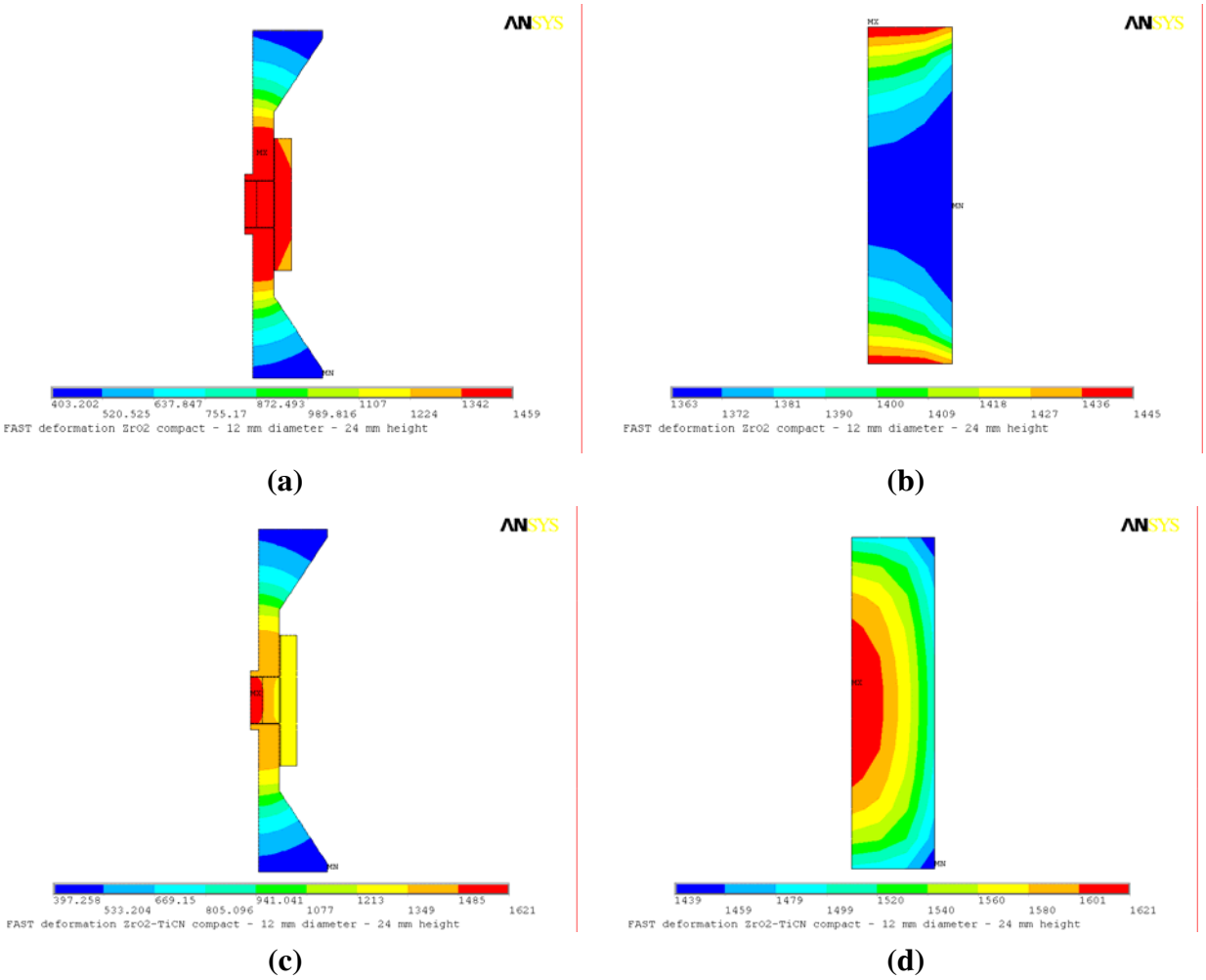

Figure 39: Temperature distributions inside the FAST tool (left) and the deforming sample (right) at the onset of deformation in case a 3Y-ZrO_2 (a-b) and ZrO_2-$TiC_{0.5}N_{0.5}$ (60/40) sample is deformed inside a 30 mm diameter FAST tool set-up at a pyrometer temperature of 1450°C.

However, when 20 mm diameter SiC discs are used to separate the cylindrical sample from the punches, a more homogeneous temperature distribution can be generated inside the deforming sample, as shown in Figure 40 (a), and the temperature distribution is very similar compared to the temperature distribution inside a 3Y-ZrO_2 sample (Figure 39). Moreover, the deformation curve of the ZrO_2-TiCN (60/40) sample, using SiC discs at 1450°C, as shown in Figure 40 (b), is very similar to that of the same material without SiC discs, deformed at a pyrometer

temperature of 1300°C. Therefore, we believe that the electrical current mainly influences the deformation by the creation of a locally overheated zone inside the deforming sample. The enhanced deformation of the TiCN containing composite over the WC containing composite can be attributed to a partial dissolution of Ti^{4+} into 3Y-ZrO_2 due to a chemical reaction between both components, as suggested by the enhanced deformation of a 5 mol% TiO_2 doped 3Y-ZrO_2 specimen compared to an undoped 3Y-ZrO_2 specimen (Figure 41 (a)) and the enhanced damping of the doped material at elevated temperature, as compared to undoped 3Y-ZrO_2.

Conclusions

The deformation of densified materials in the FAST set-up opens up the prospect of producing more complicated shapes in the FAST process than simple cylinders. The deformation behaviour can not be properly understood without an accurate thermal-electrical modelling of the experiments.

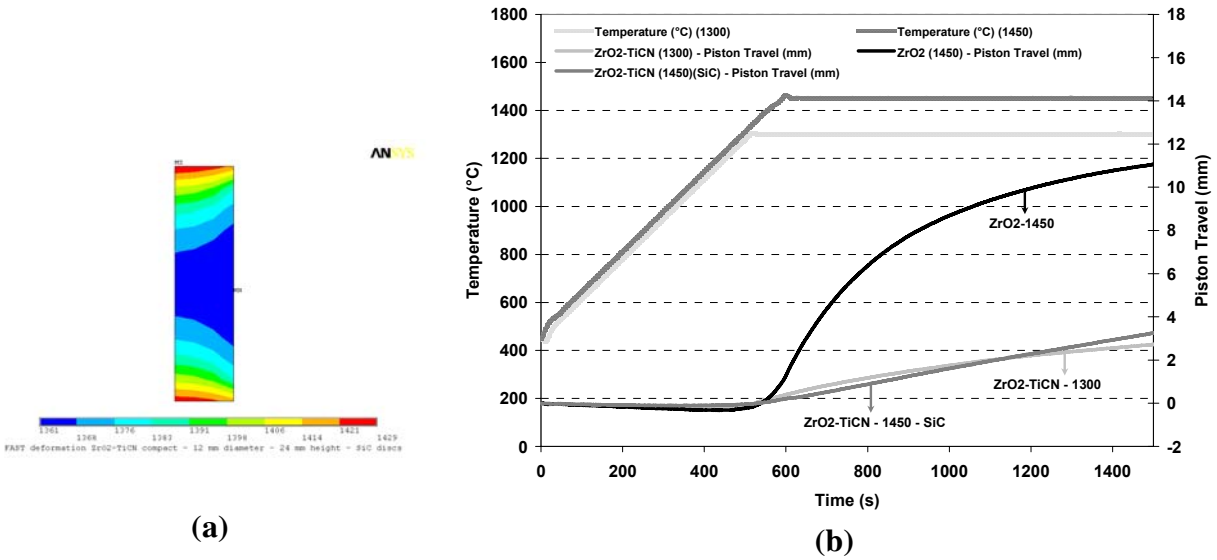

Figure 40: ***Temperature distributions inside the deforming ZrO_2-TiCN (60/40) sample at the onset of deformation (a) and the concomitant deformation curve (b) when it is deformed inside a 30 mm diameter FAST tool set-up, using SiC discs to separate the sample from the graphite punches, at a pyrometer temperature of 1300°C.***

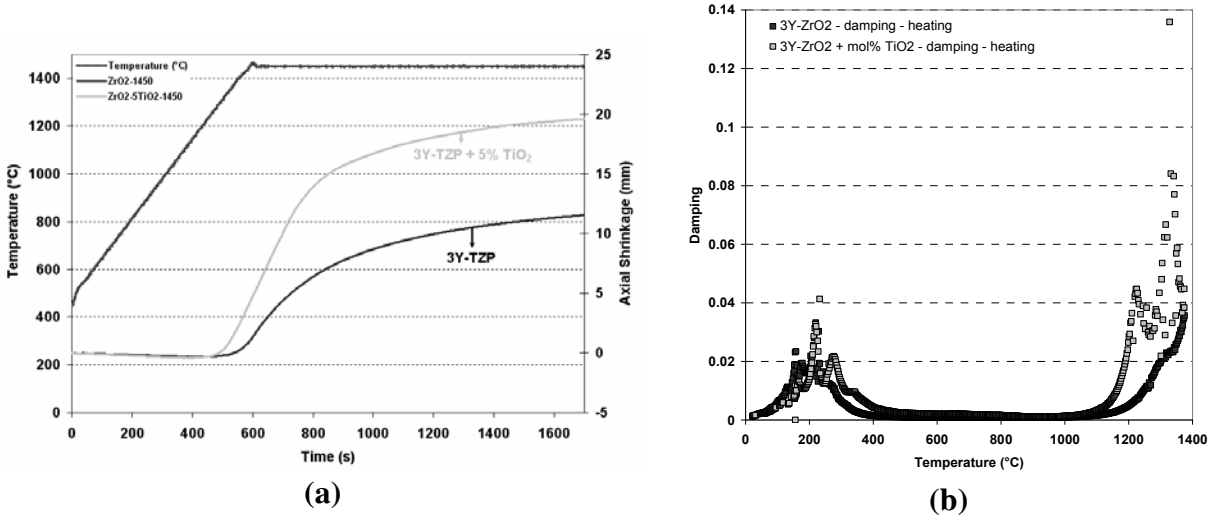

Figure 41: Comparison of the high temperature deformation (a) and damping (b) characteristics of undoped and 5 mol% TiO_2 doped 3Y-ZrO_2.

10. Overview of Case studies

1. Use of silicon carbide for space mirrors applications

One of the **envisaged applications for SiC suggested by AMOS** was lightweight and stiff mirror elements for use in space. This requires a smooth pore free silicon carbide surface. Pore free silicon carbide can not be obtained by standard hot pressing or pressureless sintering. **By FAST experiments at 2100°C encouraging densification results were obtained for a micrometre sized SiC powder** but some residual porosity remained. Further optimization of the FAST cycle and of the additives level with a nanosized powder could lead to the desired result. This was not possible within the context and time span of this project due to the difficulty of obtaining nanosized powders in sufficient quantity within the time span of the project.

2. Densification of yttria coated *m*-ZrO_2 powder supplied by Umicore

Different Y-ZrO_2-Al_2O_3 (70/30) (vol%) composites with different amounts of yttria (2, 2.5 and 3 mol% Y_2O_3) were prepared by mixing Al_2O_3 (Taimicron, TM-DAR) and Y_2O_3 coated *m*-ZrO_2 powder (Umicore). The Y_2O_3 coating was obtained after calcination (800°C, 1h, air) of an $Y(NO_3)_3$ salt that was mixed with the received *m*-ZrO_2 powder. The Y-ZrO_2 grain size and concomitant Y-ZrO_2 phase transformability could be optimised by changing the yttria stabiliser content and sintering temperature/time.

3. Densification of WC-Co-diamond mixtures supplied by Diarotech

Two different WC-Co-diamond mixtures, containing either coarse or fine grained diamond particles (Diarotech), were successfully densified by means of FAST at 1100°C, applying a pressure of 100 MPa.

4. Densification and characterisation of TiO_2/TiO_x powders from Bekaert

Both in case of bead-milled (5000 rpm, 2h) TiO_x and nanometre sized TiO_2 powder, a FAST densification temperature of 1000°C, in combination with an applied mechanical pressure of 60 MPa, were needed to densify both materials. The electrical conductivity of the bead milled TiO_x pellet was 19 S/cm, allowing the sample to be machined by electrical discharge machining (EDM).

11. Conclusions

11.1. Scientific and technical conclusions

The main lesson learnt from the R&D activities carried out on the **synthesis of SiC plasma powders** is that the production of consistent nanopowders (i.e. having reproducible properties) is possible using a RF plasma torch capable of producing at least semi industrial amounts of end product within reasonable run durations. However, tuning the process variables requires a careful study of all process related aspects, ranging from the nature of the reactants to the post processing treatment operations. The main outcome of this research is the demonstration of the pertinence of chemical engineering tools and reasoning for overall process optimization purposes. Sirris believes that each specific nanopowder would require a study similar to the one reported here if they are ever to be produced at industrial scale while maintaining acceptable product consistency. Further efforts will be needed to the extension of characterization tools and methods as well as to dispersion and functionalisation of nanopowders.

One of the **envisaged applications for SiC suggested by AMOS** was lightweight and stiff mirror elements for use in space. This requires a smooth pore free silicon carbide surface. Pore free silicon carbide can not be obtained by standard hot pressing or pressureless sintering. **By FAST experiments at 2100°C encouraging densification results were obtained for a micrometre sized SiC powder** but some residual porosity remained. Further optimization of the FAST cycle and of the additives level with a nanosized powder could lead to the desired result. This was not possible within the context and time span of this project due to the difficulty of obtaining nanosized powders in sufficient quantity within the time span of the project.

A well dispersed and stable suspension could be obtained from the commercial **TM-DAR alumina powder** by the use of the MiniCer® nanogrinder (Netzsch).

In order to gain insights into the **operating densification mechanisms** during the FAST process a series of experiments was carried out varying the pressures, heating rates, dwell temperatures as well as dwell duration. The data are still being analysed and in particular more detailed microstructural data are needed for the further elucidation. However it is clear that as the density of the alumina increases the grains also grow significantly. Further work is also in progress to compare density and microstructural evolution during FAST with the hot pressing technique.

The **elastic properties of the obtained aluminas** depended primarily on the porosity level of the samples. Other processing parameters do not have a discernible influence. Particular attention has been paid to **the modelling of the thermal conductivity as function of porosity and grain size of the aluminas.** From an extensive literature study, the Effective Medium Percolation Theory (EMPT) model appeared to be most appropriate. In order to match data on porous and very fine grained aluminas it is necessary to take into account the thermal resistivity of the grain boundaries.

Al_2O_3–WC composite powders with up to 80 vol% WC could be fully densified by means of FAST. The higher the WC content, the higher the sintering temperature needed to achieve fully dense composites. The dispersion of 20–60 vol% WC grains significantly suppressed Al_2O_3 grain growth, resulting in ultrafine grained composites with high stiffness. T**he FAST sintered Al_2O_3–WC composites with 40 or 60 vol% WC combine an excellent hardness of 24 GPa with a quite acceptable fracture toughness of 4 MPa.m$^{1/2}$ and a high flexural strength of 1000–1200 MPa.** The electrical conductivity of these composites is high enough for the materials to be suitable for electrical discharging machining.

As part of **a case study together with Umicore** an unstabilised nanosized **zirconia powder** was characterised. The large fraction of the tetragonal structure testifies to the fine primary particle size for this powder. This powder among others was also used in the development of zirconia based composites.

The fracture toughness of the **ZrO_2-Al_2O_3 composites** was mainly dependent on a) the Y-ZrO_2 grain size, which was directly influenced by the temperature and the stabiliser content, b) the type and c) amount of stabiliser. Increasing temperatures and decreasing stabiliser contents (3→ 2.5 → 2Y) resulted in increased Y-ZrO_2 transformability and toughness values up to 6 MPa.m$^{1/2}$

Also for **electrically conductive ZrO_2-$TiC_{0.5}N_{0.5}$ (60/40) composites** a number of process variables were investigated. With respect to the stabilisers the highest toughness was obtained for 1Y2Nd-ZrO_2 matrices which were tougher compared to 3Y-ZrO_2 matrices with values **up to 9 MPa.m$^{1/2}$**reached. Generally, the mechanical properties of the processed composite materials decreased with decreasing TiCN particle size. This was attributed to a partial dissolution of TiCN in Y-ZrO_2 which increases as the contact area between the two phases increases. Further proof for this hypothesis is being sought. In contrast for **ZrO_2-WC (60/40) (vol%) composites** we observed improved mechanical properties compared to ZrO_2-TiCN (60/40)

composite materials, due to the absence of any chemical interaction between the Y-ZrO_2 matrix and the secondary WC phase.

The **thermal properties of ZrO_2-TiN ceramic composites** were investigated and modelled. Among the analytical models the Maxwell model appears to approximate the experimental data more closely. A numerical object oriented finite element technique (OOF) was also used. In this approach actual pictures of the microstructure are the starting point. The OOF approach leads to a realistic estimate of the thermal conductivity values compared to experimentally determined values. There is also a good correspondence with the analytically calculated values using the Maxwell model.

In a **case study together with Bekaert on TiO_x / TiO_2 materials**, the main conclusions are that it was possible to retain the crystallographic structure of the TiO_x phase after densification with FAST. In contrast this was not possible for the TiO_2 phase with anatase structure which had transformed to the rutile structure after densification. For the latter the thermal diffusivity was measured and shown to decrease substantially from 25°C to 300°C.

Fully dense, binderless WC ceramics can be obtained by FAST whereby the grain size of the initial starting powder (150 nm) was maintained in the fully densified material. **This is an example of a material that could only be made by FAST and where indeed the promise of the technique has been fully realised.** This material exhibits exceptional mechanical properties such as a Vickers hardness of 28 GPa and a 3-point bending strength of nearly 1 GPa.

Within a case study with Diarotech the densification of **WC-Co materials with a dispersion of diamond particles** was investigated. The first experiments yielded promising results.

In the FAST technology **the electrical and thermal properties of the die assembly** play a crucial role in the temperature distribution that can be achieved. The **mechanical properties of the die material also determine the pressures that can be applied** to assist the densification. Hence research on the development of a die set-up which allows the application of higher pressures than the currently used graphite dies are very worthwhile. Within the project a TZM die assembly was successfully designed and experiments in this die set-up simulated. From these simulations emerged that the resistance in the set-up was too low and would have led to overheating of the electrodes. Incorporation of steel plates between the protection plates and the electrodes and horizontal graphite paper between the

punches and the protection plates are necessary. The TZM die allows the use of significantly higher pressures up to 200 MPa than the traditional graphite dies although its maximum use temperature is limited to 1200°C.

Another limitation of the FAST technology is that at present only rather simple shapes such as discs can be obtained. In order to make **more complicated shapes** possible we have investigated the deformation behaviour of fully dense material and have observed **super plastic deformation rates** which opens prospects of more complex shaping. In order to understand this deformation behaviour one needs an accurate thermal-electrical modelling of the experiments.

11.2. Support to innovation and transfer of knowledge

At 6 months intervals the research partners met with the project follow-up committee which included among others representatives from the Following industrial actors: Bekaert; Diarotech; Umicore; AMOS; Halliburton; Magotteaux and EB Consult. These meetings have allowed these industries to develop a general assessment of the technology. The work plan included case studies driven by four industrial members of the Follow-up committee. These four case studies have given the industrial members the opportunity to evaluate the FAST technology on nanopowders for their specific interests.

The novel approach based on chemical engineering tools and reasoning as used by Sirris to tune the process variables of the synthesis of consistent nanopowders is being further exploited to provide specific powders to several industrial partners. Sirris is also ready to transfer the necessary knowledge to partners who would be interested in scaling the synthesis up to an industrial scale.

K.U.Leuven, Sirris and INISMa participated in a Symposium on “Nanopoeders: Een stand van zaken” - “Nanopowders: the present state of affairs” organised by the Flemish centre for Powder Technology (VCPT vzw.) at the Technical College De Nayer in St-Katelijne-Waver on Wednesday 23 May 2007. Prof. J. Vleugels (K.U.Leuven) gave a talk about “Production of nanopowders – a review”, Mr. F. Cambier (Sirris) gave a presentation on “Plasma technology for the production of nanopowders in Belgium”, Dr. M. Poorteman (INISMa) gave a presentation on “Characterisation of nanopowders by electro-acoustic measurements“.

INISMa took part in June 2007 in the "10th International Conference and Exhibition of the European Ceramic Society". This allowed to collect updated information on the

state-of-the-art in terms of SPS sintering, as well as on the elaboration and characterization of nanoceramic materials.

Prof. J. Vleugels participated in the Thematic Day on: “Keramiek, al eeuwenlang gebruikt in de modernste producten”, “Ceramics used for Centuries in the most Advanced Products” at the Mikrocentrum, Eindhoven (NL), on 13 December 2007 and gave a presentation on “Trends in the Development of Technical Ceramics”.

Prof. O. Van der Biest participated in the Conference EURO PM2007 from 15-17 October 2007 in Toulouse (France). He gave a presentation on “Pulsed electric current sintering of WC based hardmetals and ZrO2 based ceramic composites” co-authors S.G. Huang, J. Vleugels. He also participated in the satellite EuroPM2007 Hardmetal Workshop and gave an invited lecture on “Thermal Processing of Advanced Hardmetal Compositions” with co-authors Shuigen Huang, Jef Vleugels. In this presentation the use of FAST and microwave sintering was discussed.

Prof. O. Van der Biest attended the 32nd International Conference & Exposition on Advanced Ceramics and Composites organised in Daytona (U.S.) from 27 January till 1 February 2008. He gave an invited lecture on “Modelling of Field Assisted Sintering Technology (FAST) and its Application to Electro-conductive Ceramic Systems” with co-authors K. Vanmeensel, S. Huang, J. Vleugels, A. Laptev.

Prof. O. Van der Biest attended the Conference on “Advanced Processing for Novel Functional Materials” in Dresden from 23 January till 25 January. He gave a lecture by invitation on “SPS of Advanced Hard Materials” with co-authors Kim Vanmeensel, A. Laptev, Shuigen Huang, Jef Vleugels. Jean-Pierre Erauw (INISMa) also attended this Conference where several sessions were specifically devoted to SPS sintering.

Prof. O. Van der Biest attended the IC4N-2008 Conference, the 1st International Conference “From Nanoparticles and Nanomaterials to Nanodevices and Nanosystems” organized in Halkidiki (Greece) from 15 June till 19 June 2008. He gave an invited lecture on “Bulk Nanoceramics and Nanocomposites Processed by Field Assisted Sintering Technology (FAST)” with co-authors K. Vanmeensel and J. Vleugels.

Prof. O. Van der Biest attended the IC4N-2009 Conference, the 2nd International Conference “From Nanoparticles and Nanomaterials to Nanodevices and Nanosystems” organized in Rhodos (Greece) from 28 June till 3 July 2009. He gave an invited lecture on “Issues in the Upscaling of the PECS technology for the

manufacturing of bulk nanocomposites" with co-authors K. Vanmeensel and J. Vleugels.

Sirris also placed in its newsletter Techniline (French - Dutch) diffused in addition to 6.000 specimens a summary of the project in order to attracting certain industrialists interested by the subject. Thus firms like Magotteaux, Halliburton and Diarotech showed their interest for this study. Sirris held with one of the industrial members of the Follow-up committee a meeting aiming to better targeting its particular expectations. With this occasion it was given to us to specify to him the state of the art as regards the use of ceramics like material of tools in contact with glass and specificities of nanometric materials and the technique of sintering used in the project.

Sirris continued their activity as regards follow-up of standardization in the field of the nanotechnology. In 2007, we took part in the full session which was held in Brussels, in March 2007. This "forum" makes it possible to collect relevant information for project NACER, so much in terms of techniques of nanostructured material characterization (in particular of powders) that in terms of risks related to the handling of nanopowders.

In addition, since 2006, BCRC-INISMa ensures the representation of the NBN within the European and International technical normalization committees, CEN/TC 352 and ISO/TC 229 respectively and contributes to the working of some of the related working groups.

12. Overview of publications, oral and poster presentations

Journal Publications

[1] Huang S.G., Vanmeensel K., Van der Biest O., Vleugels J., Pulsed electric current sintering and characterization of ultrafine Al_2O_3-WC composites, Materials Science and Engineering A, 2010, 527:584.

[2] Jothinathan E., Vanmeensel K., Vleugels J., Van der Biest O., Synthesis of nano-crystalline apatite type electrolyte powders for solid oxide fuel cells, Journal of the European Ceramic Society, 2010, 30:1699.

[3] Vanmeensel K., Huang S.G., Laptev A., Salehi S.A., Swarnakar A.K., Van der Biest O., Vleugels J., Pulsed electric current sintering of electrically conductive ceramics, Journal of Materials Science, 2008, 43:6435.

Publications in Conference Proceedings

[1] Vanmeensel K., Jothinathan E., Huang S.G., Van der Biest O., Vleugels J., High Pressure Pulsed Electric Current Sintering, Proceedings of the 11th International Conference and Exhibition of the European Ceramic Society, Krakow, Poland, 21-25 June, 2009.

[2] Staverescu A.L., Vanmeensel K., Vleugels J., Van der Biest O., Processing and characterization of Pulsed Electric Current Sintered (Y-ZrO_2)-Al_2O_3 (70/30) (vol%) ceramic nanocomposites, Proceedings of the 11th International Conference and Exhibition of the European Ceramic Society, Krakow, Poland, 21-25 June, 2009.

[3] Demuynck M., Erauw J.P., Vanmeensel K., Van der Biest O., Delannay F., Cambier F., Densification of alumina and alumina based composites by SPS and other conventional sintering techniques: Influence of sintering conditions and sintering modes, Proceedings of the 11th International Conference and Exhibition of the ECerS, Krakow, Poland, 21-25 June, 2009.

Oral and poster presentations

[1] Demuynck M., Erauw J.P., Vanmeensel K., Van der Biest O., Delannay F., Cambier F., Densification of alumina and alumina based composites by SPS and other conventional sintering techniques: Influence of sintering conditions and sintering modes, 11th International Conference and Exhibition of the ECerS, Krakow, Poland, 21-25 June, 2009.

[2] Erauw J.P., Demuynck M., Van der Biest O., Cambier F., Densification kinetics of alumina compacts undergoing field assisted sintering, International workshop on Spark Plasma Sintering, Avignon, France, 6-8 October, 2008.

[3] Erauw J.P., Demuynck M., Van der Biest O., Cambier F., Densification kinetics of alumina compacts undergoing field assisted sintering, International Conference "Sintering 2008", San Diego, USA, 17-21 November, 2008.

[4] Vanmeensel K., Vleugels J., Van der Biest O., Current path/Temperature distribution during SPS, International workshop on Spark Plasma Sintering, Avignon, France, 6-8 October, 2008.

[5] Staverescu A.L., Vanmeensel K., Vleugels J., Van der Biest O., Electrically conductive ceramic nanocomposites densified by Pulsed Electric Current Sintering, Proceeedings of the European Congress on Advanced Materials and Processes (EUROMAT 2009), Glasgow, United Kingdom, 7-10 September, 2009.

[6] Van der Biest O., Vanmeensel K., Staverescu A.L., Malek O., Sheng H., Swarnakar A.K., Laptev A., Vleugels J., Bulk nanoceramics and nanocomposites processed using the Pulsed Electric Current Sintering Technique, Proceedings of the Materials Science and Technology (MS&T) 2009 Conference, Pittsburgh, 25-29 October, 2009.

ACKNOWLEDGEMENTS

We are indebted to Belspo for the financial support of this research.

Sirris thank also Technord Automation who helped us for implementing and enhancing the process control systems, Industrial Robotics Automation who designed a very useful device for the monitoring of the solid precursor injection rates, as well as Nanopole and Aseptic Technologies for numerous fruitful discussions.

REFERENCES

[1] Yanagisawa O., Kuramoto H., Matsugi K., Komatsu M., Observation of particle behaviour in copper powder compact during pulsed electric discharge, Materials Science and Engineering A, 2003, 350(1-2):184-189;
Mamedov V., Spark plasma sintering as advanced PM sintering method, Powder Metallurgy, 2002, 45(4):322-328;
Shen Z., Nygren M. Microstructural prototyping of ceramics by kinetic engineering: Applications of spark plasma sintering, Chemical Record, 2005, 5(3):173-184.

[2] Jiang Z.L., Liao L.X., Liu M.D., Catalytic Method for the Determination of Traces of Tungsten by Linear Scan Voltammetry, Analytica Chimica Acta, 1995, 300:107.

[3] Malakhova N.A., Popkova G.N., Wittmann G., Kalnichevskaia L.N., Brainina K.Z., Anodic stripping voltammetry of tungsten at graphite electrodes, Electroanalysis, 1996, 8:375.

[4] Rahier A., Lunardi S., Triki C., Practical measurement of silicon in low alloy steels by differential pulse stripping voltammetry, SCK-CEN Open BLG report.

[5] Rahier A., Analytical Determination of Total Carbon and Sulphur in Solid Samples by Full Combustion and Integrated NDIR Detection, SCK-CEN Open BLG report, BLG-1013, 2005.

[6] Vandeperre L., Van Der Biest O., Bouyer F., Persello J., Foissy A., Electrophoretic deposition of silicon carbide ceramics, Journal of The European Ceramic Society, 1997,17(2):373–376.

[7] Ref 1: Munro R.G., Evaluated Material Properties for a Sintered Alumina, Journal of the American Ceramic Society, 1997, 80 (8):1919-1928;
Ref 2: Castanet R., Selected Data on the Thermodynamic Properties of Alumina, High Temperatures - High Pressures, 1984, 16: 449-457;
Ref 3: Furukawa G.T., Douglas T.B., McCoskey R.E., Ginnings D.C., Thermal Properties of Aluminum Oxide from 0° to 1200 °K, Journal of Research of the National Bureau of Standards, 1956, 57(2): 67-82;
Ref 4: Miyayama M., Koumoto K., Yanagida H., Engineering Properties of Single Oxides Engineered Materials Handbook, 1991, 4:748-757, edited by S.J. Schneider, Jr., published by ASM International.

[8] Smith D., Fayette S., Grandjean S., Martin C., Thermal Resistance of Grain Boundaries in Alumina Ceramics and Refractories, J. Am. Ceram. Soc., 2003, 86(1) 105:11;
Landauer R., The Electrical Resistance of Binary Metallic Mixtures, J. Appl.Phys., 1952, 23, 779:84.

[9] Vanmeensel K., Laptev A., Hennicke J., Vleugels J., Van der Biest O., Modelling of the temperature distribution during field assisted sintering, Acta Materialia, 2005, 53:4379-4388.